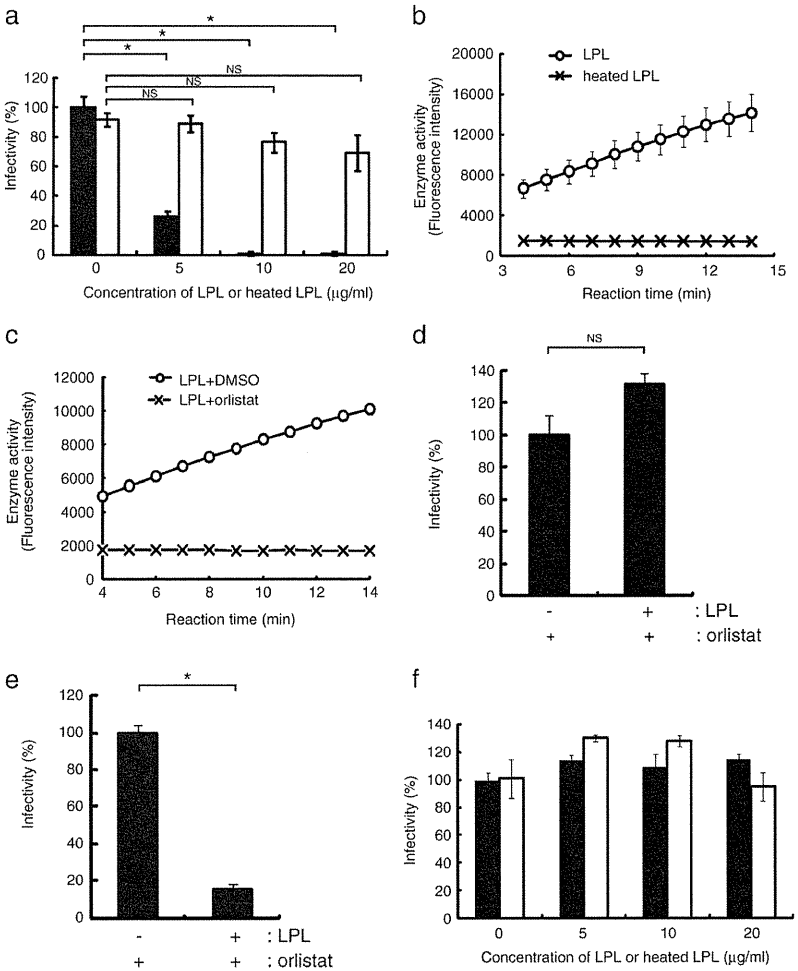

Fig. 1. LPL treatment reduced infectivity of the HCV-bearing medium in a dose-dependent manner. a. The HCV-bearing medium was pretreated with bovine LPL (•) or heat-inactivated LPL (□) (Fig. 2b) at 37 °C for 1 h before inoculation with HuH7.5 cells. Cells were fixed at 24 h post-inoculation and subjected to immunofluorescence staining. The mean percentage of HCV-positive cells relative to LPL-untreated medium is shown with the standard deviation (n=3). Statistically significant differences ($p<0.001$) are indicated by asterisks (Student's *t*-test): NS (not significant, $p>0.01$). b. Activities of LPL and inactivated LPL by heating at 100 °C for 5 min were determined. The mean value and standard deviation are shown (n=3). c. Activities of LPL on incubation with orlistat were determined. LPL (10 μg/ml) and orlistat (25 μg/ml) were mixed and subjected to determine lipase activity. Orlistat completely inhibited LPL activity. The mean value and standard deviation are shown (n=3). d. The HCV-bearing medium was pretreated with LPL (10 μg/ml) and orlistat (25 μg/ml) at 37 °C for 1 h before inoculation. Cells were subjected to immunofluorescence staining at 24 h post-inoculation. The mean percentage of HCV-positive cells relative to LPL-untreated medium is shown with the standard deviation (n=3). There was no statistically significant difference observed (Student's *t*-test): NS $p>0.01$. e. Orlistat (25 μg/ml) was added just before HuH7.5 cells were inoculated with the HCV-bearing medium pretreated with LPL (10 μg/ml). Cells were subjected to immunofluorescence staining at 24 h post-inoculation. The mean percentage of HCV-positive cells relative to LPL-untreated medium is shown with the standard deviation (n=3). Statistically significant differences are indicated by asterisks (Student's *t*-test): *$p<0.001$. f. SeV, whose genome contains the gene coding Green Fluorescent Protein (GFP), was pretreated with bovine LPL (•) or heat-inactivated LPL (□) (Fig. 2b) at 37 °C for 1 h before inoculation with HeLa cells. Expression of GFP in infected cells was observed under microscope at 24 h post-inoculation. The mean percentage of SeV-positive cells relative to LPL-untreated medium is shown with the standard deviation (n=3). LPL did not significantly affect the infectivity of SeV ($p>0.01$).

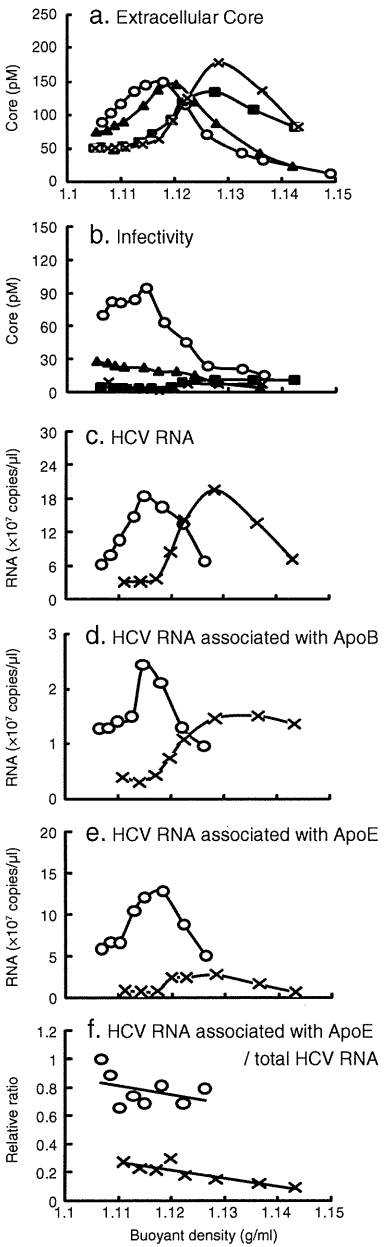

of HCV RNA in the complex associating with ApoE from LPL-treated sample was remarkably reduced (Fig. 2e). Thus, it is indicated that HCV is associated with both ApoB and ApoE but that the association with ApoE is more closely related to HCV infectivity than that with ApoB.

The ratio of HCV RNA in the complex associating with ApoE to the total HCV RNA was dramatically lower in LPL-treated samples than in PBS-treated samples (Fig. 2f). HCV with the same buoyant density showed a different ratio of the association with ApoE between LPL-treated and -untreated samples (Fig. 2f). It is indicated that HCV with the same buoyant density might have heterogeneous characteristics, especially in the association with ApoE. Though LPL affects the buoyant density of HCV, buoyant density may not become a direct indicator of HCV infectivity.

LPL and HTGL reduced HCV infectivity

Generally, two successive lipolytic steps, sequentially catalyzed by LPL and HTGL, convert VLDL through IDL to LDL (Braun and Severson, 1992; Connelly, 1999; Mead et al., 2002; S.-Fojo et al., 2004). Hepatocytes produce HTGL but not LPL (Braun and Severson, 1992; Connelly, 1999). If HuH7.5 cells produce HTGL into culture medium, addition of LPL to the HCV-bearing medium from HuH7.5 cells would lead to two successive lipolytic actions by exogenous LPL and endogeneous HTGL. To analyze this possibility, we examined HTGL expression in HuH7.5 cells. Expression of LPL mRNA in hepatocyte-derived cell lines, HuH7.5 and HepG2, was lower compared to that in the 293T cell line derived from kidney (Fig. 3a). We observed higher expression of HTGL mRNA in HuH7.5 and HepG than in 293T (Fig. 3a). HTGL activity was detected in medium from HuH7.5 cells, which was higher than that in medium from 293T cells (Fig. 3b) and showed good agreement to the level of mRNA (Fig. 3a), though HTGL activity was not detected in medium from HepG2 cells.

Then, to evaluate the role of HTGL on LPL-induced reduction of HCV infectivity, the HCV-bearing medium was incubated with LPL in the presence of a neutralizing antibody against HTGL and infectivity was measured. Since LPL activity itself was not affected by the anti-HTGL antibody treatment (data not shown), we expected that HCV-associated lipoprotein should be protected against HTGL in the presence of the anti-HTGL antibody. In fact, LPL-induced reduction in HCV infectivity was partly suppressed by the presence of the anti-HTGL antibody (Fig. 3c). The infectivity was not fully restored after treatment with the anti-HTGL antibody from the LPL-induced suppressive status, which indicates that HTGL plays a partial role in the LPL effect but that LPL also plays a role. This result implied that two lipases could reduce HCV infectivity through changing the lipoprotein-like structure and that, conversely, infectivity of HCV was regulated by the lipoprotein-like structure that associated with HCV.

HTGL reduced HCV infectivity through its catalytic activity, irrespective of LPL activity

To confirm the reductive effect of HTGL on HCV infectivity, the endogenous expression of HTGL was suppressed by siRNA specific to

Fig. 2. Shift of buoyant density of HCV as well as detachment of ApoE by LPL treatment. The HCV-bearing medium treated with PBS or LPL was subjected to centrifugation in an iodixanol gradient. After ultracentrifugation, aliquots of 30 consecutive fractions were collected and analyzed for (a) Core, (b) infectivity, (c) HCV RNA, and HCV RNA in (d) ApoB-associated and (e) ApoE-associated complexes. For a and b, PBS (○), 5 (▲), 50 (■), and 500 (×) μg/ml of LPL-treated samples, and for c–f, PBS (○) and 500 (×) μg/ml of LPL-treated samples were subjected. a. Core in each fraction was measured by ELISA (Ortho Clinical Diagnostics). b. HuH7.5 cells were inoculated with aliquots of each fraction for 2 h. Core ELISA of the culture medium was performed at 24 h post-inoculation. c. RNA was extracted from each fraction and subjected to cDNA synthesis followed by quantitative PCR. d. Measurement of HCV RNA in the complexes associated with ApoB. e. Measurement of HCV RNA in the complexes associated with ApoE. f. Ratio of HCV RNA in the complexes associated with ApoE versus the total HCV RNA in each fraction. The values were obtained by dividing the amounts of RNA of Fig. 3e by those of Fig. 3c.

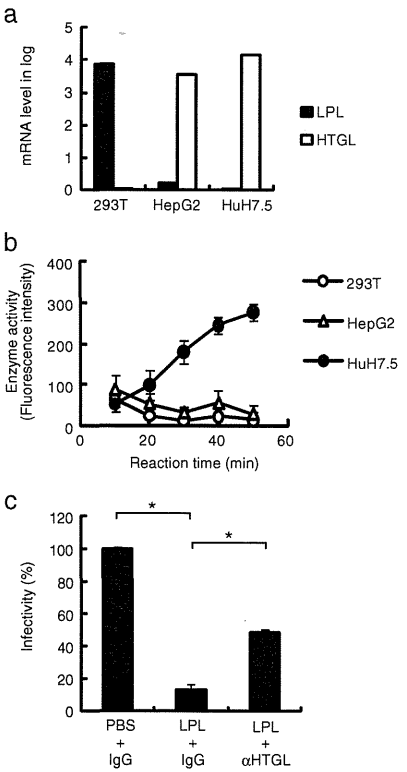

Fig. 3. Treatment of the HCV-bearing medium with exogenous LPL led to subsequent digestion by endogenously produced HTGL, resulting in loss of HCV infectivity. a. Expression of LPL and HTGL in HuH7.5, HepG2 and 293T cells. The mean of LPL mRNA expression level in 293T cells relative to the level in HuH7.5 cells is shown with standard deviation (n=3) and vice versa for HTGL (n=3). b. Validation of HTGL activity. The culture medium from HuH7.5, HepG2 and 293T cells was concentrated to 20 times using centricon YM-30 (Millipore), and was analyzed for HTGL activity. The mean and standard deviation are shown (n=3). c. The HCV-bearing medium was incubated with anti-HTGL antibody before LPL treatment. HuH7.5 cells were inoculated with the medium and then subjected to immunofluorescence staining at 24 h post-inoculation. The mean percentage of HCV-positive cells relative to medium incubated with PBS and IgG is shown with the standard deviation (n=3). Statistically significant differences are indicated by asterisks (Student's *t*-test): $^*p<0.001$.

HTGL (Fig. 4a). The level of HTGL mRNA in cells transfected with siRNA targeting HTGL was lower than one 6th of the control cells transfected with non-target siRNA (Fig. 4a). The activity of secreted HTGL was slightly lower in HTGL knockdown cells than the control (Fir. 4b). It may be because HTGL is so stable at protein level that its activity remains 48 h after transfection of siRNA. The presence of infectious HCV in the cells as well as the amounts of Core secreted into the culture medium was not significantly different between HTGL knockdown cells and the control (Fig. 4a). ApoB and ApoE were secreted at the same level from HTGL knockdown cells and the control cells (Fig. 4c). These results indicate that HTGL knockdown did not affect the production of either HCV or lipoproteins. Interestingly, the infectivity of the culture medium was about 2 folds higher than that in culture medium from control cells (Fig. 4a). The HCV-bearing medium from HTGL knockdown cells was ultracentrifuged through iodixanol gradients. We collected 80 fractions from the gradients and analyzed for Core. The Core peak was shifted to a lower buoyant density in the medium from HTGL knockdown cells compared to the control (Fig. 4d). Thus, HTGL could hydrolyze HCV-associated lipoproteins in the medium derived from HuH7.5 cells irrespective of LPL, leading to a reduction of infectivity.

Discussion

Our results indicate that bovine LPL reduced HCV infectivity through its catalytic activity. Since the same doses of LPL did not impair the infectivity of SeV (Fig. 1f), it is likely that HCV-associated lipoprotein is targeted by the LPL and that the lipoprotein associating with HCV plays a pivotal role in HCV infectivity. Previously, it was shown that LPL-Ps disrupted HCV (Thomssen and Bonk, 2002) and that bovine LPL suppressed HCV infectivity through uncertain mechanisms within cells after bridging HCV with cells by bovine LPL (Andréo et al., 2007). We detected Core and HCV RNA from the LPL-treated HCV-bearing medium almost at the same level as the untreated medium (Figs. 2a and c). Thus, bovine LPL at the concentration used in this study did not destroy the HCV structure as reported by LPL-Ps (Thomssen and Bonk, 2002). LPL seems to have at least two distinct functions to reduce HCV infectivity; one is through its de-lipidation activity observed here and another is its suppressive activity observed after being associated with cells (Andréo et al., 2007). We used an LPL inhibitor, orlistat, to delineate these two suppressive functions of LPL on HCV. After incubation of the HCV-bearing medium with LPL at a concentration of 10 μg/ml, orlistat was added so that catalytic activity of LPL could be suppressed upon contact of HCV with cells. HCV infectivity was significantly reduced even under this condition (Fig. 1e). This result indicates that de-lipidation by LPL is a major cause of HCV inactivation. However, it is worth mentioning that the residual infectivity was higher than that observed in the conditions of infection assay conducted without orlistat (Fig. 1e, compare the lane with the same dose (10 μg/ml) of LPL in Fig. 1a), which indicates the presence of another inactivating mechanism suggested by Andréo et al. (2007) though the contribution is not as high.

The experiments using neutralizing antibody against HTGL (Fig. 3c) indicated that both LPL and HTGL have some roles in LPL-induced reduction in HCV infectivity. Knockdown of HTGL resulted in HCV with higher infectivity and a lower density in the medium (Figs. 4a and d). HTGL is the predominant enzyme in the lipolysis of IDL, but also hydrolyzes TG in all lipoproteins to some extent (Connelly, 1999). Thus, it is suggested that endogenous HTGL has lipolytic activity on HCV-associated lipoprotein irrespective to LPL functions. Taking account of the effect of LPL and HTGL on HCV infectivity, their expression is disadvantageous for HCV. There were not much differences in expressions of LPL and HTGL between HuH7.5 cells and HepG2 cells (Fig. 3a), suggesting that expression of lipases does not explain HuH7.5 as an excellent cell line for HCV.

Our study shows that LPL and/or HTGL change(s) the nature of HCV-associated lipoproteins, leading to reduced HCV infectivity. This indicates that the association of HCV with certain lipoprotein-like VLDL is important for HCV infectivity. Recently, ApoE was shown to be important for HCV infectivity as a ligand of the HCV receptor (Owen et al., 2009). It is conceivable that the reduction of ApoE in accordance to lipolysis of HCV associating lipoproteins is a direct cause of the reduction of HCV infectivity.

We used bovine LPL at 2–20 μg/ml to reduce HCV infectivity (Fig. 1a). It is expected that the same doses of human LPL could reduce HCV infectivity. However, heparin-treated human plasma contains around 100 ng/ml of LPL; most of LPL is bound to heparan sulfate proteoglycan (HSPG) at the cell surface and

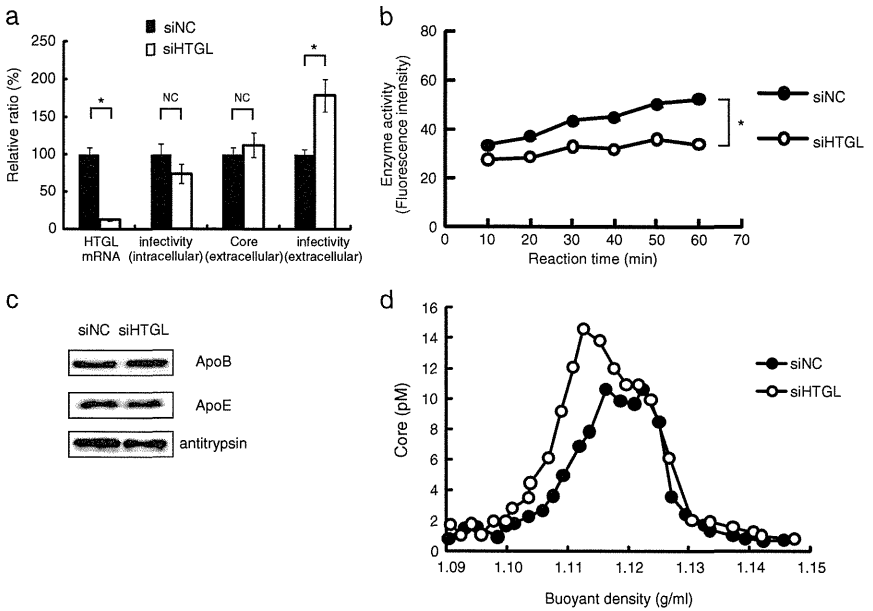

Fig. 4. HCV with higher infectivity and a lower buoyant density in the medium from HTGL knockdown cells. a. HTGL mRNA, infectivity of HCV within cells, extracellular Core and infectivity of HCV in the medium are shown. The mean percentages relative to control cells are shown with the standard deviation (mRNA, Core; n=3, infectivity; n=5). Statistically significant differences in HTGL mRNA level and extracellular infectivity are indicated by asterisks (Student's *t*-test): $^*p<0.001$. There was no statistically significant difference in intracellular infectivity and extracellular core (Student's *t*-test): NS $p>0.01$. b. Activities of HTGL were determined. After secretion, most of the HTGL is bound to heparan sulfate proteoglycans (HSPG) at the cell surface (Connelly, 1999; S.-Fojo et al., 2004). Both HTGLs bound and unbound to HSPG are expected to act on lipoproteins in the medium. Thus, in order to evaluate activities of HTGL acting on lipoproteins in the medium, heparin (10 U/ml) was added to the medium to release HTGL bound to HSPG at 24 h post-transfection of siRNA. The medium was harvested at 48 h post-transfection, passed through 0.45 μm filter (Iwaki) to eliminate cell debris and used for the assay. Statistically significant difference in HTGL activity at 60 min is indicated by asterisks (Student's *t*-test): $^*p<0.001$. c. Detection of apolipoproteins (ApoB and ApoE) and α-1 antitrypsin as standard secreted in culture medium from HTGL knockdown cells and control cells. d. Buoyant density of HCV produced from HTGL knockdown cells. The HCV-bearing medium from HTGL knockdown cells was subjected to centrifugation in an iodixanol gradient. After ultracentrifugation, aliquots of 80 consecutive fractions were collected and analyzed for Core by ELISA. The data are presented from 25 fractions around Core peak from a single representative experiment of three experiments. There was a significant difference in the buoyant density of the Core peak between HTGL knockdown cells and the control (Student's *t*-test, $p<0.001$).

heparin leads to a release of LPL bound to HSPG (Kern et al., 1990). Therefore, it is conceivable that HCV infectivity could be reduced through activities of LPL in the circulation at a lesser efficiency than observed in this work. Here, we demonstrated that the hydrolyzing activity of HTGL as well as LPL affects HCV infectivity. Considering this lipase-induced reduction in HCV infectivity in the circulation, it is important for virus to infect the proximal hepatocytes before entering circulation. In other words, the activities of LPL and/or HTGL may be one host mechanism to resist invasion and spread of HCV.

Materials and methods

Cell culture

HuH7.5, HeLa, 293T and HepG2 cells were maintained in DMEM supplemented with 10% FBS, 100 U/ml penicillin and 100 μg/ml streptomycin.

Virus source

HuH7.5 cells were transfected with HCV 2a strain, JFH1 RNA genome and maintained in DMEM supplemented with 10% FBS, 100 U/ml penicillin and 100 μg/ml streptomycin. Three days before harvest, medium was replaced with Opti-Pro (Invitrogen) supplemented with 0.1% BSA. Culture medium was filtered with 0.45 μm filter (Iwaki) and used as virus source (the HCV-bearing medium).

HCV infectivity

To determine HCV infectivity in the medium, HuH7.5 cells were inoculated with the HCV-bearing medium (MOI of 0.5) at 37 °C for 2 h. Cells were washed with PBS and incubated in DMEM supplemented with 10% FBS, 100 U/ml penicillin and 100 μg/ml streptomycin. Cells were fixed at 24 h post-inoculation and subjected to immunofluorescence staining using serum from a HCV-positive individual to detect HCV-infected cells. Three to five fields under microscope were randomly selected. Cells in a field were counted and the percentage of HCV-positive cells to total cells (around 500–1000) was calculated.

To determine HCV infectivity within cells, cells were collected by trypsinization. After washing with PBS, cells were incubated with water and passed through a 27-gauge needle (Terumo) at ten times. After centrifugation, supernatant was passed through a 0.45 μm filter (Iwaki) and inoculated to HuH7.5 cells. Immunofluorescence staining was performed as mentioned above.

Lipase activity

Total lipase test (Progen) and hepatic lipase select test (Progen) were used to examine LPL activity and HTGL activity, respectively, according to the manufacturer's protocol.

Iodixanol density gradients

The HCV-bearing medium was concentrated around 50 times using amicon ultra-15 100k (Millipore) and treated with PBS or 5, 50, or 500 μg/ml of LPL at 37 °C for 1 h. The samples were applied to the top of a linear gradient formed from 17–37% iodixanol-containing PBS and spun at 36,000 rpm for 18 h at 4 °C using a SRP 41 Hitachi Ultracentrifuge rotor. Aliquots of 30 consecutive fractions were collected and used for analyses of Core, infectivity, HCV RNA, and immunoprecipitation with anti-ApoB or anti-ApoE antibodies.

For analysis of the HCV-bearing medium from HTGL knockdown cells, the concentrated samples were applied to the top of a gradient from 14–54% iodixanol-containing PBS and spun at 34,000 rpm for 20 h at 4 °C. A total of 80 consecutive fractions were collected and used for analyses of Core.

Quantification of HCV RNA

RNA was extracted from fractions of the iodixanol gradient using an RNeasy mini kit (Qiagen). Complementary DNA was prepared by incubating RNA with SuperScript III (Invitrogen) and 737R primer, a reverse RNA primer of HCV genome (Sugiyama et al., 2009). Quantitative PCR analysis was performed by 7500 Fast Real Time PCR System (Applied Biosystems). Taqman probe and primers were as follows: probe 733FB (Sugiyama et al., 2009), forward 5′-CCCTCCCGGGAGAGCCATAGTG-3′, reverse 5′-GTCTCGCGGGGGCACGCCCAAAT-3′. The copy number of HCV was determined by the standard-curve method with serial dilutions of the synthesized full-length HCV RNA.

Immunoprecipitation

Fractions from iodixanol gradient were incubated with anti-ApoB antibody (Biodesign International) or anti-ApoE antibody (Chemicon International) for 2 h at room temperature. Protein G sepharose (GE) was added and the immunocomplex was collected by centrifugation. The pellets were used for RNA extraction.

Expression of LPL and HTGL

RNA was extracted from cells using RNeasy mini kit (Qiagen). Complementary DNA was prepared by incubating RNA with SuperScript III (Invitrogen) and oligo(dT) as an universal primer. Quantitative PCR analysis was performed with primers specific for LPL (Lindegaard et al., 2005), for HTGL (Sirvent et al., 2004), and for GAPDH (Suzuki et al., 2008). The LPL and HTGL mRNA expression level was calibrated with the level of GAPDH mRNA expression.

Neutralization of HTGL

The HCV-bearing medium was incubated with IgG rabbit (Santa Cruz) or anti-HTGL antibody (sc-21007, Santa Cruz) at 4 °C overnight, followed by PBS or LPL treatment at 37 °C for 1 h. HuH7.5 cells were inoculated with the medium at 37 °C for 2 h and subjected to immunofluorescence staining as explained above.

Knockdown of HTGL

siRNA (siGENOME SMART pool M-008743-00-0005, Thermo) at a final concentration of 40 nM was transfected with HuH7.5 cells using siLentFect reagent (Bio-Rad). The HCV-bearing medium (MOI = 0.5) was inoculated with cells at 4 h post-transfection. Then, fresh medium was replaced 2 h later. At 24 h post-transfection, medium was replaced with Opti-pro (Invitrogen) supplemented with 0.1% BSA. At 48 h post-transfection, culture medium and cells were used for analyses of RNA, infectivity, Western blotting and buoyant density.

Western blotting

Western blotting was performed using anti-ApoB antibody (Biodesign International), anti-ApoE antibody (Innogenetics) and anti-α-1 antitrypsin antibody (Biodesign). Detection was carried out using ECL plus reagent (GE).

Supplementary materials related to this article can be found online at doi:10.1016/j.virol.2010.08.011.

Acknowledgments

We are grateful to Drs. T. Wakita and C. Rice for their kind gifts of JFH1 and HuH7.5 cells, respectively. We thank H. Kato, R. Shiina, E. Sugawara, R. Tobita, and H. Yamamoto (Chiba Institute of Technology) for their technical assistance. This study was supported by Grants-in-Aid for Scientific Research from the Ministry of Health, Labor, and Welfare of Japan and from the Ministry of Education, Culture, Sports, Science, and Technology.

References

André, P., K.-Pradel, F., Deforges, S., Perret, M., Berland, J.L., Sodoyer, M., Pol, S., Bréchot, C., P.-Baccalà, G., Lotteau, V., 2002. Characterization of low- and very-low-density hepatitis C virus RNA-containing particles. J. Virol. 76, 6919–6928.

Andréo, U., Maillard, P., Kalinina, O., Walic, M., Meurs, E., Martinot, M., Marcellin, P., Budkowska, A., 2007. Lipoprotein lipase mediates hepatitis C virus (HCV) cell entry and inhibit HCV infection. Cell. Microbiol. 9, 2445–2456.

Braun, J.E.A., Severson, D.L., 1992. Regulation of the synthesis, processing and translocation of lipoprotein lipase. Biochem. J. 287, 337–347.

Chang, K.-S., Jiang, J., Cai, Z., Luo, G., 2007. Human apolipoprotien E is required for infectivity and production of hepatitis C virus in cell culture. J. Virol. 81, 13783–13793.

Connelly, P.W., 1999. The role of hepatic lipase in lipoprotein metabolism. Clin. Chim. Acta 286, 243–255.

Gastaminza, P., Cheng, G., Wieland, S., Zhong, J., Liao, W., Chisari, F.V., 2008. Cellular determinants of hepatitis C virus assembly, maturation, degradation, and secretion. J. Viol. 82, 2120–2129.

Huang, H., Son, F., Owen, D.M., Li, W., Chen, Y., Gale Jr., M., Ye, J., 2007. Hepatits C virus production by human hepatocytes dependent on assembly and secretion of very low-density lipoprotein. Proc. Natl Acad. Sci. 104, 5848–5853.

Icard, V., Diaz, O., Scholtes, C., P.-Cocon, L., Ramière, C., Bartenschlager, R., Penin, F., Lotteau, V., André, P., 2009. Secretion of hepatitis C virus envelope glycoproteins depends on assembly of apolipoprotein B positive lipoproteins. PLoS ONE 4, e4233.

Jiang, J., Luo, G., 2009. Apolipoprotein E but not B is required for the formation of infectious hepatitis C virus particles. J. Virol. 83, 12680–12691.

Kern, P.A., Martin, R.A., Carty, J., Goldberg, I.J., Ong, J.M., 1990. Identification of lipoprotein lipase immunoreactive protein in pre- and posthepain plasma from normal subjects and patients with type I hyperlipoproteinemia. J. Lipid Res. 31, 17–26.

Lindegaard, M.L.S., Olivecrona, G., Christoffersen, C., Kratky, D., Hannibal, J., Petersen, B.L., Zechner, R., Damm, P., Nielsen, L.B., 2005. Endothelial and lipoprotein lipases in human and mouse placenta. J. Lipid Res. 46, 2339–2346.

Mead, J.L., Irvine, S.A., Ramji, D.P., 2002. Lipoprotein lipase: structure, function, regulation, and role in disease. J. Mol. Med. 80, 753–769.

Olofsson, S.-O., Borèn, J., 2005. Apolipoprotein B: a clinically important apolipoprotein which assembles atherogenic lipoproteins and promotes the development of atherosclerosis. J. Intern. Med. 258, 395–410.

Owen, D.M., Huang, H., Ye, J., Gale Jr., M., 2009. Apolipoprotein E on hepatitis C virion facilitates infection through interaction with low-density lipoprotein receptor. Virology 394, 99–108.

S.-Fojo, S., G.-Navarro, H., Freeman, L., Wagner, E., Nong, Z., 2004. Hepatic lipase, lipoprotein metabolism, and atherogenesis. Arterioscler. Thromb. Vasc. Biol. 24, 1750–1754.

Sirvent, A., Verhoeven, A.J.M., Jansen, H., Kosykh, V., Darteil, R.J., Hum, D.W., Fruchart, J.-C., Staels, B., 2004. Farnesoid X receptor represses hepatic lipase gene expression. J. Lipid Res. 45, 2110–2115.

Sugiyama, K., Suzuki, K., Nakazawa, T., Funami, K., Hishiki, T., Ogawa, K., Saito, S., Shimotohno, K.W., Suzuki, T., Shimizu, Y., Tobiba, R., Hijikata, M., Takaku, H., Shimotohno, K., 2009. Genetic analysis of Hepatitis C virus with defective genome and its infectivity in vitro. J. Virol. 83, 6922–6928.

Suzuki, K., Nakamura, K., Iwata, Y., Sekine, Y., Kawai, M., Sugihara, G., Tsuchiya, K.J., Suda, S., Matsuzaki, H., Takei, N., Hashimoto, K., Mori, N., 2008. Decreased expression of reelin receptor VLDLR in peripheral lymphocytes of drug-naïve schizophrenic patients. Schizophrenia Res. 98, 148–156.

Thomssen, R., Bonk, S., Propfe, C., Heermann, K.-H., Köchel, H.G., Uy, A., 1992. Association of hepatitis C virus in human sera with b-lipoprotein. Med. Microbiol. Immunol. 181, 293–300.

Thomssen, R., Bonk, S., Thiele, A., 1993. Density heterogeneities of hepatitis C virus in human sera due to the binding of β-lipoproteins and immunoglobulins. Med. Microbiol. Immunol. 182, 329–334.

Thomssen, R., Bonk, S., 2002. Virolytic action of lipoprotein lipase on hepatitis C virus in human sera. Med. Microbiol. Immunol. 191, 17–24.

JOURNAL OF VIROLOGY, Nov. 2010, p. 11761–11770
0022-538X/10/$12.00 doi:10.1128/JVI.00638-10

Vol. 84, No. 22

Sphingomyelin Activates Hepatitis C Virus RNA Polymerase in a Genotype-Specific Manner▽†

Leiyun Weng,[1] Yuichi Hirata,[2] Masaaki Arai,[3] Michinori Kohara,[2] Takaji Wakita,[4] Koichi Watashi,[4,5] Kunitada Shimotohno,[5,6] Ying He,[7] Jin Zhong,[7] and Tetsuya Toyoda[1]*

Units of Viral Genome Regulation[1] and Viral Hepatitis,[7] Institut Pasteur of Shanghai, Key Laboratory of Molecular Virology and Immunology, Chinese Academy of Sciences, 411 Hefei Road, 200025 Shanghai, People's Republic of China; Department of Microbiology and Cell Biology, Tokyo Metropolitan Institute of Medical Biology, 3-18-22 Honkomagome, Bunkyo-Ku, Tokyo 113-8613, Japan[2]; Pharmacology Laboratory, Pharmacology Department V, Mitsubishi Tanabe Pharma Corporation, 1000 Kamoshida-cho, Aoba-ku, Yokohama 227-0033, Japan[3]; Department of Virology II, National Institute of Health, 1-23-1 Toyama, Shinjuku, Tokyo 132-8640, Japan[4]; Laboratory of Human Tumor Viruses, Department of Viral Oncology, Institute for Virus Research, Kyoto University, Kyoto 606-8507, Japan[5]; and Chiba Institute of Technology, 2-17-1 Tsudamuna, Narashino, Chiba 275-0016, Japan[6]

Received 25 March 2010/Accepted 27 August 2010

Hepatitis C virus (HCV) replication and infection depend on the lipid components of the cell, and replication is inhibited by inhibitors of sphingomyelin biosynthesis. We found that sphingomyelin bound to and activated genotype 1b RNA-dependent RNA polymerase (RdRp) by enhancing its template binding activity. Sphingomyelin also bound to 1a and JFH1 (genotype 2a) RdRps but did not activate them. Sphingomyelin did not bind to or activate J6CF (2a) RdRp. The sphingomyelin binding domain (SBD) of HCV RdRp was mapped to the helix-turn-helix structure (residues 231 to 260), which was essential for sphingomyelin binding and activation. Helix structures (residues 231 to 241 and 247 to 260) are important for RdRp activation, and 238S and 248E are important for maintaining the helix structures for template binding and RdRp activation by sphingomyelin. 241Q in helix 1 and the negatively charged 244D at the apex of the turn are important for sphingomyelin binding. Both amino acids are on the surface of the RdRp molecule. The polarity of the phosphocholine of sphingomyelin is important for HCV RdRp activation. However, phosphocholine did not activate RdRp. Twenty sphingomyelin molecules activated one RdRp molecule. The biochemical effect of sphingomyelin on HCV RdRp activity was virologically confirmed by the HCV replicon system. We also found that the SBD was the lipid raft membrane localization domain of HCV NS5B because JFH1 (2a) replicon cells harboring NS5B with the mutation A242C/S244D moved to the lipid raft while the wild type did not localize there. This agreed with the myriocin sensitivity of the mutant replicon. This sphingomyelin interaction is a target for HCV infection because most HCV RdRps have 241Q.

Hepatitis C virus (HCV) has a positive-stranded RNA genome and belongs to the family *Flaviviridae* (21). HCV chronically infects more than 130 million people worldwide (34), and HCV infection often induces liver cirrhosis and hepatocellular carcinoma (19, 28). To date, pegylated interferon (PEG-IFN) and ribavirin are the standard treatments for HCV infection. However, many patients cannot tolerate their serious side effects. Therefore, the development of new and safer therapeutic methods with better efficacy is urgently needed.

Lipids play important roles in HCV infection and replication. For example, the HCV core associates with lipid droplets and recruits nonstructural proteins and replication complexes to lipid droplet-associated membranes which are involved in the production of infectious virus particles (24). HCV RNA replication depends on viral protein association with raft membranes (2, 30). The association of cholesterol and sphingolipid with HCV particles is also important for virion maturation and infectivity (3). The inhibitors of the sphingolipid biosynthetic pathway, ISP-1 and HPA-12, which specifically inhibit serine palmitoyltransferase (SPT) (23) and ceramide trafficking from the endoplasmic reticulum (ER) to the Golgi apparatus (37), suppress HCV virus production in cell culture but not viral RNA replication by the JFH1 replicon (3). Other serine SPT inhibitors (myriocin and NA255) inhibit genotype 1b replication (4, 29, 33). Very-low-density lipoprotein (VLDL) also interacts with the HCV virion (15).

Sakamoto et al. reported that sphingomyelin bound to HCV RNA-dependent polymerase (RdRp) at the sphingomyelin binding domain (SBD; amino acids 230 to 263 of RdRp) to recruit HCV RdRp on the lipid rafts, where the HCV complex assembles, and that NA255 suppressed HCV replication by releasing HCV RdRp from the lipid rafts (29). In the present study, we analyzed the effect of sphingomyelin on HCV RdRp activity *in vitro* and found that sphingomyelin activated HCV RdRp activity in a genotype-specific manner. We also determined the sphingomyelin activation domain and the activation mechanism. Finally, we confirmed our biochemical data by a HCV replicon system.

* Corresponding author. Mailing address: Unit of Viral Genome Regulation, Institut Pasteur of Shanghai, Chinese Academy of Sciences, 411 Hefei Road, 200025 Shanghai, People's Republic of China. Phone and fax: 86 21 6385 1621. E-mail: ttoyoda@amber.plala.or.jp.

† Supplemental material for this article may be found at http://jvi.asm.org.

▽ Published ahead of print on 15 September 2010.

MATERIALS AND METHODS

HCV RNA polymerase. A C-terminal 21-amino-acid deletion was made to the HCV RdRps of strains HCR6 (genotype 1b) (36), NN (1b) (35), Con1 (1b) (5), JFH1 (2a) (36), J6CF (2a) (25), H77 (1a) (7), and RMT (1a), and the mutants were purified from bacteria as described previously (36). HCR6 (1b) RdRp with the mutation L245A [RdRp(L245A)] or I253A [RdRp(I253A)] or the double mutation L245A and I253A [RdRp(L245A/I253A)]; JFH1 (2a) RdRp with the mutation(s) A242C/S244D, A242, S244D, or T251Q; J6CF (2a) RdRp with the mutation(s) R241Q, S244D, or R241Q/S244D; and H77 (1a) RdRp(A238S/Q248E) were introduced using an *in vitro* mutagenesis kit (Stratagene) and the oligonucleotides listed in Table S1 in the supplemental material. HCR6 (1b) His_6-tagged RdRp(L245A/I253A) was removed from pET21b/KM (36) and cloned into the BamHI/XhoI site of pGEX-6P-3 (GE), resulting in pGEXHCVHCR6RdRp(L245A/I253A).

***In vitro* HCV transcription.** *In vitro* HCV transcription was performed as described previously (36). Briefly, following 30 min of preincubation without ATP, CTP, or UTP, 100 nM HCV RdRp was incubated in 50 mM Tris-HCl (pH 8.0), 200 mM monopotassium glutamate, 3.5 mM $MnCl_2$, 1 mM dithiothreitol (DTT), 0.5 mM GTP, 50 μM ATP, 50 μM CTP, 5 μM [α-^{32}P]UTP, 200 nM RNA template (SL12-1S), 100 U/ml human placental RNase inhibitor, and the lipid (amount indicated below) at 29°C for 90 min. ^{32}P-labeled RNA products were subjected to 6% polyacrylamide gel electrophoresis (PAGE) containing 8 M urea. The resulting autoradiograph was analyzed with a Typhoon Trio plus image analyzer (GE).

RNA filter binding assay. An RNA filter binding assay was performed as described previously (36). Briefly, 100 nM HCV RdRp and 100 nM ^{32}P-labeled RNA template (SL12-1S) were incubated with or without 0.01 mg/ml egg yolk sphingomyelin in 25 μl of 50 mM Tris-HCl (pH 7.5), 200 mM monopotassium glutamate, 3.5 mM $MnCl_2$, and 1 mM DTT at 29°C for 30 min. After incubation, the solutions were diluted with 0.5 ml of TE (50 mM Tris-HCl [pH 7.5], 1 mM EDTA) buffer and filtered through nitrocellulose membranes (0.45-μm pore size; Millipore). The filter was washed five times with TE buffer, and the bound radioisotope was analyzed by Typhoon Trio plus after being dried.

Enzyme-linked immunosorbent assay (ELISA). Ninety-six-well microtiter plates (Corning) were coated with 250 ng of egg yolk sphingomyelin in ethanol by evaporation at room temperature. After the wells were blocked with phosphate-buffered saline (PBS) and 3% bovine serum albumin (BSA), they were incubated with 1 pmol of the HCV RdRp of HCR6 (1b) wild type (wt) or L245A, I253A, or L245A/I253A mutant; NN (1b); H77 (1a); RMT (1a); J6CF (2a); or JFH1 (2a) wt or A242C/S244D, A242, S244D, or T251Q mutant in Tris-buffered saline (50 mM Tris-HCl [pH 7.5] and 150 mM NaCl) for 1.5 h at room temperature. After being blocked with 3% BSA, the bound HCV RdRp was detected by adding rabbit anti-HCV RdRp serum (1:5,000) (see Fig. S1 in the supplemental material) (17) before incubation with a horseradish peroxidase (HRP)-conjugated anti-rabbit IgG antibody (1:5,000; Southern Biotech). The optical density at 450 nm (OD_{450}) was measured with a Spectra Max 190 spectrophotometer (Molecular Devices) using a TMB (3,3′,5,5′-tetramethylbenzidine) Liquid Substrate System (Sigma).

HCV subgenomic replicon. A D244S mutation was introduced into the HCV strain NN (1b) subgenomic replicon pLMH14 (35), resulting in pLMH(NN)5B(D244S) [where 5B(D244S) is the NS5B protein with the mutation D244S]. The A242C/S244D mutation was introduced into the HCV JFH1 (2a) replicon, pSGR-JFH1/luc (25), resulting in pSGR-JFH1/luc5B(A242C/S244D). The HpaI and XbaI fragment of pSGR-JFH1 (18) was replaced with that of pSGR-JFH1/luc5B(A242C/S244D), resulting in pSGR-JFH15B(A242C/S244D). The A238S/Q248E mutation was introduced into HCV H77 (1a) replicon pHCVrep13(S2204I)/Neo (7) after the neomycin gene was replaced by the firefly luciferase gene [pH77(I)/luc] by insertion of AflII and AscI sites (see Table S1 in the supplemental material), resulting in pH77(I)/luc5B(A238S/Q248E). Subgenomic replicon RNA was transcribed *in vitro* by T7 RNA polymerase using MegaScript (Ambion) after the replicon plasmids were linearized by XbaI (strain NN and JFH1 replicons) or HpaI (strain H77 replicon). Subgenomic replicon RNA was stored at −80°C after being purified by phenol-chloroform extraction and ethanol precipitation.

Replicon assay with myriocin. Huh7.5.1 cells were kindly provided by F. Chisari and were maintained in Dulbecco's modified Eagle's medium (DMEM; Gibco) with 10% fetal bovine serum (FBS; Gibco) (38). HCV replicon RNA (10 μg) was transfected into 4×10^6 Huh7.5.1 cells (1×10^7/ml) in OptiMEM I (Gibco) by electroporation (GenePulser Xcell; Bio-Rad) at 270 V, 100 Ω, and 950 μF. After transfection, the cells were plated in 12-well plates incubated in DMEM–10% FBS. At 6 h after transfection, cells were treated with 0, 5, and 50 nM myriocin. At 4, 54, and 78 h after transfection (48 and 72 h after myriocin treatment), the cells were harvested, and luciferase activity was measured using a Dual-Glo luciferase assay kit and a GloMax 96 Microplate Luminometer (Promega). Luciferase activity was normalized against the activity at 4 h after transfection (26).

HCV JFH1 wt and NS5B(A242C/S244D) replicon cells. Huh7/scr cells were kindly provided by F. Chisari of the Scripps Research Institute and were maintained in Dulbecco's modified Eagle's medium (Gibco) with 10% fetal bovine serum (Gibco). RNA (10 μg each) from SGR-JFH1 and SGR-JFH1 with the mutations A242C/S244D in NS5B [NS5B(A242C/S244D) was transfected into 4×10^6 Huh7/scr cells (1×10^7/ml) in OptiMEM I (GIBCO) by electroporation (GenePulser Xcell; Bio-Rad) at 270 V, 100 Ω, and 950 μF. After transfection, the cells were plated in 10-cm dishes and incubated in DMEM–10% FBS with 1.0 and 0.5 mg/ml G418 (Gibco). JFH1 wt and NS5B(A242C/S244D) replicon cells were maintained in DMEM–10% FBS and 0.5 mg/ml G418.

Membrane floating assay. JFH1 wt and NS5B(A242C/S244D) replicon cells were suspended in two packed cell volumes of hypotonic buffer (10 mM HEPES-NaOH [pH 7.6], 10 mM KCl, 1.5 mM $MgCl_2$, 2 mM DTT, and 1 tablet/25 ml of EDTA-free protease inhibitor cocktail tablets [Roche]) and disrupted by 30 strokes of homogenization in a Dounce homogenizer using a tight-fitting pestle at 4°C. After nuclei were removed by centrifugation at 2,000 rpm for 10 min at 4°C, the supernatant (postnuclear supernatant [PNS]) was treated with 1% Triton X-100 in TNE buffer (25 mM Tris-HCl [pH 7.6] 150 mM NaCl, 1 mM EDTA) for 30 min on ice. The lysates were supplemented with 40% sucrose and centrifuged at 38,000 rpm in a Beckman SW41 Ti rotor (Beckman Coulter) overlaid with 30% and 10% sucrose in TNE buffer at 4°C for 14 h.

Western blotting. Western blotting using anti-HCV RdRp (17), rabbit anti-NS3 (32), anti-NS5A (16) and anti-caveolin-2 was performed as previously published (17).

Reagent. Egg yolk sphingomyelin, cholesterol phosphocholine, myriocin, and rabbit anti-caveolin-2 antibodies were purchased from Sigma. Hexanoyl sphingomyelin, C_6-ceramide, C_8-β-D-glucosyl ceramide, and C_8-β-D-lactosyl ceramide were purchased from Avanti Polar Lipids. [α-^{32}P]UTP was purchased from New England Nuclear.

Statistical analysis. Significant differences were evaluated using *P* values calculated from a Student's *t* test.

Nucleotide sequence accession number. The sequence of HCV RMT has been deposited in the GenBank under accession number AB520610.

RESULTS

Sphingomyelin activation of HCV RNA polymerases of various genotypes. There are several sequence variations in the sphingomyelin binding domain (SBD; amino acids 231 to 260 of HCV RdRp) among HCV genotypes (see Fig. 7A). In order to compare the RdRps of different genotypes of HCV, we purified RdRp from genotypes 1b (strains HCR6, NN, and Con1), 1a (H77 and MRT), and 2a (JFH1 and J6CF) (see Fig. S2 in the supplemental material). First, the effect of ethanol on HCV HCR6 (1b) RdRp transcription was examined because lipids were suspended in ethanol before they were added to the HCV transcription reaction mixture. We found that 2% ethanol did not inhibit HCV transcription (see Fig. S3 in the supplemental material); therefore, all subsequent experiments were performed using less than 2% ethanol.

The kinetics of sphingomyelin activation were analyzed using egg yolk sphingomyelin for HCR6 (1b) RdRp wt (Fig. 1A) and subtype 2a (JFH1 and J6CF) RdRps (Fig. 1B), and *N*-hexanoyl-D-*erythro*-sphingosylphosphorylcholine (hexanoyl sphingomyelin) was used for HCR6 (1b) RdRp wt (Fig. 1C) and subtype 1a (H77 and RMT) RdRps (Fig. 1D). The egg yolk sphingomyelin activation curve of HCR6 (1b) RdRp wt at low concentrations (<0.01 mg/ml) was sigmoid. The transcription activity of HCR6 (1b) RdRp wt increased in a dose-dependent manner. It was activated 11-fold at 0.01 mg/ml and then plateaued (14-fold activation) at 0.1 mg/ml. However, JFH1 (2a) and J6CF (2a) RdRps were activated 2.5-fold and 2.2-fold, respectively, at 0.01 mg/ml sphingomyelin, at which point they plateaued.

Egg yolk sphingomyelin is a mixture. In order to obtain the optimal molar ratio for sphingomyelin activation of HCR6 (1b)

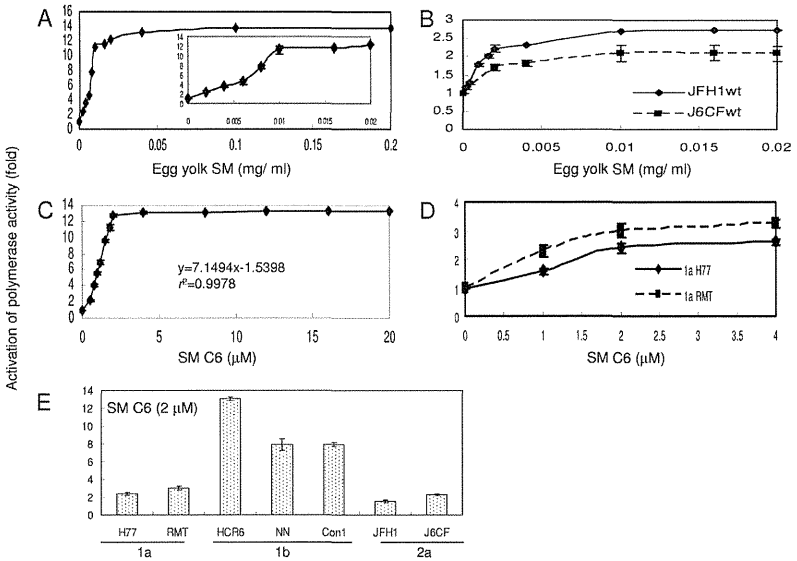

FIG. 1. Sphingomyelin activation of HCV RNA polymerases. (A) Activation kinetics of HCV HCR6 (1b) RdRp wt by egg yolk sphingomyelin (SM). The inset shows activation produced by 0 to 0.02 mg/ml egg yolk sphingomyelin. Activation kinetics of HCV 2a (JFH1 and J6CF) RdRps by egg yolk sphingomyelin (B) and of HCV HCR6 (1b) RdRp wt by hexanoyl sphingomyelin (SM C6) (C). In panel C, the first order of the graph was fitted by linear regression; the calculated equation is indicated in the graph. (D) Activation kinetics of HCV 1a (H77 and RMT) RdRps by hexanoyl sphingomyelin. (E) Activation effect of hexanoyl sphingomyelin on HCV RdRp of various genotypes. HCV RdRp (100 nM) was incubated with or without 2 μM SM C6. The names of the RdRps are indicated below the graph. Mean ± standard deviation of the activation ratio was calculated from three independent experiments.

RdRp wt, its activation kinetics were calculated using hexanoyl sphingomyelin (Fig. 1C, SM C6). The equation for the first-order ratio of hexanoyl sphingomyelin activation according to linear regression fitting was as follows: $y = 7.1494x - 1.5398$, where y is the activation ratio and x is the sphingomyelin concentration ($r^2 = 0.9978$). RdRp activation had almost plateaued at 2 μM hexanoyl sphingomyelin. The activation kinetics of JFH1 (2a) and J6CF (2a) RdRps in egg yolk sphingomyelin were biphasic and plateaued at 0.01 mg/ml. Those of RMT (1a) and H77 (1a) RdRps in hexanoyl sphingomyelin were also biphasic and plateaued at 2 μM. The curve of the first order was fitted by linear regression. The molar ratio of RdRp to hexanoyl sphingomyelin at its plateau was calculated as 1:20.

Because RdRp activation had almost plateaued at 2 μM hexanoyl sphingomyelin, we compared the effect of sphingomyelin on 100 M concentrations of RNA polymerases of the HCV 1a, 1b, and 2a genotypes using 2 μM hexanoyl sphingomyelin (Fig. 1E and Table 1).

Helix-turn-helix structure for sphingomyelin binding and activation. Sphingomyelin binds to the SBD peptide (see HCV SBD in Fig. 7) (29). Initially, we tested whether SBD was the sphingomyelin binding site in HCV RdRp by ELISA (Fig. 2A and Table 1). When the L245 and I253 residues of the SBD peptide were mutated to A, sphingomyelin binding activity was lost (29). We introduced the same mutations in HCV HCR6 (1b) RdRp and purified HCR6 (1b) RdRp with mutations L245A, I253A, and L245A/I253A. Because the C-terminal His-tagged HCR6 RdRp(L245A/I253A) was not soluble, it was solubilized by tagging of glutathione *S*-transferase (GST) sequence at the N terminus but lost polymerase activity. As the L245A/I253A mutant had lost its polymerase activity, polymerase activation was tested only for L245A and I253A (Fig. 2B and Table 1). These results confirmed that SBD located in the finger domain (residues 230E to 263G) successfully achieved sphingomyelin binding in HCV RdRp and that sphingomyelin did not bind to the SBD when the helix-turn-helix structure had been destroyed by the L245A or I253A mutation (29).

The sphingomyelin binding activities of genotype 1a and 2a RdRps were also tested (Fig. 2 and Table 1). Both JFH1 and J6CF were tested for genotype 2a because J6CF (2a) RdRp had an additional amino acid difference at position 241 in the SBD, and its sphingomyelin binding activity was very low (Fig. 2A and 7A; Table 1). J6CF (2a) RdRp(R241Q) showed the same sphingomyelin binding activity as HCR6 (1b) RdRp wt, indicating that 241Q was the critical amino acid for sphingomyelin binding. J6CF (2a) RdRp(S244D) and RdRp(R241Q/S244D) also showed higher sphingomyelin binding activity

TABLE 1. Summary of sphingomyelin activation of HCV RNA polymerase activities

Parameter	Value for the parameter by RdRp genotype, strain, and variant[a]																									
	1b									1a					2a											
	HCR6						NN	Con1	RMT	H77				J6CF					JFH1							
	wt	L245A	I253A	L245A/I253A	D244S	wt	wt	wt	wt	A238S/Q248E	wt	R241Q	S244D	R241Q/S244D	wt	A242C	S244D	A242C/S244D	T251Q
SM binding (%)[b]	100	24.3	30.8	15.5	78.7	93.4	117	144	86.7	82.5	19.3	118	53.1	80.2	70.4	75.5	93.1	92.4	80.7
Activation of polymerase (*n*-fold)[c]	13.0 (11.2)[d]	(2.8)[d]	(2.5)[d]	ND	3.6	7.9	7.9	3.0	2.0	8.1	2.3	4.3	5.6	3.4	1.6	1.0	3.1	4.4	1.8
Activation of RNA binding (*n*-fold)[e]	4.5	2.6	1.7	ND	1.9	ND	ND	ND	ND	1.4	3.3	1.5	3.6	3.2	1.7	1.3	ND	ND	1.4	ND

[a] Numbers were averaged from three independent experiments. ND, not done.
[b] Egg yolk sphingomyelin (SM; 250 ng) was used.
[c] Hexanoyl sphingomyelin (2 μM) was used.
[d] Egg yolk sphingomyelin (0.01 mg/ml) was used.

than the wt ($P < 0.001$) but lower binding than the R241Q mutant. However, S244D showed higher RdRp activation than R241Q ($P < 0.005$), while the RdRp activation ratio of the double mutant (R241Q/S244D) was lower than that of S244D or R241Q, although all of them activated RdRp with sphingomyelin ($P < 0.005$) (Fig. 2A and C and Table 1). For JFH1, when the JFH1 RdRp SBD was modified (A242C/S244D) to allow it to bind with more sphingomyelin than the wt ($P < 0.005$), the mutant JFH1 RdRp(A242C/S244D) was activated more than the wt by sphingomyelin ($P < 0.005$) (Fig. 2A and C; Table 1). The sphingomyelin binding activity of JFH1 RdRp(T251Q) was 80.7% of that of HCR6 (1b), and its activation ratio was 1.8-fold. These results agree that SBD is both the sphingomyelin activation and binding domain and that the domains for these two activities are somehow different.

We determined which amino acid, 242C or 244D, enhanced sphingomyelin binding by comparing HCR6 (1b) and JFH1 (2a) RdRps. Sphingomyelin binding of HCR6 (1b) RdRp(D244S) was 79% of that of the wt ($P < 0.005$) (Fig. 2A and Table 1), and its activation by sphingomyelin was only 3.6-fold (Fig. 2C and Table 1). The sphingomyelin binding of JFH1 (2a) RdRp(A242C) and RdRp(S244D) increased to 75.5% and 93.1%, respectively, of HCR6 (1b) RdRp wt (Fig. 2A and Table 1). This was significantly higher than that of JFH1 (2a) RdRp wt ($P < 0.005$), and the sphingomyelin activation of JFH1 (2a) RdRp(A242C) and RdRp(S244D) was increased 1.0-fold and 3.1-fold, respectively ($P < 0.005$) (Fig. 2C and Table 1). From these mutation analyses of the J6CF and JFH1 RdRps, we concluded that 244D enhanced sphingomyelin binding and RdRp activation.

HCV 1a RdRps were not activated even though sphingomyelin bound to them (Fig. 1E and 2A and Table 1). We then tried to elucidate the domains responsible for sphingomyelin activation. There are 14 amino acids (residues 19, 25, 81, 111, 120, 131, 184, 270, 272, 329, 436, 464, 487, and 540) unique to genotype 1a RdRp in the region of residues 1 to 570 and two amino acid differences unique to 1a RdRp in SBD, i.e., 238A and 248Q (see Fig. 6A). Initially, we focused on the SBD and introduced the A238S and Q248E mutations into the H77 (2a) RdRp SBD (Fig. 2A and D and Table 1). The sphingomyelin binding activity of H77 (2a) RdRp(A238S/Q248E) was similar to that of H77 (2a) RdRp wt. The sphingomyelin activation ratio of H77 (2a) RdRp(A238S/Q248E) was increased 8.1-fold, leading us to conclude that these mutations are essential to sphingomyelin activation.

Effect of lipids on HCV RNA polymerase activity. In order to elucidate the structure of the lipids involved in activation of HCV RdRp, D-lactosyl-β-1,1′-*N*-octanoyl-D-*erythro*-sphingosine [C_8-lactosyl(β) ceramide], D-glucosyl-β1-17-N-octanoyl-D-*erythro*-sphingosine (C_8-β-D-glucosyl ceramide), *N*-hexanoyl-D-*erythro*-sphingosine (C_6-ceramide), and cholesterol were tested for their abilities to activate RdRp. The relative polymerase activities of 100 nM HCV HCR6 (1b) RdRp activated with 0.01 mg/ml egg yolk sphingomyelin, 2 μM hexanoyl sphingomyelin, 8 μM C_8-lactosyl(β) ceramide, 12 μM C_8-β-D-glucosyl ceramide, 12 μM C_6-ceramide, and 0.02 mg/ml cholesterol were 11.2, 13.0, 5.66, 4.19, 1.12, and 2.25 of that without lipids, respectively (Fig. 3A). The amount of lipids that gave the maximum activation was calculated from the kinetics of the lipids bound to HCR6 (1b) and JFH1 (2a) RdRps (Fig. 3B and

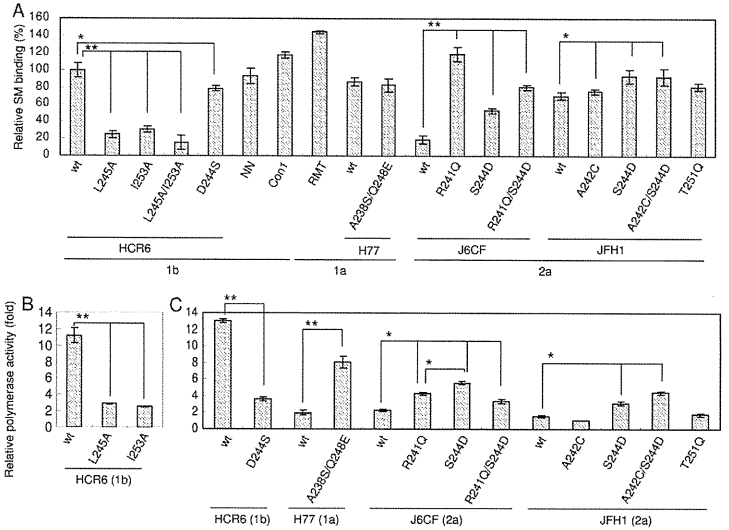

FIG. 2. Sphingomyelin binding and activation of HCV RNA polymerase sphingomyelin binding domain mutants. Names of RdRps are indicated below the graphs. (A) Egg yolk sphingomyelin (SM) binding activity relative to that of HCR6 (1b) RdRp wt. Mean ± standard deviation of the binding was calculated from three independent experiments. (B) Egg yolk sphingomyelin activation of HCR6 (1b) RdRps. RdRps (100 nM) were incubated with or without 0.01 mg/ml egg yolk sphingomyelin. (C) Hexanoyl sphingomyelin activation of the RdRps (RdRp names are indicated below the graphs). HCV RdRps (100 nM) were incubated with or without 2 μM hexanoyl sphingomyelin. The mean ± standard deviation of the activation ratio was calculated from three independent experiments. *, $P < 0.005$; ** $P < 0.001$.

C). C_8-lactosyl(β) ceramide and C_8-β-D-glucosyl ceramide activated HCR6 (1b) RdRp compared with the linear regression kinetics of the reaction with hexanoyl sphingomyelin as it plateaued (Fig. 1C and 3B). Cholesterol activated HCR6 (1b) RdRp slightly but did not activate JFH1 (2a) RdRp (Fig. 3C). We therefore concluded that the phosphocholine of sphingomyelin bound to the SBD of HCV RdRp because the order of HCV RdRp activation was hexanoyl sphingomyelin > C_8-lactosyl(β) ceramide > C_8-β-D-glucosyl ceramide, and C_6-ceramide did not activate HCV HCR6 (1b) RdRp. The polarity of the phosphocholine of sphingomyelin is important for HCV RdRp activation (see Fig. S5 in the supplemental material).

In order to test whether phosphocholine activated HCV RdRp (Fig. 3D), HCR6 (1b) RdRp was incubated with 0.4, 2, 20, 100, and 400 μg and 2, 4, 11, 54, and 100 mg of phosphocholine. Up to 400 μg of phosphocholine did not affect RdRp activity, but more than 2 mg of phosphocholine inhibited RdRp activity.

Effect of sphingomyelin on the template RNA binding of HCV RNA polymerase. The mechanism of HCV RdRp activation was analyzed. RNA polymerase changes its conformation throughout the different transcription steps, and template binding is the first step of transcription (9). Therefore, the effect of sphingomyelin on template RNA binding activity was tested (Fig. 4A and Table 1). Sphingomyelin enhanced the template RNA binding of HCR6 (1b) RdRp wt but not that of JFH1 (2a), H6CF (2a), or H77 (1a) wt RdRp. When the A238S/Q248E mutation was introduced into H77 (1a) RdRp, the RNA binding was enhanced. J6CF (2a) RdRp R241Q and S244D mutants showed similar enhancement of RNA binding, but the R241Q/S244D double mutant did not. The activation effect of RNA binding of HCR6 (1b) RdRp mutants L245A, I253A, and D244S was lower than that of RdRp wt. JFH1 (2a) RdRp wt and RdRp(A242C/S244D) showed similar RNA binding activation levels. Based on a comparison of the sphingomyelin activation of HCR6 (1b) RdRp wt and its mutants which lost sphingomyelin binding with J6CF (2a) RdRp wt and the R241Q and S244D mutants and H77 (1a) RdRp wt and the A238S/Q248E mutant, we concluded that polymerase activation by sphingomyelin was induced mainly via activation of the template RNA binding of RdRp. RNA binding activity of JFH1 (2a) RdRp wt and RdRp(A242C/S244D) was almost saturated because RNA binding of these RdRps was not activated by sphingomyelin (see Fig. S4 in the supplemental material).

HCV RdRp has to be bound with sphingomyelin before or at the same time as it binds to template RNA. After RdRp had bound to the template RNA, sphingomyelin did not enhance template RNA binding strongly (Fig. 4B).

Effect of the sphingomyelin binding domain mutations for HCV replicon activity with myriocin. In order to confirm sphingomyelin activation of HCV polymerase activity in a viral replication system, HCV replicon activity of the loss-of-function mutant HCV NN (1b) NS5B(D244S) and the gain-of-function mutants H77 (1a) NS5B(A238S/Q248E) and JFH1 (2a) NS5B(A242C/S244D) were compared with 5 and 50 nM myriocin treatment for 72 h (Fig. 5).

First, HCV replicon activity was compared as the relative luciferase activity (Fig. 5A). Both JFH1 (2a) wt and NS5B(A242C/S244D) replicons showed similar and strong replicon activity ($133 \times 10^3 \pm 12 \times 10^3$ and $138 \times 10^3 \pm 8.5 \times 10^3$, respectively). JFH1 (2a) wt replicon was resistant to myriocin treatment, as reported by Aizaki et al. using other SPT inhibitors (3). The JFH1 (2a) NS5B(A242C/S244D) replicon became sensitive to myriocin but still showed higher replicon activity than NN (1b) or H77 (1a) replicons even at 50 nM myriocin.

To analyze the effect of mutations precisely, the replicon activity relative to each wt strain was compared (Fig. 5B). The JFH1 (2a) wt replicon with 50 nM myriocin showed the same luciferase activity as the wt without myriocin (102% ± 9.6%). JFH1 (2a) NS5B(A242C/S244D) replicon activity was the same as that of the wt without myriocin (103% ± 12%); with 5 nM myriocin it was 84.1% ± 6.6% of the wt level, but with 50 nM myriocin it was 70.3% ± 5.3% of the wt level, which was significantly lower ($P < 0.01$). NN (1b) wt replicon activity was 45.3% ± 6.6% with 5 nM myriocin and 21.7% ± 2.9% with 50 nM myriocin relative to the wt level without myriocin. NN (1b) NS5B(D244S) replicon activity was 72.2% ± 12% without myriocin ($P < 0.05$), 44.0% ± 7.4% with 5 nM myriocin, and 38.1% ± 4.2% with 50 nM myriocin relative to wt level without myriocin, which was significantly higher ($P < 0.01$). Thus, NN (1b) NS5B(D244S) showed lower replicon activity than the wt

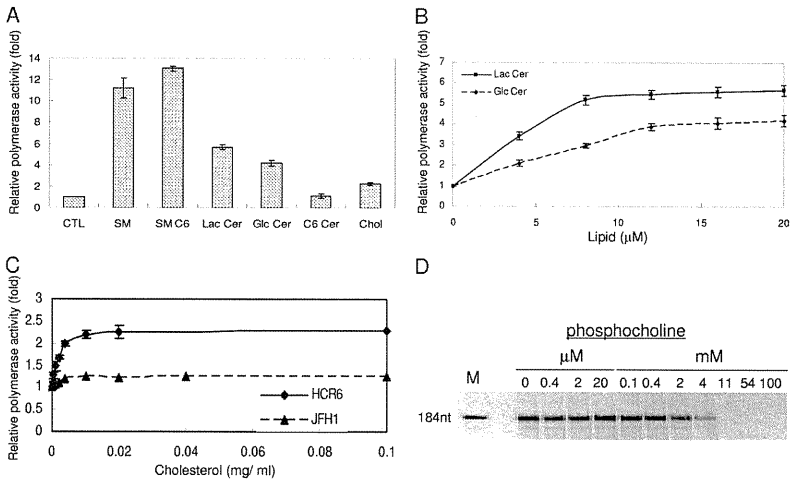

FIG. 3. HCV RNA polymerase activation effect of lipids. (A) Lipid activation of HCR6 (1b) RdRp wt. HCV HCR6 (1b) RdRp wt (100 nM) was incubated with or without (control [CTL]) 0.01 mg/ml egg yolk sphingomyelin (SM), 2 μM hexanoyl sphingomyelin (SM C6), 8 μM C_8-lactosyl(β) ceramide (Lac Cer), 12 μM C_8-β-D-glucosyl ceramide (Glc Cer), 12 μM C_6-ceramide (C6 Cer), or 0.02 mg/ml cholesterol (chol). (B) Activation kinetics of C_8-lactosyl(β) ceramide (Lac Cer) and C_8-β-D-glucosyl ceramide (Glc Cer) on HCR6 (1) RdRp. (C) Activation kinetics of cholesterol on HCR6 (1b) and JFH1 (12a) RdRps. (D) The effect of phosphocholine on HCR6 (1b) RdRp. The mean ± standard deviation of the activation ratio was calculated from three independent experiments.

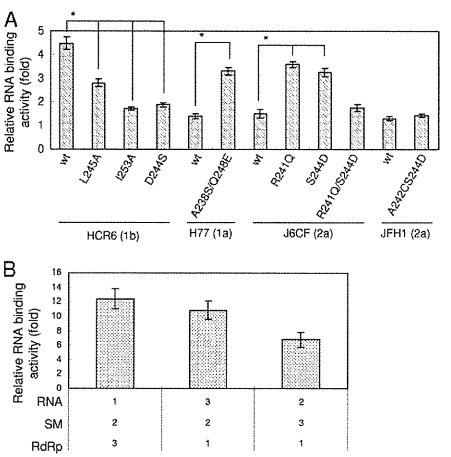

FIG. 4. Sphingomyelin activation of the RNA binding activity of HCV RNA polymerase. (A) Sphingomyelin activation of RNA filter binding of HCV RdRps (RdRp names are indicated below the graph). RdRps and ^{32}P-labeled RNA template (SL12-1S) were incubated with or without egg yolk sphingomyelin (SM), before filtration. (B) Effect of the order of sphingomyelin treatment. Numbers below the graph indicate the order in which the reagents were added. The graph represents the ratio to RNA binding without sphingomyelin. The mean ± standard deviation of the activation ratio was calculated from three independent experiments. *, $P < 0.01$.

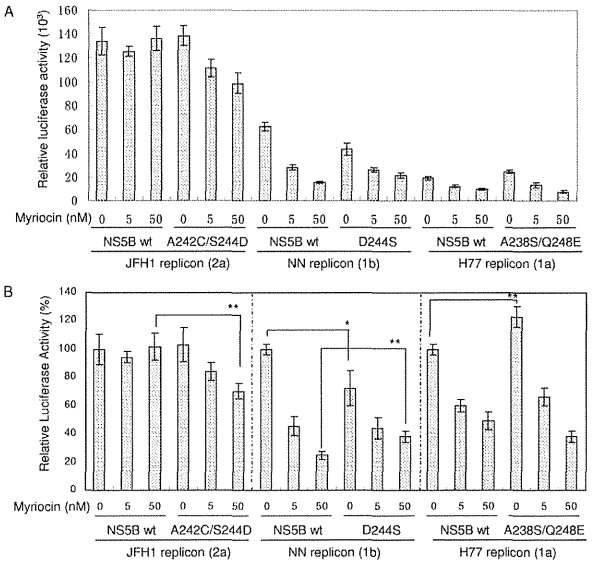

FIG. 5. Myriocin inhibition of HCV replicon activity. Huh7.5.1 cells were incubated with myriocin after transfection with the HCV replicons indicated below the graphs. Means ± standard deviations of the relative luciferase activity at 72 h after myriocin treatment compared to activity at 4 h after transfection (A) and to that of each wt without myriocin (B) were calculated from three independent measurements. *, $P < 0.05$; **, $P < 0.01$.

and was less sensitive to myriocin than the wt. H77 (1a) wt replicon activity was 59.9% ± 4.2% with 5 nM myriocin and 49.2% ± 6.4% with 50 nM myriocin relative to the wt level without myriocin. H77 (1a) NS5B(A238S/Q248E) replicon activity was 123% ± 7.1% without myriocin ($P < 0.01$), 66.1% ± 6.3% with 5 nM myriocin, and 38.0% ± 4.1% with 50 nM myriocin relative to wt level without myriocin. Both H77 (1a) wt and NS5B(A238S/Q248E) replicons were sensitive to myriocin, and the replicon activity of NS5B(A238S/Q248E) was higher than that of the wt.

JFH1 (2a) RdRp(A242C/S244D) localized in the DRM fractions. Myriocin sensitivity of JFH1 (2a) NS5B(A242C/S244D) replicon indicates the importance of 244D in JFH1 NS5B for sphingomyelin binding. To further confirm the role of 244D for recruitment of HCV RdRp to the detergent-resistant membrane (DRM), where the HCV replication complex exists, we compared the distribution of NS5A and NS5B of JFH1 (2a) wt and NS5B(A242C/S244D) in their replicon cells by sucrose density gradient centrifugation of the DRM (Fig. 6). NS5A proteins of both JFH1 (2a) wt and NS5B(A242C/S244D) replicons localized in the DRM fraction where caveolin-2 was present (11, 27), but most of NS5B wt localized in the Triton-soluble fractions. NS5B of JFH1 (2a) NS5B(A242C/S244D) replicon was shifted to the DRM fraction from the soluble fraction. The shift of NS5B(A242C/S244D) localization into the DRM demonstrated that SBD was the DRM localization domain of NS5B and that residue 244D was important for this localization.

DISCUSSION

Hepatitis C virus is an envelope virus, and the lipid components of the virion play important roles in HCV infectivity and virion assembly (3, 15, 20, 24). HCV replication complexes localize in lipid raft structures/DRMs in the membrane fractions of subgenomic replicon cells (30). Lipid rafts are composed mainly of sphingomyelin, cholesterol, and glycosphingolipids. Most reports regarding the relationship between lipids and HCV have examined virion assembly, infectivity, and the localization of HCV, but their biochemical interactions have not been reported. Our findings clearly demonstrate that sphingomyelin plays an important role not only in HCV replication complex formation and its localization but also in HCV RdRp activity.

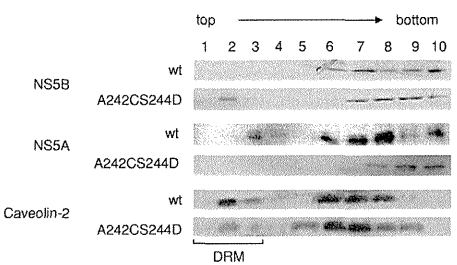

FIG. 6. Membrane floating assay of JFH1 wt and NS5B(A242C/S244D) replicon cells. The PNS fractions of HCV JFH1 (2a) wt and NS5B(A242C/S244D) replicon cells were treated with 1% Triton X-100 in TNE buffer for 30 min at 4°C and subjected to 10 to 40% sucrose gradient centrifugation in TNE buffer. Each fraction was subjected to 10% SDS-PAGE, followed by Western blotting with anti-NS5A, -NS5B, and -caveolin-2 antibodies. Fractions are numbered as indicated at the top of the panel. The DRM fractions (fractions 1 to 3) are indicated.

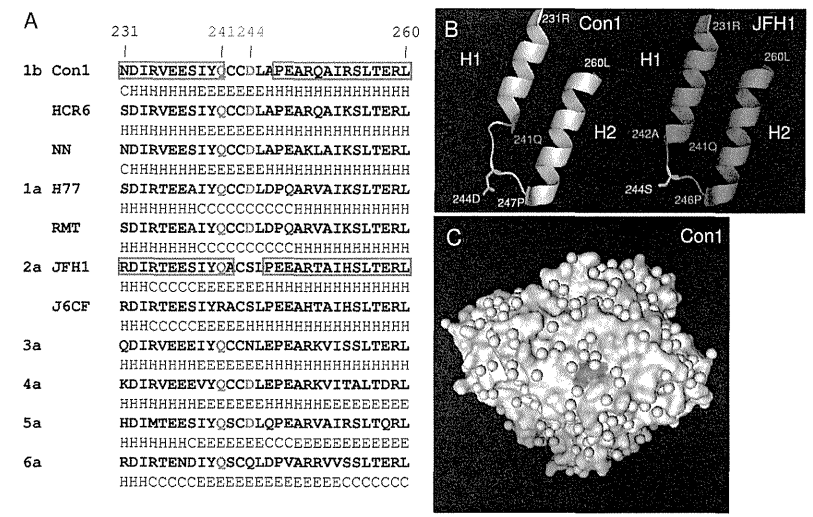

FIG. 7. Sphingomyelin binding domain (SBD) of HCV RNA polymerase. (A) The SBDs (231N to 260L) of HCV RdRps are aligned together with their secondary structure predicted by the Chou-Fasman program (10). The predicted secondary structure is indicated below the sequence as follows: H, α-helix; E, β-sheet; and C, coil. The α-helix structures of HCV Con1 (1b) RdRp and JFH1 (2a) RdRp are boxed in red. Residues 241Q and 244D are indicated in red and green, respectively. The 238A and 248E of the H77 and RMT (1a) RdRps are indicated in purple. GenBank accession numbers of HCV genotypes 3a, 4a, 5a, and 6a are GU814263 (12), GU814265 (12), Y13184 (8), and Y12083 (1), respectively. (B) Comparison of the SBDs of HCV Con1 (1b) (yellow) and JFH1 (2a) RdRps (magenta). The starting and ending amino acids of H1 and H2 are indicated. The sphingomyelin binding site, 241Q, is indicated in red, and 244D of Con1 (1b) and 244S of JFH1 (2a) RdRp are indicated in green. (C) Surface model of HCV Con1 (1b) RdRp. SBD is indicated in yellow, and 241Q and 244D are indicated in red and green, respectively. The structures of the Con1 and JFH1 RdRps were constructed by PyMOL, version 1.1.1 (http://www.pymol.org/). PDB numbers of Con1 (1b) RdRp and JFH1 (2a) RdRp are 3FQL (14) and 3I5K (31), respectively.

The helix-turn-helix structure of the SBD (residues 230 to 263), which is located between RNA polymerase motifs A and B, has been proposed as the sphingomyelin binding domain of HCV RdRp (29). We compared the SBD of Con1 (1b) (Protein Data Bank [PDB] 3FQL) (14) and JFH1 (2a) (PDB 3I5K) (31) and the secondary structure of the amino acids (201 to 290) in the SBD predicted by the Chou-Fasman program (10) (Fig. 7; see also Fig. S5 in the supplemental material) because the helix structures of the SBD of Con1 (helix 1 [H1], 231N to 241Q; helix 2 [H2], 247A to 260L) and JFH1 (H1, 231R to 242A; H2, 246P to 260L) RdRp fit with those predicted by the Chou-Fasman program. The structures contributing to sphingomyelin binding and activation are H1 and H2 and the junction (turn) between the two helix structures that are similar to the human immunodeficiency virus (HIV) gp120 V3 domain, prion protein (PrP), and β-amyloid peptide (13, 22). Although Con1 (1b) RdRp has a shorter helix structure than JFH1 (2a) RdRp (Fig. 6B), the structures of their SBDs are very similar (Fig. 7; see also Fig. S5). When the helix-turn-helix structure of the SBD was destroyed (HCR6 genotype 1b RdRp mutants L245A and I253A), the RdRp lost sphingomyelin binding activity and lost its activation (Fig. 2).

In order to study the structure-function relationship of the SBD and sphingomyelin, we compared the SBD of genotype 1a, 1b and 2a RdRps and particularly focused on residue 244D in the turn and residues 241Q and 238S/248E in the helix domains. The polar amino acid 241Q and the negatively charged 244D of Con1 (1b) RdRp located on the surface of the RdRp molecule bind and interact with the positively charged choline residue of sphingomyelin (Fig. 7C; see also Fig. S5 in the supplemental material). The positively charged 241R repels the choline residue of sphingomyelin, and as a result, J6CF (a) RdRp wt did not bind to sphingomyelin. J6CF (2a) RdRp(R241Q) showed almost the same sphingomyelin binding activity as HCR6 (1b) RdRp wt. This ionic interaction between SBD and sphingomyelin agrees with the activation of lipids with different sphingosine structures and fatty acid chains (Fig. 3A). JFH1 (2a) RdRp does not interact well with sphingomyelin because it does not have the negatively charged

amino acids at the tip of its turn structure. Once its 244S was changed to D, more sphingomyelin bound to JFH1 (2a) RdRp and activated the RdRp (Fig. 2A and C). The reason for the low activation of J6CF (2a) RdRp(R241Q/S244D) is not clear. Sometimes mutations affect the entire conformation of the molecule. In conclusion, from the comparison of sphingomyelin binding and activation of HCR6 (1b), J6CF (2a), and JFH1 (2a) RdRp SBD mutants, 241Q is the essential amino acid for sphingomyelin binding in the SBD. Amino acid 244D enhanced both binding and RdRp activation.

The *in vitro* sphingomyelin binding and RdRp activation experiments indicate that sphingomyelin binding and its RdRp activation are different biochemical reactions because we found controversial activation rates for sphingomyelin binding and RdRp activation among J6CF (2a) RdRp mutants (Fig. 2). The relationship between sphingomyelin binding and the activation of polymerase activity was studied by comparing genotype 1b and 1a RdRps, both of which bind to sphingomyelin (Fig. 2). However, 1a RdRp is not activated by sphingomyelin because both of the helix structures of 1a RdRp are probably terminated at 238A and 248Q, making its helix structures shorter than those of 1b RdRp (Fig. 6A). The length of the helix structure may be essential for sphingomyelin activation because RdRp changes its structure to bind to template RNA when sphingomyelin binds to SBD (Fig. 4).

HCV RdRp changes its conformations at the early stages of transcription initiation, including the template RNA binding step (6, 9). Sphingomyelin binding is likely to change the conformation of 1b RdRp to recruit template RNA and initiate transcription efficiently. Comparison of the activation ratio of RNA binding and polymerase activity of 1b RdRp, J6CF (2a) RdRp wt and R241Q and S244D mutants, and JFH1 (2a) RdRp wt and mutant A242C/S244D suggests that steps other than RNA binding are also likely to be activated by sphingomyelin.

From a kinetic analysis of sphingomyelin activation (Fig. 1C and D), 20 sphingomyelin molecules are estimated to interact with the SBD of RdRp and activate it because sphingomyelin activation plateaued at 20 sphingomyelin molecules per HCV RdRp molecule. It is not clear whether 20 sphingomyelin molecules form a micelle or a layer structure. However, the structure of sphingomyelin is important for the activation of HCV RdRp because phosphocholine did not activate the RdRp (Fig. 3D).

To confirm these biochemical findings in HCV replication, we tested the effect of SBD mutations in HCV replicon systems with the SPT inhibitor myriocin (Fig. 5) (4, 33) because NA255 was not available. The loss-of-function mutant, HCV NN (1b) NS5B(D244S), showed lower replicon activity than NN (1b) wt and more resistance to 50 nM myriocin, which did not affect the viability of cells (4, 33), than the wt. The gain-of-function mutant, H77 (1a) NS5B(A238S/Q248E), showed higher replicon activity than H77 wt and retained myriocin sensitivity because it had the sphingomyelin binding sites 241Q and 244D. At 50 nM myriocin, another gain-of-function mutant, JFH1 (2a) NS5B(A242C/S244D), was inhibited although its activity was the same as that of JFH1 (2a) wt without myriocin because the JFH1 wt replicon had high replicon activity without myriocin (Fig. 5A). The JFH1 replicon activity may be maximal in the system; therefore, the JFH1 (2a) NS5B(A242C/S244D) replicon did not show higher activity than JFH1 (2a) wt without myriocin while H77 (1a) NS5B(A238S/Q248E) showed higher replicon activity than H77 wt.

The binding and RdRp activation activity of the amino acid 244 mutants by sphingomyelin did not differ greatly from the wt *in vitro*. However, the myriocin sensitivity of JFH1 (2a) NS5B(S244D) was demonstrated clearly. That of H77 (1a) NS5B(A238S/Q248E) indicated that sphingomyelin binding was the target of myriocin inhibition, not the sphingomyelin activation of RdRp. These data confirm the importance of 241Q, 244D, and the helix structure in SBD for HCV replication in the cells.

Sphingomyelin is the major component of the lipid raft structure/DRM where the HCV genome replicates. To confirm that the SBD is the membrane binding site of HCV RdRp, we analyzed the localization of NS5B of JFH1 (2a) wt and NS5B(A242C/S244D) replicons by membrane floating assay (Fig. 6). JFH1 (2a) NS5B wt did not localize in the DRM. However, the localization of NS5B of the JFH1 (2a) NS5B(A242C/S244D) replicon shifted to the DRM from the soluble fractions. Previously, HCV NS5B was believed to localize in the DRM by its C-terminal hydrophobic sequences (21). However, our data demonstrate that the SBD is the membrane localization domain of HCV NS5B, which agrees with the myriocin sensitivity of JFH1 (2a) NS5B(A242C/S244D) replicons (Fig. 5) and the release of HCV 1b NS5B from the DRM by another SPT inhibitor, NA255 (29).

This is the first report of RNA polymerase activation by lipids. Twenty sphingomyelin molecules interact with SBD, particularly with residues 241Q and 244D of HCV (1b) RdRp, and change the conformation of the RdRp in order to recruit RNA templates. At the same time, HCV RdRp molecules may be aligned on the sphingomyelin layer formed via interactions between the hydrocarbon chains of sphingosine and fatty acids via placement of their SBD into the layer (Fig. 7C). Consistent with previous research (3, 23, 37), our findings explain why the inhibitors of the sphingolipid biosynthetic pathway influence subgenomic replicons derived from HCV genotypes 1a and 1b but not those derived from JFH1 (2a) (Fig. 5). Most HCV isolates have 241Q in NS5B, and some of them also have 244D (Fig. 7A). These sphingomyelin interactions are new targets for the treatment of HCV.

ACKNOWLEDGMENTS

We thank C. Rice and R. Bartenshlager for the HCV H77 and Con1 plasmids, respectively. We also thank F. Chisari for Huh7.5.1 and Huh7/src cells.

This work was supported by a grant-in-aid from the Chinese Academy of Sciences (O514P51131 and KSCX1-YW-10), the Chinese 973 project (2009CB522504), and the Chinese National Science and Technology Major Project (2008ZX10002-014).

REFERENCES

1. **Adams, N. J., R. W. Chamberlain, L. A. Taylor, F. Davidson, C. K. Lin, R. M. Elliott, and P. Simmonds.** 1997. Complete coding sequence of hepatitis C virus genotype 6a. Biochem. Biophys. Res. Commun. **234:**393–396.
2. **Aizaki, H., K. J. Lee, V. M. Sung, H. Ishiko, and M. M. Lai.** 2004. Characterization of the hepatitis C virus RNA replication complex associated with lipid rafts. Virology **324:**450–461.
3. **Aizaki, H., K. Morikawa, M. Fukasawa, H. Hara, Y. Inoue, H. Tani, K. Saito, M. Nishijima, K. Hanada, Y. Matsuura, M. M. Lai, T. Miyamura, T. Wakita, and T. Suzuki.** 2008. Critical role of virion-associated cholesterol and sphingolipid in hepatitis C virus infection. J. Virol. **82:**5715–5724.
4. **Amemiya, F., S. Maekawa, Y. Itakura, A. Kanayama, A. Matsui, S. Takano, T. Yamaguchi, J. Itakura, T. Kitamura, T. Inoue, M. Sakamoto, K. Yamauchi, S. Okada, A. Yamashita, N. Sakamoto, M. Itoh, and N. Enomoto.** 2008. Targeting lipid metabolism in the treatment of hepatitis C virus infection. J. Infect. Dis. **197:**361–370.
5. **Binder, M., D. Quinkert, O. Bochkarova, R. Klein, N. Kezmic, R. Bartenschlager, and V. Lohmann.** 2007. Identification of determinants involved in initiation of hepatitis C virus RNA synthesis by using intergenotypic replicase chimeras. J. Virol. **81:**5270–5283.
6. **Biswal, B. K., M. M. Cherney, M. Wang, L. Chan, C. G. Yannopoulos, D. Bilimoria, O. Nicolas, J. Bedard, and M. N. James.** 2005. Crystal structures of the RNA-dependent RNA polymerase genotype 2a of hepatitis C virus reveal two conformations and suggest mechanisms of inhibition by non-nucleoside inhibitors. J. Biol. Chem. **280:**18202–18210.
7. **Blight, K. J., J. A. McKeating, J. Marcotrigiano, and C. M. Rice.** 2003. Efficient replication of hepatitis C virus genotype 1a RNAs in cell culture. J. Virol. **77:**3181–3190.
8. **Chamberlain, R. W., N. J. Adams, L. A. Taylor, P. Simmonds, and R. M. Elliott.** 1997. The complete coding sequence of hepatitis C virus genotype 5a, the predominant genotype in South Africa. Biochem. Biophys. Res. Commun. **236:**44–49.
9. **Chinnaswamy, S., I. Yarbrough, S. Palaninathan, C. T. Kumar, V. Vijayaraghavan, B. Demeler, S. M. Lemon, J. C. Sacchettini, and C. C. Kao.** 2008. A locking mechanism regulates RNA synthesis and host protein interaction by the hepatitis C virus polymerase. J. Biol. Chem. **283:**20535–20546.
10. **Chou, P. Y., and G. D. Fasman.** 1974. Prediction of protein conformation. Biochemistry **13:**222–245.
11. **Fujimoto, T., H. Kogo, K. Ishiguro, K. Tauchi, and R. Nomura.** 2001. Caveolin-2 is targeted to lipid droplets, a new "membrane domain" in the cell. J. Cell Biol. **152:**1079–1085.
12. **Gottwein, J. M., T. K. Scheel, B. Callendret, Y. P. Li, H. B. Eccleston, R. E. Engle, S. Govindarajan, W. Satterfield, R. H. Purcell, C. M. Walker, and J. Bukh.** Novel infectious cDNA clones of hepatitis C virus genotype 3a (strain S52) and 4a (strain ED43): genetic analyses and *in vivo* pathogenesis studies. J. Virol. **84:**5277–5293.
13. **Hammache, D., G. Pieroni, N. Yahi, O. Delezay, N. Koch, H. Lafont, C. Tamalet, and J. Fantini.** 1998. Specific interaction of HIV-1 and HIV-2 surface envelope glycoproteins with monolayers of galactosylceramide and ganglioside GM3. J. Biol. Chem. **273:**7967–7971.
14. **Hang, J. Q., Y. Yang, S. F. Harris, V. Leveque, H. J. Whittington, S. Rajyaguru, G. Ao-Ieong, M. F. McCown, A. Wong, A. M. Giannetti, S. Le Pogam, F. Talamas, N. Cammack, I. Najera, and K. Klumpp.** 2009. Slow binding inhibition and mechanism of resistance of non-nucleoside polymerase inhibitors of hepatitis C virus. J. Biol. Chem. **284:**15517–15529.
15. **Huang, H., F. Sun, D. M. Owen, W. Li, Y. Chen, M. Gale, Jr., and J. Ye.** 2007. Hepatitis C virus production by human hepatocytes dependent on assembly and secretion of very low-density lipoproteins. Proc. Natl. Acad. Sci. U. S. A. **104:**5848–5853.
16. **Ishii, N., K. Watashi, T. Hishiki, K. Goto, D. Inoue, M. Hijikata, T. Wakita, N. Kato, and K. Shimotohno.** 2006. Diverse effects of cyclosporine on hepatitis C virus strain replication. J. Virol. **80:**4510–4520.
17. **Kashiwagi, T., K. Hara, M. Kohara, K. Kohara, J. Iwahashi, N. Hamada, H. Yoshino, and T. Toyoda.** 2002. Kinetic analysis of C-terminally truncated RNA-dependent RNA polymerase of hepatitis C virus. Biochem. Biophys. Res. Commun. **290:**1188–1194.
18. **Kato, T., T. Date, M. Miyamoto, A. Furusaka, K. Tokushige, M. Mizokami, and T. Wakita.** 2003. Efficient replication of the genotype 2a hepatitis C virus subgenomic replicon. Gastroenterology **125:**1808–1817.
19. **Kiyosawa, K., T. Sodeyama, E. Tanaka, Y. Gibo, K. Yoshizawa, Y. Nakano, S. Furuta, Y. Akahane, K. Nishioka, R. H. Purcell, et al.** 1990. Interrelationship of blood transfusion, non-A, non-B hepatitis and hepatocellular carcinoma: analysis by detection of antibody to hepatitis C virus. Hepatology **12:**671–675.
20. **Lambot, M., S. Fretier, A. Op De Beeck, B. Quatannens, S. Lestavel, V. Clavey, and J. Dubuisson.** 2002. Reconstitution of hepatitis C virus envelope glycoproteins into liposomes as a surrogate model to study virus attachment. J. Biol. Chem. **277:**20625–20630.
21. **Lemon, S., C. Walker, M. Alter, and M. Yi.** 2007. Hepatitis C virus, p. 1253–1304. *In* D. M. Knipe, P. M. Howley, D. E. Griffin, R. A. Lamb, M. A. Martin, B. Roizman, and S. E. Straus (ed.), Fields virology, 5th ed. Lippincott Williams & Wilkins, Philadelphia, PA.
22. **Mahfoud, R., N. Garmy, M. Maresca, N. Yahi, A. Puigserver, and J. Fantini.** 2002. Identification of a common sphingolipid-binding domain in Alzheimer, prion, and HIV-1 proteins. J. Biol. Chem. **277:**11292–11296.
23. **Miyake, Y., Y. Kozutsumi, S. Nakamura, T. Fujita, and T. Kawasaki.** 1995. Serine palmitoyltransferase is the primary target of a sphingosine-like immunosuppressant, ISP-1/myriocin. Biochem. Biophys. Res. Commun. **211:**396–403.
24. **Miyanari, Y., K. Atsuzawa, N. Usuda, K. Watashi, T. Hishiki, M. Zayas, R. Bartenschlager, T. Wakita, M. Hijikata, and K. Shimotohno.** 2007. The lipid droplet is an important organelle for hepatitis C virus production. Nat. Cell Biol. **9:**1089–1097.
25. **Murayama, A., T. Date, K. Morikawa, D. Akazawa, M. Miyamoto, M. Kaga, K. Ishii, T. Suzuki, T. Kato, M. Mizokami, and T. Wakita.** 2007. The NS3 helicase and NS5B-to-3′X regions are important for efficient hepatitis C virus strain JFH-1 replication in Huh7 cells. J. Virol. **81:**8030–8040.
26. **Murayama, A., L. Weng, T. Date, D. Akazawa, X. Tian, T. Suzuki, T. Kato, Y. Tanaka, M. Mizokami, T. Wakita, and T. Toyoda.** 2010. RNA polymerase activity and specific RNA structure are required for efficient HCV replication in cultured cells. PLoS Pathog. **6:**e1000885.
27. **Ostermeyer, A. G., J. M. Paci, Y. Zeng, D. M. Lublin, S. Munro, and D. A. Brown.** 2001. Accumulation of caveolin in the endoplasmic reticulum redirects the protein to lipid storage droplets. J. Cell Biol. **152:**1071–1078.
28. **Saito, I., T. Miyamura, A. Ohbayashi, H. Harada, T. Katayama, S. Kikuchi, Y. Watanabe, S. Koi, M. Onji, Y. Ohta, et al.** 1990. Hepatitis C virus infection is associated with the development of hepatocellular carcinoma. Proc. Natl. Acad. Sci. U. S. A. **87:**6547–6549.
29. **Sakamoto, H., K. Okamoto, M. Aoki, H. Kato, A. Katsume, A. Ohta, T. Tsukuda, N. Shimma, Y. Aoki, M. Arisawa, M. Kohara, and M. Sudoh.** 2005. Host sphingolipid biosynthesis as a target for hepatitis C virus therapy. Nat. Chem. Biol. **1:**333–337.
30. **Shi, S. T., K. J. Lee, H. Aizaki, S. B. Hwang, and M. M. Lai.** 2003. Hepatitis C virus RNA replication occurs on a detergent-resistant membrane that cofractionates with caveolin-2. J. Virol. **77:**4160–4168.
31. **Simister, P., M. Schmitt, M. Geitmann, O. Wicht, U. H. Danielson, R. Klein, S. Bressanelli, and V. Lohmann.** 2009. Structural and functional analysis of hepatitis C virus strain JFH1 polymerase. J. Virol. **83:**11926–11939.
32. **Tsukiyama-Kohara, K., S. Tone, I. Maruyama, K. Inoue, A. Katsume, H. Nuriya, H. Ohmori, J. Ohkawa, K. Taira, Y. Hoshikawa, F. Shibasaki, M. Reth, Y. Minatogawa, and M. Kohara.** 2004. Activation of the CKI-CDK-Rb-E2F pathway in full genome hepatitis C virus-expressing cells. J. Biol. Chem. **279:**14531–14541.
33. **Umehara, T., M. Sudoh, F. Yasui, C. Matsuda, Y. Hayashi, K. Chayama, and M. Kohara.** 2006. Serine palmitoyltransferase inhibitor suppresses HCV replication in a mouse model. Biochem. Biophys. Res. Commun. **346:**67–73.
34. **Wasley, A., and M. J. Alter.** 2000. Epidemiology of hepatitis C: geographic differences and temporal trends. Semin. Liver Dis. **20:**1–16.
35. **Watashi, K., N. Ishii, M. Hijikata, D. Inoue, T. Murata, Y. Miyanari, and K. Shimotohno.** 2005. Cyclophilin B is a functional regulator of hepatitis C virus RNA polymerase. Mol. Cell **19:**111–122.
36. **Weng, L., J. Du, J. Zhou, J. Ding, T. Wakita, M. Kohara, and T. Toyoda.** 2009. Modification of hepatitis C virus 1b RNA polymerase to make a highly active JFH1-type polymerase by mutation of the thumb domain. Arch. Virol. **154:**765–773.
37. **Yasuda, S., H. Kitagawa, M. Ueno, H. Ishitani, M. Fukasawa, M. Nishijima, S. Kobayashi, and K. Hanada.** 2001. A novel inhibitor of ceramide trafficking from the endoplasmic reticulum to the site of sphingomyelin synthesis. J. Biol. Chem. **276:**43994–44002.
38. **Zhong, J., P. Gastaminza, G. Cheng, S. Kapadia, T. Kato, D. R. Burton, S. F. Wieland, S. L. Uprichard, T. Wakita, and F. V. Chisari.** 2005. Robust hepatitis C virus infection in vitro. Proc. Natl. Acad. Sci. U. S. A. **102:**9294–9299.

Secondary Structure of the Amino-Terminal Region of HCV NS3 and Virological Response to Pegylated Interferon Plus Ribavirin Therapy for Chronic Hepatitis C

Mai Sanjo,[1] Takafumi Saito,[1]* Rika Ishii,[1] Yuko Nishise,[1] Hiroaki Haga,[1] Kazuo Okumoto,[1] Junitsu Ito,[1] Hisayoshi Watanabe,[1] Koji Saito,[1] Hitoshi Togashi,[2] Kazuto Fukuda,[3] Yasuharu Imai,[3] Ahmed El-Shamy,[4] Lin Deng,[4] Ikuo Shoji,[4] Hak Hotta,[4] and Sumio Kawata[1]

[1]*Department of Gastroenterology, Yamagata University School of Medicine, Yamagata, Japan*
[2]*Health Administrative Center, Yamagata University, Yamagata, Japan*
[3]*Division of Gastroenterology, Ikeda Municipal Hospital, Osaka, Japan*
[4]*Division of Microbiology, Kobe University Graduate School of Medicine, Kobe, Japan*

The aim of the study was to identify a predictive marker for the virological response in hepatitis C virus 1b (HCV-1b)-infected patients treated with pegylated interferon plus ribavirin therapy. A total of 139 patients with chronic hepatitis C who received therapy for 48 weeks were enrolled. The secondary structure of the 120 residues of the amino-terminal HCV-1b non-structural region 3 (NS3) deduced from the amino acid sequence was classified into two major groups: A and B. The association between HCV NS3 protein polymorphism and virological response was analyzed in patients infected with group A ($n = 28$) and B ($n = 40$) isolates who had good adherence to both pegylated interferon and ribavirin administration (>95% of the scheduled dosage) for 48 weeks. A sustained virological response (SVR) representing successful HCV eradication occurred in 33 (49%) in the 68 patients. Of the 28 patients infected with the group A isolate, 18 (64%) were SVR, whereas of the 40 patients infected with the group B isolate only 15 (38%) were SVR. The proportion of virological responses differed significantly between the two groups ($P < 0.05$). These results suggest that polymorphism in the secondary structure of the HCV-1b NS3 amino-terminal region influences the virological response to pegylated interferon plus ribavirin therapy, and that virus grouping based on this polymorphism can contribute to prediction of the outcome of this therapy. ***J. Med. Virol. 82:1364–1370, 2010.*** © 2010 Wiley-Liss, Inc.

KEY WORDS: hepatitis C; interferon; ribavirin; interaction; polymorphism

INTRODUCTION

Hepatitis C virus (HCV) is the major pathogen that causes chronic liver diseases with a risk of progression to cirrhosis and hepatocellular carcinoma. Currently, the standard treatment for chronic hepatitis C is antiviral therapy using pegylated interferon (Peg-IFN) plus ribavirin (RBV), and this approach is most effective for eradication of HCV viremia. However, even with the widely used treatment regimen of 48 weeks, the rate of sustained virological response (SVR), which indicates eradication of viremia, is still approximately 50% for patients infected with the therapy-resistant HCV genotype 1b (HCV-1b) with a high viral load [Manns et al., 2001; Bruno et al., 2004; Hadziyannis et al., 2004]. It would be useful to predict the virological response to this therapy and to identify patients who would obtain beneficial therapeutic effects before treatment, in order to avoid any serious side effect and to eliminate those who would not be helped by the treatment. In the future it will be important to establish a protocol of tailor-made medicine for chronic hepatitis C.

Grant sponsor: Grant-in-Aid for Scientific Research; Grant number: 21590824; Grant sponsor: Global Center of Excellence program of the Japan Society for the Promotion of Science (Yamagata University School of Medicine and Kobe University Graduate School of Medicine); Grant sponsor: Ministry of Health, Labor and Welfare of Japan.

*Correspondence to: Takafumi Saito, M. D., Department of Gastroenterology, Yamagata University School of Medicine, 2-2-2 Iida-nishi, Yamagata 990-9585, Japan.
E-mail: tasaitoh@med.id.yamagata-u.ac.jp

Accepted 6 March 2010
DOI 10.1002/jmv.21818
Published online in Wiley InterScience (www.interscience.wiley.com)

Both the HCV genotype and pre-treatment viral load are major viral factors that influence the response to IFN-based antiviral therapy, but IFN resistance is also partly due to variation of the amino acid sequence encoded by HCV itself. Enomoto et al. [1996] proposed that variation of 40 amino acids within the NS5A region (aa 2,209–2,248), which is referred to as the IFN sensitivity-determining region (ISDR), is well correlated with IFN responsiveness. ISDR and its adjacent sequence bind and inhibit the enzymatic activity of a double-stranded RNA-activated protein kinase (PKR), which can have an antiviral effect, and therefore the combined region is referred to as the PKR-binding domain (PKR-BD) [Gale et al., 1997, 1998]. A correlation between sequence variation in the PKR-BD and IFN responsiveness has been reported [Nousbaum et al., 2000], and some reports show a correlation between IFN responsiveness and the sequence diversity of variable region 3 (V3) (aa 2,356–2,379) or surrounding regions near the carboxy terminus of NS5A [Murphy et al., 2002; Sarrazin et al., 2002; Puig-Basagoiti et al., 2005]. A high degree of amino acid substitution in the V3 and pre-V3 regions (aa 2,334–2,355) of NS5A, which is referred to as the IFN/RBV resistance-determining region (IRRDR) (aa 2,334–2,379), has been associated with SVR in Peg-IFN/RBV combination therapy for patients infected with HCV-1b [El-Shamy et al., 2007, 2008]. In addition to these findings in non-structural proteins of the virus, amino acid substitution in a structural region of HCV has been reported to be a predictive viral marker for the virological response to PegIFN/RBV therapy. Amino acid polymorphisms in the HCV core region (Arg70 vs. Gln70 and Leu91 vs. Met91) correlate with virological outcome and on-treatment viral kinetics in Peg-IFN/RBV therapy [Akuta et al., 2006, 2007], and a double wild-type HCV core (Arg70 and Leu91) may be a significant predictor of SVR in Peg-IFN/RBV therapy [Akuta et al., 2007].

Interactions between viral and host proteins in infected cells may influence therapeutic effects and the natural history of infection, since the HCV NS3 region has a significant effect on immunity. The amino-terminal part of this region encodes a serine protease, for which the minimum activity has been mapped to a region between aa 1,059 and 1,204 [Yamada et al., 1998]. The serine protease inactivates Cardif, a caspase recruitment domain (CARD)-containing adaptor protein that interacts with the RNA helicase retinoic acid inducible gene 1 (RIG-1)-dependent antiviral pathway in infected cells [Foy et al., 2003; Meylan et al., 2005; Evans and Seeger, 2006]. This action inhibits phosphorylation and subsequent heterodimerization of interferon regulatory factor-3 (IRF-3), which is essential for activation of IFN signaling through translocation of IRF-3 heterodimers into the nucleus, and eventually blocks IFN-beta production. In addition, inactivation of IRF-3 is postulated to influence the therapeutic effect of IFN-based antiviral therapy, because the IRF-3 heterodimer translocates into the nucleus to bind to the IFN-stimulated response element that produces many antiviral proteins, including 2′,5′-oligoadenylate synthetase and PKR [Nakaya et al., 2001; Grandvaux et al., 2002]. Collectively, these findings suggest that polymorphisms in HCV NS3 structure deduced from sequence variation may influence IFN-related signaling and the antiviral effect of IFN-based anti-HCV therapy.

We have focused on polymorphisms in the secondary structure of the viral polyprotein that interacts with host proteins involved in immunity, with the aim of identification of predictive viral markers for the response to Peg-IFN/RBV therapy. In this study, we examined the potential correlation between polymorphisms in the secondary structure of the HCV NS3 amino-terminal region and virological responses to Peg-IFN/RBV therapy in patients infected with HCV-1b with a high viral load.

PATIENTS AND METHODS

Patients and Treatment Regimen With Peg-IFN Plus Ribavirin

A total of 139 consecutive patients diagnosed with chronic hepatitis C were enrolled in the study from December 2004 to March 2007. These patients included 81 men and 58 women, and were aged from 31 to 75 years old (mean ± SD, 56.8 ± 8.7 years old). All patients were infected with HCV-1b with a high viral load of over 100 KIU/ml, and all received Peg-IFN/RBV therapy. Patients with alcoholic liver injury, autoimmune liver disease, and those who had symptoms of decompensated cirrhosis including ascites were excluded. Briefly, all patients were treated with a combination of Peg-IFN-alpha 2b (Pegintron®; Schering-Plough, Kenilworth, NJ) and RBV (Rebetol®; Schering-Plough) for 48 weeks. Peg-IFN was administered subcutaneously once a week and RBV was given orally twice a day for the total dose. The dosages were determined on the basis of body weight according to the Japanese standard prescription information supplied by the Japanese Ministry of Health, Labour and Welfare, and there was a limit for calculating the optimized dose: patients with body weights of 35–45, 46–60, 61–75, and 76–90 kg were given Peg-IFN at doses of 60, 80, 100, and 120 μg, respectively, and those with body weights of <60, 60–80, and >80 kg were given RBV at doses of 600, 800, and 1,000 mg, respectively. The dose of Peg-IFN or RBV was reduced according to the Japanese standard criteria based on the white blood cell count, neutrophil count, hemoglobin concentration and platelet count [Hiramatsu et al., 2008].

Virological Tests and Response to Peg-IFN Plus Ribavirin

Virological responses were evaluated at 12 weeks after the start of treatment with an early depletion of viremia referred to as an early virological response (EVR), at the end of treatment with depletion of viremia referred to as an end of treatment virological response (ETR), and at 24 weeks after completion of treatment,

with a clinical outcome of a sustained virological response (SVR) representing successful HCV eradication. All patients were negative for hepatitis B surface antigen. Quantification of serum HCV RNA was performed using an RT-PCR-based commercial kit (Amplicor HCV monitor test, ver. 2.0, Roche Diagnostics, Tokyo, Japan). This Amplicor HCV RNA assay has a lower limit of detection of 50 IU/ml. SVR was determined by monitering negativity for HCV RNA monthly for 6 months. The real-time PCR assay kit (COBAS TaqMan HCV Auto, Roche Diagnostics) for more precise quantitation of HCV viremia has recently become available and pre-treatment viral titers were re-evaluated using preserved serum samples. This real-time PCR assay has a lower limit of detection of 15 IU/ml. The study protocol was approved by the Ethics Committee of Yamagata University Hospital. Informed consent was obtained from all patients.

PCR Amplification of the Amino-Terminal Region of NS3

RNA was extracted from 50 μl of serum using an RNeasy Mini kit (Qiagen, Tokyo, Japan). To amplify the region of the HCV genome encoding the amino-terminal region of NS3 (1,027–1,206), a one-step PCR was performed in a tube using the Superscript One-Step RT-PCR kit with Platinum Taq (Gibco-BRL, Tokyo, Japan) and an outer set of primers: NS3-F1 (sense primer; 5′-ACA CCG CGG CGT GTG GGG ACA T-3′; nucleotides 3,295–3,316) and NS3-AS2 (antisense primer; 5′-GCT CTT GCC GCT GCC AGT GGG A-3′; nucleotides 4,040–4,019), as reported previously [Ogata et al., 2002a, 2003]. PCR was initially performed at 45°C for 30 min at RT and then at 94°C for 2 min, followed by the first-round PCR for forty 3-min cycles at 94°, 55°, and 72°C for 1 min each. The second-round PCR was performed with *Pfu* DNA polymerase (Promega, Tokyo, Japan) and an inner set of primers: NS3-F3 (sense primer; 5′-CAG GGG TGG CGG CTC CTT-3′; nucleotides 3,390–3,407) and NS3-AS1 (antisense primer; 5′-GCC ACT TGG AAT GTT TGC GGT A-3′; nucleotides 4,006–3,985). The second-round PCR was performed for 35 cycles, with each cycle consisting of 1 min at 94°C, 1.5 min at 55°C, and 3 min at 72°C. This method allowed amplification of the corresponding portion of the HCV genome from HCV-1b RNA-positive samples. The amplified fragments were purified with a QIAquick PCR purification kit (Qiagen) and directly sequenced (without being subcloned) in both directions using a dRhodamine Terminator Cycle Sequencing Ready Reaction kit and an ABI 377 sequencer (Applied Biosystems, Tokyo, Japan).

Classification of the Secondary Structure of the HCV-1b NS3 Amino-Terminal Region

The secondary structure of the amino-terminal region of HCV NS3 was predicted by computer-assisted Robson analysis [Garnier et al., 1978] with Genetyx-Mac software (ver.10.1; Software Development Co., Tokyo, Japan). Previously, the full-length secondary structure of the HCV-1b NS3 region was analyzed, and this showed that the secondary structure deduced from the carboxy-terminal 60 residues was well conserved in terms of linear structure, without any turn structure [Ogata et al., 2002a]. We have shown that the secondary structure of the 120 residues in the amino-terminal region of HCV-1b NS3 can be classified into two major groups: A and B (Fig. 1) [Ogata et al., 2002a, 2003]. Briefly, the criteria for this classification are as follows: in group A isolates, the carboxy-terminal 20 residues (aa 1,125–1,146) are oriented leftward relative to a domain composed of the remaining amino-terminal region; whereas in group B isolates, the same 20 residues are oriented rightward relative to the rest of the amino-terminal domain.

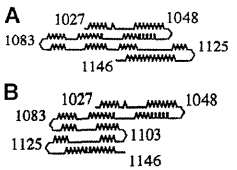

Fig. 1. Secondary structure of the 120 amino-terminal residues of HCV-1b nonstructural 3 (NS3) region classified into two major groups: A and B. The looped, zigzag, straight, and bent lines represent α-helix, β-sheet, coil, and turn structures, respectively. The numbers indicate amino acid positions. **A**: Group A, (**B**) Group B.

Analysis of Amino Acid Substitutions in the Core Region

To amplify a region of the HCV genome encoding the core region including positions 70 and 91, reverse transcription and the first-round PCR were performed in a tube by the Superscript One-Step RT-PCR kit with Platinum *Taq* (Gibco-BRL) and an outer set of primers, followed by second-round PCR with an inner set of primers in accordance with procedures reported previously [Ogata et al., 2002b]. The sequences of the amplified fragments were determined by direct sequencing.

Statistical Analysis

Data were analyzed by a χ^2 test for independence with a two-by-two contingency table and a Student *t*-test. A *P*-value <0.05 was considered significant.

RESULTS

Virological Response *and Adherence* to the Peg-IFN Plus Ribavirin Regimen

Rates of virological responses in patients treated with PegIFN/RBV combination therapy for 48 weeks are shown in Figure 2. Of the 139 patients enrolled in the study, SVR, non-SVR and cessation of therapy occurred in 58 (42%), 62 (45%), and 19 (14%), respectively. Serious

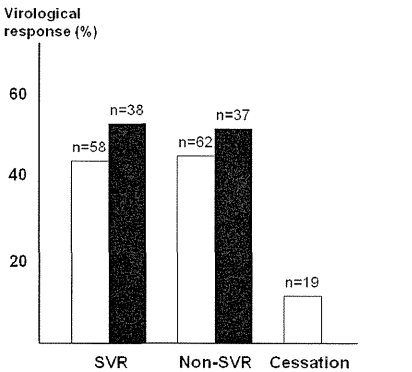

Fig. 2. Virological response in patients treated with peginterferon plus ribavirin for 48 weeks. The results are shown for all 139 subjects (open bars) and for 75 cases with good adherence of >80% of the scheduled dosages (closed bars). SVR, sustained virological response.

adverse events that necessitated discontinuation of this therapy were depression in one patient, thyroid function disorder in 2, general itching in 2, infection in 2, anorexia in 2, occurrence of hepatocellular carcinoma in 2, and a decreased neutrophil count in 2. Six patients also terminated this therapy at their own request. Of the 139 patients, 75 (54%) received >80% of the scheduled dosage of Peg-IFN and RBV designated before treatment, and of these 75 cases SVR and non-SVR occurred in 38 (51%) and 37 (49%), respectively.

Prevalence of Types of Secondary Structure of the Amino-Terminal Region of HCV NS3

The prevalence of the types of secondary structure of HCV NS3 in the 139 subjects is shown in Table I. Among these subjects, 43 (31%), 70 (50%), and 26 (19%) were classified into groups A, B, and others, including 3 of mixed type (A plus B) and 23 of non-A, non-B type. Of the 75 cases with good adherence to administration of >80% of the scheduled dosage, 28 (37%), 40 (53%) and 7 (9%) were classified into groups A, B, and others. The amino acid data of group A and B in the cases with good adherence to administration are available in the DDBJ/EMBL/GenBank databases with the accession numbers AB548070–AB548137. Our analysis revealed no specific correlations between amino acid sequences and the secondary structure deduced by the Robson method, as we have reported previously [Ogata et al., 2003].

TABLE I. Prevalence of the HCV NS3 Secondary Structure Type

	Group A (%)	Group B (%)	Others (%)
Enrolled cases (n = 139)	43 (31)	70 (50)	26 (19)
Adherent cases (n = 75)	28 (37)	40 (53)	7 (9)

Characteristics of Adherent Patients Based on Different HCV NS3 Structure Types

The virological responses to Peg-IFN/RBV combination therapy for patients infected with group A and B isolates were assessed in the 68 subjects with good adherence to the scheduled dosage of Peg-IFN and RBV. The characteristics of patients infected with group A and B isolates are shown in Table II. Age, gender, pre-treatment level of serum HCV RNA and ALT, and frequency of fibrosis stage did not differ significantly between the two groups. Peg-IFN/RBV combination therapy was completed in all the patients, and the total administered dosages of Peg-IFN and RBV was >95% of the scheduled dosage in both groups.

Relationship Between Virological Responses and Polymorphisms in the HCV NS3 Amino-Terminal Region

In the 68 patients who received >95% of the scheduled doses of Peg-IFN and RBV for 48 weeks, SVR and non-SVR occurred in 33 (49%) and 35 (51%), respectively. The EVR, ETR, and SVR rates in patients infected with group A and B isolates are shown in Table III. There was a significant difference in the rates of EVR between subjects infected with group A and B isolates: EVR was achieved in 19 of 28 (68%) patients with group A infection, compared to 17 of 40 (43%) with group B infection ($P < 0.05$). The final outcome also differed significantly between subjects infected with group A and B isolates: SVR was achieved in 18 of 28 (64%) patients with group A infection, compared to 15 of 40 (38%) with group B infection ($P < 0.05$).

Polymorphisms in Core Amino Acids 70/91 and in the HCV NS3 Secondary Structure

The wild-type core sequence (Arg70, Leu91) has been associated with SVR in Peg-IFN/RBV combination therapy, while the non-double wild-type containing one or two substitutions at positions 70 and/or 91 was associated with non-SVR [Akuta et al., 2007]. Therefore, we examined substitutions at positions 70 and 91 in the HCV core region in pre-treatment serum samples of 44 cases that were available for testing. The double wild-type 70/91 sequence was found in 22 of the 44 cases (50%), of which 12 were SVR and 10 were non-SVR. Combination analysis of polymorphisms of the HCV core 70/91 positions and the NS3 amino-terminal region showed that 10 (83%) of the 12 SVR cases and only 3 (30%) of the 10 non-SVR cases with the double wild-type core had a group A polymorphism in HCV NS3 (Table IV). Thus, combination analysis of the core and NS3 regions may improve prediction of the outcome of Peg-IFN/RBV therapy.

TABLE II. Characteristics of Adherent Patients Infected With HCV Group A and B Isolates

	Group A (n = 28)	Group B (n = 40)	P
Age (years)	55.5 ± 9.5	55.5 ± 8.9	NS[a]
Sex (men/women)	18/10	21/19	NS[b]
Pre-treatment HCV RNA (KIU/ml)	1,635 ± 930	2,087 ± 1,422	NS[a]
Alanine aminotransferase level (U/L)	80 ± 62	71 ± 47	NS[a]
Stage of liver fibrosis			
F1 or F2/F3 or F4	19/9	28/12	NS[b]
Drug adherence dosage (%)			
Pegylated interferon	97.7 ± 5.2	95.2 ± 7.3	NS[a]
Ribavirin	96.8 ± 6.4	95.3 ± 7.7	NS[a]

NS, not significant.
[a]t-test.
[b]χ^2 test.

Re-Evaluation of Pre-Treatment HCV Viremia Status Using Real-Time PCR

Since the viral titer before treatment is a major predictive marker of the outcome of Peg-IFN/RBV therapy, we re-evaluated the pre-treatment viral titers more precisely using preserved serum samples taken within 1 month before treatment, using a real-time PCR assay. The pre-treatment viral titers did not differ significantly between sera with group A and B isolates (5.98 ± 0.94 vs. 6.25 ± 0.62 logIU/ml) (Table V). The secondary structure polymorphisms of HCV NS3 were independent of the pre-treatment viral titers.

DISCUSSION

Antiviral therapy with Peg-IFN/RBV for 48 weeks fails to eradicate HCV in about half of patients infected with a high titer of HCV genotype 1b, and the severe adverse events and high costs associated with this therapy require outcome prediction to allow targeted treatment for chronic hepatitis C. The pre-treatment viral titer, viral factors that influence the virological response to IFN-based anti-HCV therapy have been widely investigated. Viral kinetics showing prompt seronegativity after the start of treatment is a critical factor for achieving SVR, and thus the possible correlation between an early virological response and genetic sequence variation of the HCV has been studied. In particular, amino acid substitutions in the HCV core region at positions 70 and 91 or multiple mutations detected in the IRRDR of the HCV NS5A region are useful markers for predicting EVR and subsequent SVR.

TABLE III. Virological Responses in Subjects With Different Polymorphisms in the Secondary Structure of HCV NS3

	EVR*	ETR**	SVR*
Group A (n = 28)	19 (68%)	23 (82%)	18 (64%)
Group B (n = 40)	17 (43%)	25 (63%)	15 (38%)

EVR: early virological response at 12 weeks after the start of treatment.
ETR: virological response at the end of treatment.
SVR: sustained virological response 24 weeks after completion of treatment.
*$P < 0.05$.
**$P = 0.08$; χ^2 test.

To date, the influence of several single amino acid substitutions and accumulation of these changes in the viral genome on the effect of IFN-based anti-HCV therapy has been examined. Since interactions between host and viral proteins in infected cells may influence the therapeutic effect of an antiviral agent, we focused on the association of structural polymorphism of a viral protein with the effect of Peg-IFN/RBV combination therapy in this study. Our results suggest that polymorphism analysis of secondary structure deduced from sequence variations in the HCV NS3 amino-terminal region can be used to predict viral responses to this therapy.

Amino acid sequences of the HCV NS3 amino-terminal region, which encodes a serine protease, vary greatly among HCV isolates. Interactions between HCV NS3 and host proteins may influence both oncogenesis and immunity, and thus elucidation of the biological significance of these interactions could result in a new prognostic marker for HCC or a predictive marker for anti-HCV therapy. First, HCV NS3 interacts with the p53 tumor suppressor to suppress p53-dependent apoptosis or p21 transcriptional activity [Ishido and Hotta, 1998; Kwun et al., 2001; Deng et al., 2006]. Transfection of a plasmid expressing the amino-terminal portion of HCV NS3 induces cell transformation in vitro, and transplanted cells proliferate with sarcoma-like features in vivo [Sakamuro et al., 1995]. These findings suggest that NS3 may be involved in the oncogenic pathway in HCV infection. We have shown that the secondary structure of the 120-residue amino-terminal region of NS3 (1,027–1,146) is classifiable into two major groups: A and B. This region encodes a serine protease and also includes p53-binding sites. Our

TABLE IV. Treatment Outcome of Cases With a Double Wild-Type Core Region and Different HCV NS3 Structural Polymorphism

	Group A (%)	Group B (%)	P
SVR (n = 12)	10 (83)	2 (17)	0.02[a]
Non-SVR (n = 10)	3 (30)	7 (70)	

SVR, sustained virological response.
[a]χ^2 test.

TABLE V. Pre-Treatment HCV RNA Levels Measured by Real-Time PCR for Subjects With Different HCV NS3 Structural Polymorphism

	Group A	Group B	P
SVR (n = 33)	5.78 ± 1.05	6.I3 ± 0.71	NS[a]
Non-SVR (n = 35)	6.33 ± 0.59	6.32 ± 0.55	NS[a]
Total (n = 68)	5.98 ± 0.94	6.25 ± 0.62	NS[a]

SVR, sustained virological response. NS, not significant.
[a]t test.

previous cross-sectional studies revealed that the prevalence of group B infection is significantly higher in HCC cases than in non-HCC cases [Ogata et al., 2003], and that the group B infection is an independent risk factor for development of HCC in patients with chronic HCV infection [Nishise et al., 2007]. Second, NS3 interacts with host proteins associated with IFN signaling and thus influences cellular immunity. Since the serine protease encoded by the amino-terminal region of NS3 inhibits the IFN-signaling pathway, polymorphism of this region is likely to influence the effect of Peg-IFN/RBV combination therapy.

Several factors associated with the virological response to this therapy are well known, with adherence to both IFN and RBV strongly influencing outcome [Pearlman, 2004; Arase et al., 2005; Yamada et al., 2008]. In this study, we analyzed 75 cases in which >80% of the scheduled dosage of both drugs was administered. Of these cases, 28 (37%) and 40 (53%) were infected with group A and B isolates, respectively, which were similar rates to those for the 139 cases in the overall study. Age, gender, viral load before treatment, ALT level, proportion of fibrosis stage and adherence to Peg-IFN and RBV did not differ between the group A and B cases. However, the frequencies of SVR and EVR were significantly higher in group A, and those for non-EVR and non-SVR were significantly higher in group B. The results suggest that infection with the group B isolate, which correlates with a higher rate of HCC, is resistant to Peg-IFN/RBV therapy. The pre-treatment viremia status in the 68 cases with group A or B isolates showed no significant differences between the two groups of patients. Therefore, these results suggest that the secondary structure of the HCV NS3 amino-terminal region may be useful for prediction of the outcome of Peg-IFN/RBV combination therapy. In this initial study setting, the relationship of these polymorphisms to the frequency of rapid viral response at 4 weeks after the start of treatment was not evaluated. It will be important to assess this relationship in a future study.

The polymorphism in HCV core region (Arg70/Leu91) is a useful predictive marker for virological responses in Peg-IFN/RBV therapy [Akuta et al., 2007]. Interestingly, a combined analysis of polymorphisms of the core region (which encodes a structural protein) and HCV NS3 (a nonstructural protein) improved the prediction rate. Therefore, analysis of NS3 polymorphism in combination with the core structural polymorphism appears to improve prediction of the outcome of Peg-IFN/RBV therapy. A larger, multi-center prospective study would be necessary to validate the present results. In conclusion, the results of this study suggest that secondary structure polymorphism in the amino-terminal region of HCV NS3 is a useful predictive marker of the effect of Peg-IFN/RBV combination therapy for chronic hepatitis C. Although the present findings are clinically important, and will be helpful for predicting the outcome of Peg-IFN/RBV therapy, further in vitro studies will be needed to elucidate the molecular mechanism underlying the association of HCV NS3polymorphisms with clinical outcome.

REFERENCES

Akuta N, Suzuki F, Sezaki H, Suzuki Y, Hosaka T, Someya T, Kobayashi M, Saitoh S, Watahiki S, Sato J, Kobayashi M, Arase Y, Ikeda K, Kumada H. 2006. Predictive factors of virological non-response to interferon-ribavirin combination therapy for patients infected with hepatitis C virus of genotype 1b and high viral load. J Med Virol 78:83–90.

Akuta N, Suzuki F, Kawamura Y, Yatsuji H, Sezaki H, Suzuki Y, Hosaka T, Kobayashi M, Kobayashi M, Arase Y, Ikeda K, Kumada H. 2007. Predictive factors of early and sustained responses to peginterferon plus ribavirin combination therapy in Japanese patients infected with hepatitis C virus genotype 1b: Amino acid substitutions in the core region and low-density lipoprotein cholesterol levels. J Hepatol 46:403–410.

Arase Y, Ikeda K, Tsubota A, Suzuki F, Suzuki Y, Saitoh S, Kobayashi M, Akuta N, Someya T, Hosaka T, Sezaki H, Kobayashi M, Kumada H. 2005. Significance of serum ribavirin concentration in combination therapy of interferon and ribavirin for chronic hepatitis C. Intervirology 48:138–144.

Bruno S, Cammà C, Di Marco V, Rumi M, Vinci M, Camozzi M, Rebucci C, Di Bona D, Colombo M, Craxì A, Mondelli MU, Pinzello G. 2004. Peginterferon alfa-2b plus ribavirin for naïve patients with genotype 1 chronic hepatitis C: A randomized controlled trial. J Hepatol 41:474–481.

Deng L, Nagano-Fujii M, Tanaka M, Nomura-Takigawa Y, Ikeda M, Kato N, Sada K, Hotta H. 2006. NS3 protein of hepatitis C virus associated with the tumor suppressor p53 and inhibits its function in an NS3 sequence-dependent manner. J Gen Virol 87:1703–1713.

El-Shamy A, Sasayama M, Nagano-Fujii M, Sasase N, Imoto S, Kim SR, Hotta H. 2007. Prediction of efficient virological response to pegylated interferon/ribavirin combination therapy by NS5A sequences of hepatitis C virus and anti-NS5A antibodies in pre-treatment sera. Microbiol Immunol 51:471–482.

El-Shamy A, Nagano-Fujii M, Sasase N, Imoto S, Kim SR, Hotta H. 2008. Sequence variation in hepatitis C virus nonstructural protein 5A predicts clinical outcome of pegylated interferon/ribavirin combination therapy. Hepatology 48:38–47.

Enomoto N, Sakuma I, Asahina Y, Kurosaki M, Murakami T, Yamamoto C, Ogura Y, Izumi N, Marumo F, Sato C. 1996. Mutations in the nonstructural protein 5A gene and response to interferon in patients with chronic hepatitis C virus 1b infection. N Engl J Med 334:77–81.

Evans JD, Seeger C. 2006. Cardif: A protein central to innate immunity is inactivated by the HCV NS3 serine protease. Hepatology 43:615–617.

Foy E, Li K, Wang C, Sumpter R, Jr., Ikeda M, Lemon SM, Gale M, Jr. 2003. Regulation of interferon regulatory factor-3 by the hepatitis C virus serine protease. Science 300:1145–1148.

Gale MJ, Jr., Korth MJ, Tang NM, Tan SL, Hopkins DA, Dever TE, Polyak SJ, Gretch DR, Katze MG. 1997. Evidence that hepatitis C virus resistance to interferon is mediated through repression of the PKR protein kinase by the nonstructural 5A protein. Virology 230:217–227.

Gale MJ, Jr., Korth MJ, Katze MG. 1998. Repression of the PKR protein kinase by the hepatitis C virus NS5A protein: A potential mechanism of interferon resistance. Clin Diagn Virol 10:157–162.

Garnier J, Osguthorfe DJ, Robson B. 1978. Analysis of the accuracy and implications of simple methods for predicting the secondary structure of globular proteins. J Mol Biol 120:97–120.

Grandvaux N, Servant MJ, tenOever B, Sen GC, Balachandran S, Barber GN, Lin R, Hiscott J. 2002. Transcriptional profiling of interferon regulatory factor 3 target genes: Direct involvement in the regulation of interferon-stimulated genes. J Virol 76:5532–5539.

Hadziyannis SJ, Sette H, Jr., Morgan TR, Balan V, Diago M, Marcellin P, Ramadori G, Bodenheimer H, Jr., Bernstein D, Rizzetto M, Zeuzem S, Pockros PJ, Lin A, Ackrill AM. 2004. Peginterferon-alpha2a and ribavirin combination therapy in chronic hepatitis C: A randomized study of treatment duration and ribavirin dose. Ann Intern Med 140:346–355.

Hiramatsu N, Kurashige N, Oze T, Takehara T, Tamura S, Kasahara A, Oshita M, Katayama K, Yoshihara H, Imai Y, Kato M, Kawata S, Tsubouchi H, Kumada H, Okanoue T, Kakumu S, Hayashi N. 2008. Early decline of hemoglobin can predict progression of hemolytic anemia during pegylated interferon and ribavirin combination therapy in patients with chronic hepatitis C. Hepatol Res 38:52–59.

Ishido S, Hotta H. 1998. Complex formation of the nonstructural protein 3 of hepatitis C virus with the p53 tumor suppressor. FEBS Lett 438:258–262.

Kwun HJ, Jung EY, Ahn JY, Lee MN, Jang KL. 2001. p53-dependent transcriptional repression of p21(waf1) by hepatitis C virus NS3. J Gen Virol 82:2235–2241.

Manns MP, McHutchison JG, Gordon SC, Rustgi VK, Shiffman M, Reindollar R, Goodman ZD, Koury K, Ling M, Albrecht JK. 2001. Peginterferon alfa-2b plus ribavirin compared with interferon alfa-2b plus ribavirin for initial treatment of chronic hepatitis C: A randomized trial. Lancet 358:958–965.

Meylan E, Curran J, Hofmann K, Moradpour D, Binder M, Bartenschlager R, Tschopp J. 2005. Cardif is an adaptor protein in the RIG-I antiviral pathway and is targeted by hepatitis C virus. Nature 437:1167–1172.

Murphy MD, Rosen HR, Marousek GI, Chou S. 2002. Analysis of sequence configurations of the ISDR, PKR-binding domain, and V3 region as predictors of response to induction interferon-alpha and ribavirin therapy in chronic hepatitis C infection. Dig Dis Sci 47:1195–1205.

Nakaya T, Sato M, Hata N, Asagiri M, Suemori H, Noguchi S, Tanaka N, Taniguchi T. 2001. Gene induction pathways mediated by distinct IRFs during viral infection. Biochem Biophys Res Commun 283:1150–1156.

Nishise Y, Saito T, Sugahara K, Ito JI, Saito K, Togashi H, Nagano-Fujii M, Hotta H, Kawata S. 2007. Risk of hepatocellular carcinoma and secondary structure of hepatitis C virus (HCV) NS3 protein amino-terminus, in patients infected with HCV subtype 1b. J Infect Dis 196:1006–1009.

Nousbaum J, Polyak SJ, Ray SC, Sullivan DG, Larson AM, Carithers RL, Jr., Gretch DR. 2000. Prospective characterization of full-length hepatitis C virus NS5A quasispecies during induction and combination antiviral therapy. J Virol 74:9028–9038.

Ogata S, Ku Y, Yoon S, Makino S, Nagano-Fujii M, Hotta H. 2002a. Correlation between secondary structure of an amino-terminal portion of the nonstructural protein 3 (NS3) of hepatitis C virus and development of hepatocellular carcinoma. Microbiol Immunol 46:549–554.

Ogata S, Nagano-Fujii M, Ku Y, Yoon S, Hotta H. 2002b. Comparative sequence analysis of the core protein and its frameshift product, the F protein, of hepatitis C virus subtype 1b strains obtained from patients with and without hepatocellular carcinoma. J Clin Microbiol 40:3625–3630.

Ogata S, Florese RH, Nagano-Fujii M, Hidajat R, Deng L, Ku Y, Yoon S, Saito T, Kawata S, Hotta H. 2003. Identification of hepatitis C virus (HCV) subtype 1b strains that are highly, or only weakly, associated with hepatocellular carcinoma on the basis of the secondary structure of an amino-terminal portion of the HCV NS3 protein. J Clin Microbiol 41:2835–2841.

Pearlman BL. 2004. Hepatitis C treatment update. Am J Med 117:344–352.

Puig-Basagoiti F, Forns X, Furcić I, Ampurdanés S, Giménez-Barcons M, Franco S, Sánchez-Tapias JM, Saiz JC. 2005. Dynamics of hepatitis C virus NS5A quasispecies during interferon and ribavirin therapy in responder and non-responder patients with genotype 1b chronic hepatitis C. J Gen Virol 86:1067–1075.

Sakamuro D, Furukawa T, Takegami T. 1995. Hepatitis C virus nonstructural protein NS3 transforms NIH 3T3 cells. J Virol 69:3893–3896.

Sarrazin C, Herrmann E, Bruch K, Zeuzem S. 2002. Hepatitis C virus nonstructural 5A protein and interferon resistance: A new model for testing the reliability of mutational analyses. J Virol 76:11079–11090.

Yamada K, Mori A, Seki M, Kimura J, Yuasa S, Matsuura Y, Miyamura T. 1998. Critical point mutations for hepatitis C virus NS3 proteinase. Virology 246:104–112.

Yamada G, Iino S, Okuno T, Omata M, Kiyosawa K, Kumada H, Hayashi N, Sakai T. 2008. Virological response in patients with hepatitis C virus genotype 1b and a high viral load: Impact of peginterferon-alpha-2a plus ribavirin dose reductions and host-related factors. Clin Drug Investig 28:9–16.

Microbiology and Immunology

Microbiol Immunol 2010; **54**: 684–690
doi:10.1111/j.1348-0421.2010.00268.x

ORIGINAL ARTICLE

17β-estradiol inhibits the production of infectious particles of hepatitis C virus

Kazumi Hayashida*, Ikuo Shoji, Lin Deng, Da-Peng Jiang, Yoshi-Hiro Ide and Hak Hotta

Division of Microbiology, Center for Infectious Diseases, Kobe University Graduate School of Medicine, 7-5-1 Kusunoki-cho, Chuo-ku, Kobe 650-0017, Japan

ABSTRACT

Persistent infection with hepatitis C virus causes serious liver diseases, such as chronic hepatitis, hepatic cirrhosis and hepatocellular carcinoma. The male gender is one of the critical factors in progression of hepatic fibrosis due to chronic HCV infection; thus female hormones may play a role in delaying the progression of hepatic fibrosis. It has also been reported that women are more likely than men to clear HCV in the acute phase of infection. These observations lead the present authors to the question: do female hormones inhibit HCV infection? In this study using HCV J6/JFH1 and Huh-7.5 cells, the possible inhibitory effect(s) of female hormones such as 17β-estradiol (the most potent physiological estrogen) and progesterone on HCV RNA replication, HCV protein synthesis and production of HCV infectious particles (virions) were analyzed. It was found that E_2, but not P_4, significantly inhibited production of the HCV virion without inhibiting HCV RNA replication or HCV protein synthesis. E_2–mediated inhibition of HCV virion production was abolished by a nuclear estrogen receptor (ER) antagonist ICI182780. Moreover, treatment with the ERα-selective agonist 4, 4′, 4″- (4-propyl-[1H]-pyrazole-1, 3, 5-triyl)trisphenol (PPT), but not with the ERβ-selective agonist 2, 3-bis (4-hydroxyphenyl)-propionitrile (DPN) or the G protein-coupled receptor 30 (GPR30)-selective agonist 1-(4-[6-bromobenzo 1, 3 dioxol-5-yl]-3a, 4, 5, 9b-tetrahydro-3H-cyclopenta [c] quinolin-8-yl)-ethanone (G-1), significantly inhibited HCV virion production. Taken together, the present results suggest that the most potent physiological estrogen, E_2, inhibits the production of HCV infectious particles in an ERα–dependent manner.

Key words 17β-estradiol, estrogen receptor, hepatitis C virus, sex difference.

HCV, an enveloped RNA virus which belongs to the genus *Hepacivirus* within the family *Flaviviridae*, prevails in most parts of the world with an estimated number of about 170 million carriers; hence HCV infection is a major global health-care problem (1). Persistent infection with HCV causes serious liver diseases, such as chronic hepatitis, hepatic cirrhosis and hepatocellular carcinoma (2, 3). In the USA, the prevalence of anti-HCV antibodies is twice as high in men as in women (4). The male gender is thought to be one of the critical factors in progression of hepatic fibrosis in chronic HCV infection (5, 6). It has also been reported that progression of hepatic fibrosis is faster in postmenopausal than in premenopausal women, and that hormone replacement therapy with estrogen and

Correspondence
Hak Hotta, Division of Microbiology, Center for Infectious Diseases, Kobe University Graduate School of Medicine, 7-5-1 Kusunoki-cho, Chuo-ku, Kobe 650-0017, Japan.
Tel: +81 78 382 5500; fax: +81 78 382 5519; email: hotta@kobe-u.ac.jp
***Present address:** Kanonji Institute, The Research Foundation for Microbial Diseases of Osaka University, 2-9-41 Yahata-cho, Kanonji, Kagawa 768-0061, Japan.

Received 7 June 2010; revised 13 August 2010; accepted 22 August 2010.

List of Abbreviations: DMEM, Dulbecco's modified Eagle's medium; DMSO, dimethyl sulfoxide; DPN, 2, 3-bis (4-hydroxyphenyl)-propionitrile; E_2, 17β-estradiol; ER, estrogen receptor; G-1, 1-(4-[6-bromobenzo 1, 3 dioxol-5-yl]-3a, 4, 5, 9b-tetrahydro-3H-cyclopenta [c] quinolin-8-yl)-ethanone; GPR30, G protein-coupled receptor 30; HCV, hepatitis C virus; P_4, progesterone; PPT, 4, 4′, 4″- (4-propyl-[1H]-pyrazole-1, 3, 5-triyl)trisphenol; SEM, standard error of the mean.

progesterone significantly delays progression of hepatic fibrosis in postmenopausal women (6, 7). This potential innate resistance of premenopausal women to hepatic fibrosis may be attributed to female hormones, such as estrogens and progesterone. In fact, E_2, the most potent physiological estrogen, has been reported to suppress the progression of liver fibrosis and hepatocarcinogenesis (8, 9). Moreover, women are more likely than men to clear HCV in the acute phase of infection, even within a few months after infection (10). These observations imply the possibility that female hormones inhibit HCV infection, either at the level(s) of virus attachment/entry, virus RNA replication, virus protein synthesis or production of infectious virus particles (virions).

Estrogens utilize three kinds of ER; ERα, ERβ and GPR30 (11–15). Specific agonists and antagonists of ER are available and widely used to examine the roles of estrogens. In the present study, we examined the possible effects of female hormones, especially E_2 and P_4, on HCV RNA replication, protein synthesis and virion production in cultured cells.

MATERIALS AND METHODS

Cell culture and virus infection

A human hepatoma-derived cell line, Huh-7.5, which is highly permissive to HCV RNA replication (16), was kindly provided by Dr. C. M. Rice (The Rockefeller University, New York, NY, USA). The cells were maintained in phenol red-free DMEM (Sigma–Aldrich, St Louis, MO, USA) supplemented with 10% heat-inactivated and charcoal-stripped FBS (Israel Beit Haemek, Haemek, Israel), 0.1 mM non-essential amino acids (Invitrogen, Carlsbad, CA, USA), 100 IU/mL penicillin and 100 μg/mL streptomycin (Invitrogen).

The pFL-J6/JFH1 plasmid that encodes the entire viral genome of a chimeric strain of HCV-2a, J6/JFH1 (17) was kindly provided by Dr. C. M. Rice. A cell culture-adapted mutant derived from J6/JFH1 (P-47 strain) (18, 19) was used for infection experiments. The virus was inoculated into Huh-7.5 cells at a multiplicity of infection of 1.0 and incubated for 2 hr. After the residual virus had been removed by washing, the cells were cultured in the presence or absence of female hormones, and agonists and an antagonist of estrogen receptors (see below). Culture supernatants were collected at 0, 1, 2 and 3 days postinfection and virus titers were determined, as described below.

Virus titration

Culture supernatants containing HCV were serially diluted 10-fold in DMEM and inoculated into Huh-7.5 cells (2×10^5 cells per well in a 24-well plate). After incubation at 37°C for 6 hr, the cells were fed with fresh DMEM. At 24 hr postinfection, the cells were fixed with ice-cold methanol, blocked with 5% goat serum in PBS and subjected to immunofluorescence analysis using mouse monoclonal antibody against the HCV core protein (2H9) and Alexa Fluor 488-conjugated goat anti-mouse IgG (H+L, Molecular Probes, Eugene, OR, USA). Hoechst 33342 (Molecular Probes) was used for counterstaining of the nuclei. HCV-positive foci were counted under a fluorescent microscope (BX51; Olympus, Tokyo, Japan) and virus titers were expressed as focus-forming units per ml, as reported previously (18, 19).

Chemicals

E_2 and P_4 were purchased from Sigma–Aldrich (St Louis, MO, USA). ICI182780 (an antagonist of ERα and ERβ), PPT (an ERα-selective agonist) (20) and DPN (an ERβ-selective agonist) (21) were purchased from Tocris Bioscience (Bristol, UK). G-1 (a GPR30-selective agonist) (22) was purchased from Calbiochem (Darmstadt, Germany). DMSO, which was used as a solvent, was obtained from Wako Pure Chemical Industries (Osaka, Japan). The concentrations of E_2 and P_4 used in this study were 0.4 μM and 3 μM, respectively, which correspond to the estimated highest concentrations in the sera of pregnant women. ICI182780 was used at a concentration of 1 μM, PPT and DPN at 0.1, 1 and 10 μM, and G-1 at 0.1 and 1 μM. As G-1 has been reported to lose its GPR30-binding specificity at concentrations over 1 μM, a concentration of 10 μM for G-1 was not tested. The final concentration of DMSO as a control never exceeded 0.01%.

Cell viability assay

Cells plated on 96-well microtiter plates (2.0×10^4 cells/well) were inoculated with HCV and treated with E_2, P_4 or DMSO. The cell viability in each well was determined by WST-1 assay (Roche Diagnostics, Mannheim, Germany) until 3 days postinfection.

Real-time quantitative RT-PCR

Total cellular RNA was isolated using the RNAiso reagent (Takara Bio, Kyoto, Japan) and cDNA was generated using the QuantiTect Reverse Transcription system (Qiagen, Valencia, CA, USA). Real-time quantitative PCR was performed on a SYBR *Premix Ex Taq* (Takara Bio) using SYBR green chemistry in ABI PRISM 7000 (Applied Biosystems, Foster, CA, USA). Primer sets used in this study are shown below: HCV NS5B, 5′-ACCAAGCTCAAACTCACTCCA-3′ and 5′-AGCGGGGTCGGGCAC GAGACA-3′ (23); β-actin, 5′-GCGGGAAATCGTGCGTGACATT-3′ and 5′-GATGGAGTTGAAGGTAGTTTCGTG-3′.

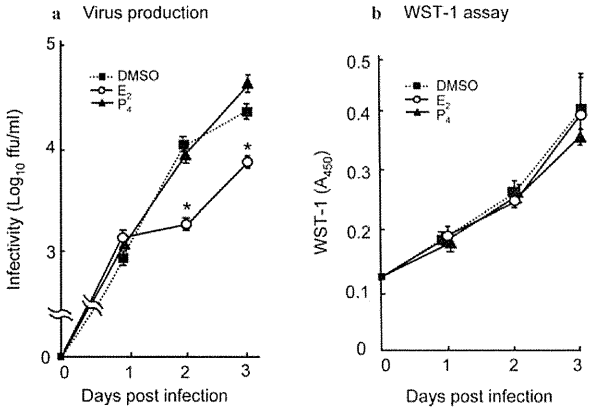

Fig. 1. Effects of E_2 and P_4 on HCV virion production and cell growth. (a) HCV virion production. Huh-7.5 cells were inoculated with HCV at a multiplicity of infection of 1.0, incubated for 2 hr, and cultured for 0, 1, 2 and 3 days after virus infection. The HCV-infected cells were treated with E_2 (0.4 μM), P_4 (3 μM) or DMSO (control) from 2 hr postinfection to sampling time (days 1, 2 and 3). The culture supernatants of HCV-infected cells were assayed for virus infectivity. Data are shown as mean ± SEM. (b) Cell growth. HCV-infected cells were treated with E_2, P_4 or DMSO (control) from 2 hr to 3 days postinfection. Cell growth in each culture was determined by WST-1 assay. Data are shown as mean ± SEM.

Immunoblotting

Cells were solubilized in lysis buffer as reported previously (18, 19). The cell lysates were subjected to 8% sodium dodecyl sulfate-polyacrylamide gel electrophoresis and transferred to polyvinylidene difluoride membrane (Millipore, Billerica, MA, USA). The membranes were incubated with mouse monoclonal antibodies against HCV NS3 (Chemicon International, Temecula, CA, USA), followed by incubation with peroxidase-conjugated goat anti-mouse IgG (Medical & Biological Laboratories Co. Ltd., Nagoya, Japan). The positive bands were visualized by using ECL detection system (GE Healthcare UK, Buckinghamshire, UK).

Statistical analysis

Results were expressed as mean ± SEM. Statistical significance was evaluated by one-way analyses of variances.

RESULTS

E_2 inhibits HCV virion production, but not HCV RNA replication or HCV protein synthesis

We first examined the effect of E_2 or P_4 treatment on HCV virion production. At 2 hr after virus inoculation, the HCV-infected Huh-7.5 cells were treated with E_2 (0.4 μM) or P_4 (3 μM) for 3 days. Culture supernatants were collected every day and titrated for viral infectivity. As shown in Figure 1a, E_2 treatment significantly suppressed HCV virion production at 2 and 3 days postinfection, whereas treatment with P_4 did not. The same treatment (E_2 or P_4) did not exert significant cytotoxicity (Fig. 1b). Next, we examined the effect of E_2 on HCV RNA replication and HCV protein synthesis under the same experimental conditions. We found that HCV RNA replication and HCV protein synthesis in both HCV-infected cells and HCV RNA replicon-harboring cells (23) were all unaffected by treatment with E_2 or P_4 (Fig. 2a–c). Moreover, treatment of the cells with E2 either prior to, or during, virus inoculation did not significantly inhibit HCV virion production (Fig. 3a). These results collectively suggest that E_2 inhibits HCV virion production, but not at the level of virus entry, RNA replication or protein synthesis. We also observed that E_2 –mediated inhibition of HCV virion production occurs in a dose-dependent manner (Fig. 3b).

A nuclear estrogen receptor antagonist, ICI182780, abolishes E_2-mediated inhibition of HCV virion production

We hypothesized that E_2 signaling through nuclear ER (ERα and ERβ) was involved in the E_2–mediated inhibition of HCV virion production. To test this possibility, we used ICI182780 (1 μM), an antagonist of ERα and ERβ. The results clearly demonstrated that treatment of cells with ICI182780 abolished E_2–mediated inhibition of HCV virion production (Fig. 4).

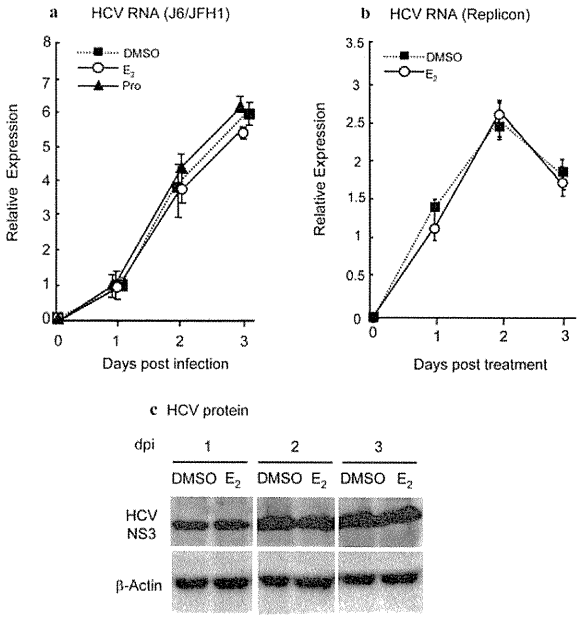

Fig. 2. Effects of E_2 and P_4 on HCV RNA replication and HCV protein synthesis. (a) HCV RNA replication. Huh-7.5 cells were inoculated with HCV at a multiplicity of infection of 1.0, incubated for 2 hr, and cultured for 0, 1, 2 and 3 days after virus infection. The HCV-infected cells were treated with E_2 (0.4 μM) or DMSO (control) from 2 hr to sampling time (days 1, 2 and 3). HCV RNA replication levels were determined by real-time quantitative RT-PCR and normalized with β-actin mRNA levels. Data are shown as mean ± SEM. (b) Huh-7.5 cells harboring a full-genomic HCV RNA replicon (23) were treated with E_2 (0.4 μM) or DMSO, and HCV RNA replication levels determined as in (a). (c) HCV protein synthesis. HCV-infected cells were treated with E2 or DMSO as in (a) and the amount of HCV protein synthesis determined by immunoblot analysis using anti-NS3 antibody. The degree of β-actin expression as determined by anti-β-actin antibody served as a control. dpi, days postinfection.

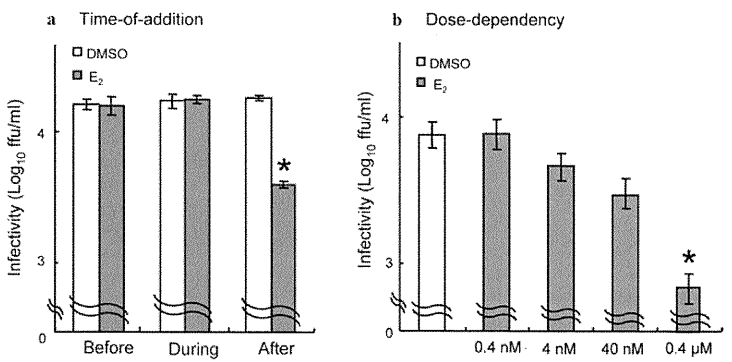

Fig. 3. Kinetic analysis of E_2–mediated inhibition of HCV virion production. (a) Time-of-addition experiment. Huh-7.5 cells were inoculated with HCV at a multiplicity of infection of 1.0, incubated for 2 hr, and cultured up to 2 days after virus infection. Treatment of the cells with E_2 (0.4 μM) was performed before or during virus inoculation for 2 hr, or after virus inoculation until sampling time (day 2). The culture supernatants of HCV-infected cells were assayed for viral infectivity. Data are shown as mean ± SEM. *$P < 0.05$, compared with DMSO control. (b) Dose–dependency experiment. Huh-7.5 cells were inoculated with HCV as in (a). The HCV-infected cells were treated with various concentrations of E_2 (0.4 nM to 0.4 μM]) from 2 hr postinfection to sampling time (day 2). The culture supernatants of HCV-infected cells were assayed for viral infectivity. Data are shown as mean ± SEM. *$P < 0.05$, compared with DMSO control.

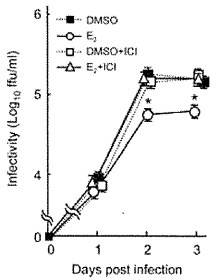

Fig. 4. Effects of ER antagonist, ICI182780, on HCV virion production. Huh-7.5 cells were inoculated with HCV at a multiplicity of infection of 1.0, incubated for 2 hr, and cultured for 0, 1, 2 and 3 days after virus infection. The HCV-infected cells were treated with E_2 (0.4 μM) and/or ICI182780 (1 μM) or DMSO (control) from 2 hr postinfection to sampling time (days 1, 2 and 3). The culture supernatants of HCV-infected cells were assayed for virus infectivity. Data are shown as mean ± SEM. *$P < 0.05$, compared with DMSO control.

Estrogen receptor-α-selective agonist 4, 4′, 4″- (4-propyl-[1H]-pyrazole-1, 3, 5-triyl) trisphenol inhibits HCV virion production

To determine which estrogen receptor(s) is/are involved in the E_2–mediated down-regulation of HCV virion production, we used receptor-specific agonists, such as PPT

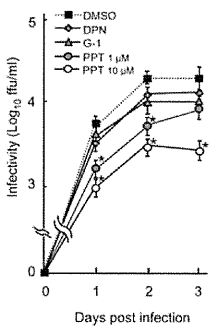

Fig. 5. Effects of ER-specific agonists on HCV virion production. Huh-7.5 cells were inoculated with HCV at a multiplicity of infection of 1.0, incubated for 2 hr, and cultured for 0, 1, 2 and 3 days after virus infection. The HCV-infected cells were treated with PPT (ERα-selective agonist; 1 and 10 μM), DPN (ERβ-selective agonist; 10 μM) or G-1 (GPR30-selective agonist; 1 μM) from 2 hr postinfection to sampling time (days 1, 2 and 3). The culture supernatants of HCV-infected cells were assayed for viral infectivity. Data are shown as mean ± SEM. *$P < 0.05$, compared with DMSO control.

(an ERα-selective agonist) (20), DPN (an ERβ-selective agonist) (21) and G-1 (a GPR30-selective agonist) (22). Treatment of cells with PPT (10 μM), but not with DPN (10 μM) or G-1 (1 μM), significantly inhibited HCV virion production (Fig. 5). PPT treatment at a concentration of 1 μM also brought about a weak, but significant, inhibition of HCV virion production at 2 days postinfection. On the other hand, PPT did not mediate significant cytotoxicity at the concentrations tested (data not shown).

DISCUSSION

We have demonstrated in the present study that treatment of Huh-7.5 cells with E_2 inhibits HCV virion production, but not HCV RNA replication or HCV protein synthesis (Figs 1 and 2). Treatment of the cells with E_2 either prior to, or during, virus inoculation did not significantly suppress HCV virion production (Fig. 3a). These results collectively suggest that E_2 inhibits HCV infection at the virion assembly/secretion level, but not at the level of virus attachment/entry, virus RNA replication or virus protein synthesis. E_2 has been reported to possess antioxidant and anti-apoptotic activities in fibrotic liver and cultured hepatocytes (24, 25). It should be noted, however, that E_2 did not exert anti-apoptotic or cytotoxic (pro-apoptotic) effect under our experimental conditions (Fig. 1b). In contrast to E_2, another female hormone, P_4, did not significantly affect HCV virion production (Fig. 1a).

E_2-mediated inhibition of HCV virion production was abolished by a nuclear ER (ERα and ERβ) antagonist, ICI182780 (Fig. 4), this result suggesting that suppression of HCV virion production may be induced by ER signal transduction. Three types of ER have been reported so far; ERα, ERβ and GPR30 (11–15). To determine which ER is involved in the suppression of HCV virion production, we used ER-specific agonists, PPT (for ERα) (20), DPN (for ERβ) (21) and G-1 (for GPR30) (22). We found that PPT, but not DPN or G-1, inhibits the production of HCV infectious particles (Fig. 5), suggesting that ERα plays an important role in the inhibition of HCV virion production. It has been reported that, in hepatocytes, ERα constitutes a minor proportion of the total ER, and that an estrogen-mediated anti-apoptotic effect is mediated principally through ERβ (26). However, the importance of ERα–mediated signal transduction should not be ignored. The rationale for this assertion is that ERα is known to be involved in lipid metabolism (27), that certain lipid metabolism disorder(s) possibly result(s) in abnormal accumulation of lipid droplets, and that such an accumulation is required for HCV virion maturation in virus-infected cells (27), that certain lipid metabolism disorder(s) possibly result(s) in abnormal accumulation of

lipid droplets, and that such an accumulation is required for HCV virion maturation in virus-infected cells (28). Also, we should not yet exclude the possible importance of ERβ and GPR30, because they may not be expressed at a sufficient level in the Huh7.5 cell line maintained in our laboratory.

Other relevant observations are that ERα interacts with HCV NS5B, the viral RNA polymerase, and promotes association of NS5B with the replication complex in human hepatoma-derived Huh-7 cells, and that tamoxifen, a competitive inhibitor of estrogens, suppresses the ERα–mediated association of NS5B with the replication complex, thereby inhibiting HCV RNA replication (29). Similarly, E_2 binding to ERα may abrogate its interaction with NS5B. However, in our experiments we did not observe E_2–mediated inhibition of HCV RNA replication (Fig. 2a,b). We therefore assume that E_2 inhibits HCV virion production through a mechanism other than E_2–ERα–NS5B interactions. Further study is needed to elucidate this issue.

In conclusion, the most potent physiological estrogen, E_2, inhibits production of HCV infectious particles in Huh-7.5 cell cultures in an ERα–dependent manner. This may explain, at least in part, why the incidence of HCV-associated liver disease is lower in premenopausal women than in postmenopausal women and men.

ACKNOWLEDGMENTS

The authors are grateful to Dr. C. M. Rice for providing Huh7.5 cells and pFL-J6/JFH1. Thanks are also due to Dr. T. Adachi for his technical advice. This study was supported in part by Health and Labor Sciences Research Grants from the Ministry of Health, Labor and Welfare, Japan, and the Japan Science and Technology/Japan International Cooperation Agencies' Science and Technology Research Partnership for Sustainable Development. This study was also carried out as part of the Japan Initiative for Global Research Network on Infectious Diseases, Ministry of Education, Culture, Sports, Science and Technology, Japan, and the Global Center of Excellence Program at Kobe University Graduate School of Medicine.

REFERENCES

1. Shepard C.W., Finelli L., Alter M.J. (2005) Global epidemiology of hepatitis C virus infection. *Lancet Infect Dis* **5:** 558–67.
2. Alberti A., Benvegnù L., Boccato S., Ferrari A., Sebastiani G. (2004) Natural history of initially mild chronic hepatitis C. *Dig Liver Dis* **36:** 646–54.
3. Davis G.L., Alter M.J., El-Serag H., Poynard T., Jennings L.W. (2010) Aging of hepatitis C virus (HCV)-infected persons in the United States: a multiple cohort model of HCV prevalence and disease progression. *Gastroenterology* **138:** 513–21.
4. Armstrong G.L., Wasley A., Simard E.P., McQuillan G.M., Kuhnert W.L., Alter M.J. (2006) The prevalence of hepatitis C virus infection in the United States, 1999 through 2002. *Ann Intern Med* **144:** 705–14.
5. Poynard T., Ratziu V., Charlotte F., Goodman Z., McHutchison J., Albrecht J. (2001) Rates and risk factors of liver fibrosis progression in patients with chronic hepatitis C. *J Hepatol* **34:** 730–9.
6. Massard J., Ratziu V., Thabut D., Moussalli J., Lebray P., Benhamou Y., Poynard T. (2006) Natural history and predictors of disease severity in chronic hepatitis C. *J Hepatol* **44:** S19–24.
7. Di Martino V., Lebray P., Myers R.P., Pannier E., Paradis V., Charlotte F., Moussalli J., Thabut D., Buffet C., Poynard T. (2004) Progression of liver fibrosis in women infected with hepatitis C: long-term benefit of estrogen exposure. *Hepatology* **40:** 1426–33.
8. Shimizu I., Yasuda M., Mizobuchi Y., Ma Y.R., Liu F., Shiba M., Horie T., Ito S. (1998) Suppressive effect of oestradiol on chemical hepatocarcinogenesis in rats. *Gut* **42:** 112–9.
9. Yasuda M., Shimizu I., Shiba M., Ito S. (1999) Suppressive effects of estradiol on dimethylnitrosamine-induced fibrosis of the liver in rats. *Hepatology* **29:** 719–27.
10. Wang C.C., Krantz E., Klarquist J., Krows M., McBride L., Scott E.P., Shaw-Stiffel T., Weston S.J., Thiede H., Wald A., Rosen H.R. (2007) Acute hepatitis C in a contemporary US cohort: modes of acquisition and factors influencing viral clearance. *J Infect Dis* **196:** 1474–82.
11. Hall J.M., Couse J.F., Korach K.S. (2001) The multifaceted mechanisms of estradiol and estrogen receptor signaling. *J Biol Chem* **276:** 36,869–72.
12. Gustafsson J.A. (2003) What pharmacologists can learn from recent advances in estrogen signaling. *Trends Pharmacol Sci* **24:** 479–85.
13. Revankar C.M., Cimino D.F., Sklar L.A., Arterburn J.B., Prossnitz E.R. (2005) A transmembrane intracellular estrogen receptor mediates rapid cell signaling. *Science* **307:** 1625–30.
14. Thomas P., Pang Y., Filardo E.J., Dong J. (2005) Identity of an estrogen membrane receptor coupled to a G protein in human breast cancer cells. *Endocrinology* **146:** 624–32.
15. Maggiolini M., Picard D. (2010) The unfolding stories of GPR30, a new membrane-bound estrogen receptor. *J Endocrinol* **204:** 105–14.
16. Blight K.J., McKeating J.A., Rice C.M. (2002) Highly permissive cell lines for subgenomic and genomic hepatitis C virus RNA replication. *J Virol* **76:** 13001–14.
17. Lindenbach B.D., Evans M.J., Syder A.J., Wolk B., Tellinghuisen T.L., Liu C.C., Maruyama T., Hynes R.O., Burton D.R., McKeating J.A., Rice C.M. (2005) Complete replication of hepatitis C virus in cell culture. *Science* **309:** 623–6.
18. Bungyoku Y., Shoji I., Makine T., Adachi T., Hayashida K., Nagano-Fujii M., Ide Y.H., Deng L., Hotta H. (2009) Efficient production of infectious hepatitis C virus with adaptive mutations in cultured hepatoma cells. *J Gen Virol* **90:** 1681–91.
19. Deng L., Adachi T., Kitayama K., Bungyoku Y., Kitazawa S., Ishido S., Shoji I., Hotta H. (2008) Hepatitis C virus infection induces apoptosis through a Bax-triggered, mitochondrion-mediated, caspase 3-dependent pathway. *J Virol* **82:** 10,375–85.
20. Stauffer S.R., Coletta C.J., Tedesco R., Nishiguchi G., Carlson K., Sun J., Katzenellenbogen B.S., Katzenellenbogen J.A. (2000) Pyrazole ligands: structure-affinity/activity relationships and estrogen receptor-alpha-selective agonists. *J Med Chem* **43:** 4934–47.
21. Meyers M.J., Sun J., Carlson K.E., Marriner G.A., Katzenellenbogen B.S., Katzenellenbogen J.A. (2001) Estrogen receptor-beta potency-selective ligands: structure-activity relationship studies of diarylpropionitriles and their acetylene and polar analogues. *J Med Chem* **44:** 4230–51.
22. Bologa C.G., Revankar C.M., Young S.M., Edwards B.S., Arterburn J.B., Kiselyov A.S., Parker M.A., Tkachenko S.E., Savchuck N.P., Sklar L.A., Oprea T.I., Prossnitz E.R. (2006) Virtual and biomolecular screening converge on a selective agonist for GPR30. *Nat Chem Biol* **2:** 207–12.
23. Kasai D., Adachi T., Deng L., Nagano-Fujii M., Sada K., Ikeda M., Kato N., Ide Y.H., Shoji I., Hotta H. (2009) HCV replication suppresses cellular glucose uptake through down-regulation of cell surface expression of glucose transporters. *J Hepatol* **50:** 883–94.
24. Liu Y., Shimizu I., Omoya T., Ito S., Gu X.S., Zuo J. (2002) Protective effect of estradiol on hepatocytic oxidative damage. *World J Gastroenterol* **8:** 363–6.
25. Lu G., Shimizu I., Cui X., Itonaga M., Tamaki K., Fukuno H., Inoue H., Honda H., Ito S. (2004) Antioxidant and antiapoptotic activities of idoxifene and estradiol in hepatic fibrosis in rats. *Life Sci* **74:** 897–907.
26. Inoue H., Shimizu I., Lu G., Itonaga M., Cui X., Okamura Y., Shono M., Honda H., Inoue S., Muramatsu M., Ito S. (2003) Idoxifene and estradiol enhance antiapoptotic activity through estrogen receptor-beta in cultured rat hepatocytes. *Dig Dis Sci* **48:** 570–80.
27. Cooke P.S., Heine P.A., Taylor J.A., Lubahn D.B. (2001) The role of estrogen and estrogen receptor-alpha in male adipose tissue. *Mol Cell Endocrinol* **178:** 147–54.
28. Miyanari Y., Atsuzawa K., Usuda N., Watashi K., Hishiki T., Zayas M., Bartenschlager R., Wakita T., Hijikata M., Shimotohno K. (2007) The lipid droplet is an important organelle for hepatitis C virus production. *Nat Cell Biol* **9:** 1089–97.
29. Watashi K., Inoue D., Hijikata M., Goto K., Aly H.H., Shimotohno K. (2007) Anti-hepatitis C virus activity of tamoxifen reveals the functional association of estrogen receptor with viral RNA polymerase NS5B. *J Biol Chem* **282:** 32,765–72.

Hepatology Research

Hepatology Research 2010; **40**: 1248–1253 doi: 10.1111/j.1872-034X.2010.00730.x

Short Communication

Gene expression profile of Li23, a new human hepatoma cell line that enables robust hepatitis C virus replication: Comparison with HuH-7 and other hepatic cell lines

Kyoko Mori,* Masanori Ikeda, Yasuo Ariumi and Nobuyuki Kato*

Department of Tumor Virology, Okayama University Graduate School of Medicine, Dentistry and Pharmaceutical Sciences, Okayama, Japan

Aim: Human hepatoma cell line HuH-7-derived cells are currently the only cell culture system used for robust hepatitis C virus (HCV) replication. We recently found a new human hepatoma cell line, Li23, that enables robust HCV replication. Although both cell lines had similar liver-specific expression profiles, the overall profile of Li23 seemed to differ considerably from that of HuH-7. To understand this difference, the expression profile of Li23 cells was further characterized by a comparison with that of HuH-7 cells.

Methods: cDNA microarray analysis using Li23 and HuH-7 cells was performed. Li23-derived ORL8c cells and HuH-7-derived RSc cells, in which HCV could infect and efficiently replicate, were also used for the microarray analysis. For the comparative analysis by reverse transcription polymerase chain reaction (RT–PCR), human hepatoma cell lines (HuH-6, HepG2, HLE, HLF and PLC/PRF/5) and immortalized hepatocyte cell line (PH5CH8) were also used.

Results: Microarray analysis of Li23 versus HuH-7 cells selected 80 probes to represent highly expressed genes that have ratios of more than 30 (Li23/HuH-7) or 20 (HuH-7/Li23). Among them, 17 known genes were picked up for further analysis. The expression levels of most of these genes in Li23 and HuH-7 cells were retained in ORL8c and RSc cells, respectively. Comparative analysis by RT–PCR using several other hepatic cell lines resulted in the classification of 17 genes into three types, and identified three genes showing Li23-specific expression profiles.

Conclusion: Li23 is a new hepatoma cell line whose expression profile is distinct from those of frequently used hepatic cell lines.

Key words: hepatitis C virus, hepatoma cell line, HuH-7, Li23, microarray

INTRODUCTION

HUH-7, A HUMAN hepatoma cell line,[1] is frequently used in the research of hepatitis C virus (HCV), since an HCV replicon system enabling HCV subgenomic RNA replication was developed using HuH-7 cells.[2] Even with the use of an efficient HCV production system developed in 2005,[3] HuH-7-derived cells are still used as the only cell line for persistent HCV production systems.

We previously developed HCV replicon systems[4,5] and an HCV production system[6] using HuH-7-derived cells. Furthermore, we recently found a new human hepatoma cell line, Li23, that enables robust HCV RNA replication and persistent HCV production.[7] In that study, using microarray analysis, we excluded the possibility that the obtained Li23-derived cells were derived from contamination of HuH-7-derived cells used for HCV replication.[7] In addition, we noticed that the gene expression profile of Li23 cells seemed considerably different from that of HuH-7 cells. Therefore, we assumed that the Li23 cell line possesses a unique expression profile among widely used human hepatoma cell lines. To evaluate this assumption, we further characterized the expression profile of Li23 cells by comparing it with those of other human hepatoma cell lines, including HuH-7,[1] HuH-6,[8] HepG2,[9] HLE,[10] HLF[10] and PLC/PRF/5.[11] Human immortalized hepatocyte cell line PH5CH8[12] was also used for the comparison. Here, we show that the Li23 cell line possesses a distinct expression profile among hepatic cell lines.

Correspondence: Professor Nobuyuki Kato, Department of Tumor Virology, Okayama University Graduate School of Medicine, Dentistry and Pharmaceutical Sciences, Okayama 700-8558, Japan. Email: nkato@md.okayama-u.ac.jp

*These authors contributed equally to this work.

Received 21 July 2010; revision 16 August 2010; accepted 17 August 2010.

METHODS

Cell culture

HUH-7, HUH-6, HEPG2, HLE, HLF and PLC/PRF/5 cells were cultured in Dulbecco's modified Eagle's medium supplemented with 10% fetal bovine serum. Li23 and PH5CH8 cells were maintained as described previously.[7] Cured cells (Li23-derived ORL8c and HuH-7-derived RSc), from which the HCV RNA had been eliminated by interferon (IFN) treatment, were also maintained as described previously.[7]

cDNA microarray analysis

Li23, ORL8c, HuH-7 and RSc cells (1×10^6 each) were plated onto 10-cm diameter dishes and cultured for 2 days. Total RNA from these cells were prepared using the RNeasy extraction kit (QIAGEN, Hilden, Germany). cDNA microarray analysis was performed according to the methods described previously.[7] Differentially expressed genes were selected by comparing the arrays from Li23 and HuH-7 cells. The selected genes were further compared with the array from ORL8c or RSc cells.

Reverse transcription polymerase chain reaction

Reverse transcription polymerase chain reaction (RT–PCR) was performed to detect cellular mRNA as described previously.[13] Briefly, total RNA (2 μg) was reverse-transcribed with M-MLV reverse transcriptase (Invitrogen, San Diego, CA, USA) using an oligo dT primer (Invitrogen) according to the manufacturer's protocol. One-tenth of the synthesized cDNA was used for PCR. The primers arranged for this study are listed in Table 1. In addition, we used primer sets for New York esophageal squamous cell carcinoma 1 (NY-ESO-1), β-defensin-1 (DEFB1), lectin, galactoside-binding, soluble 3 (LGALS3)/Galectin-3, melanoma-specific antigen family A6 (MAGEA6), UDP glycosyltransferase 2 family polypeptide B4 (UGT2B4), transmembrane 4 superfamily member 3 (TM4SF3), insulin-like growth factor binding protein 2 (IGFBP2), arylacetamide deacetylase (AADAC), albumin and glyceraldehyde-3-phosphate dehydrogenase (GAPDH), as described previously.[7]

RESULTS

Genes showing pronounced differences in gene expression between Li23- and HuH-7-derived cells

WE RECENTLY ESTABLISHED several Li23-derived cell lines showing robust HCV RNA replication.[7] In convenient microarray analysis using these cell lines, we noticed that the gene expression profile of Li23 cells differed considerably from that of HuH-7 cells, and that several genes, including cancer antigens such as NY-ESO-1 and MAGEA6, were highly expressed in Li23 cells but were not expressed in HuH-7 cells.[7] However, it

Table 1 Primers used for reverse transcription polymerase chain reaction analysis

Gene (accession no.)	Direction	Nucleotide sequence (5′–3′)	Products (bp)
Cancer antigen 45, A5	Forward	TGGAGATGACCTAGAATGCAG	218
(CT45A5); NM_001007551	Reverse	CTCGTCTCATACATCTTGCTG	
Four-and-a-half LIM domain 1	Forward	GGAATCACTTACCAGGATCAG	243
(FHL1; NM_001449)	Reverse	TTTGCAGTGGAAGCAGTAGTC	
Thymosin β4, X-linked	Forward	ACCAGACTTCGCTCGTACTC	179
(TMSB4X; NM_021109)	Reverse	TCGCCTGCTTGCTTCTCCTG	
Lectin, galactoside-binding, soluble 1	Forward	CAACACCATCGTGTGCAACAG	253
(LGALS1; NM_002305)	Reverse	CAGCTGCCATGTAGTTGATGG	
Interferon-induced transmembrane protein 2	Forward	CCTCTTCATGAACACCTGCTG	184
(IFITM2; NM_006435)	Reverse	CACTGGGATGATGATGAGCAG	
Apolipoproteins A1	Forward	ACTGTGTACGTGGATGTGCTC	273
(APOA1; X02162)	Reverse	CTTCTTCTGGAAGTCGTCCAG	
α-2-HS-glycoprotein	Forward	AACCGAACTGCGATGATCCAG	248
(AHSG; NM_001622)	Reverse	TTCGACAGCATGCTCCTTCAG	
Gap junction protein-α 1	Forward	CATCTTCATGCTGGTGGTGTC	253
(GJA1; NM_000165)	Reverse	GTTTCTGTCGCCAGTAACCAG	

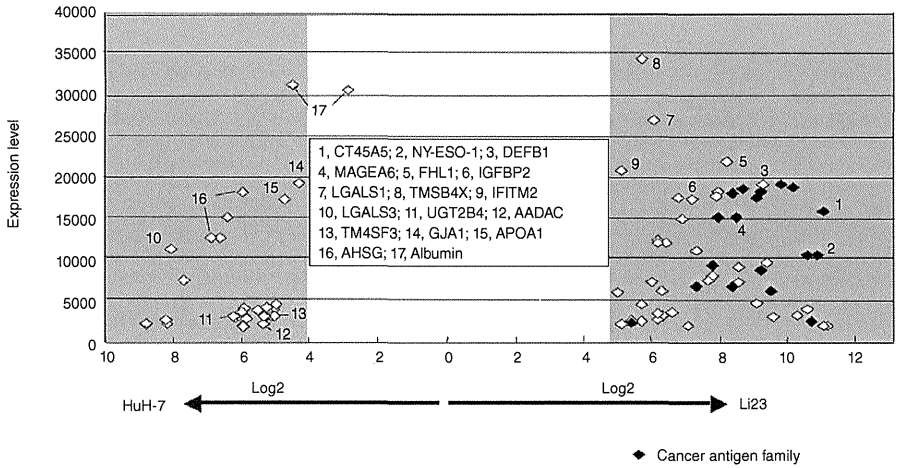

Figure 1 Genes showing pronounced differences in gene expression between Li23 and HuH-7 cells. The probes showing expression levels of more than 2000 and ratios of more than 30 (Li23/HuH-7) or 20 (HuH-7/Li23) are presented.

is unclear whether the expression profiles of these genes are characteristics of Li23 cells.

To clarify this point, comprehensive microarray analysis using Li23 and HuH-7 cells was performed. This revealed 4119 and 3570 probes whose expression levels were upregulated and downregulated at ratios of more than 2 and less than 0.5 in Li23 versus HuH-7 cells, respectively. From among these probes, we selected those showing ratios of more than 30 (Li23/HuH-7) and 20 (HuH-7/Li23), and further selected the probes showing expression levels of more than 2000 (actual value of measurement). By these selections, 80 probes were assigned (Fig. 1). The most distinguishing characteristic of the comparison is that the cancer antigen family (18 probes) was highly expressed in Li23 cells but was not highly expressed in HuH-7 cells (Fig. 1). From these probes, 14 known genes showing expression levels above 10 000 (#1–10 and #14–17 in Fig. 1) and three additional known genes (#11–13 in Fig. 1) were chosen as representative genes for further analysis.

Regarding the total of 17 genes, the expression levels in Li23 versus ORL8c or HuH-7 versus RSc were compared. The expression levels of most of the 17 genes were maintained between Li23 and ORL8c cells or between HuH-7 and RSc cells (Table 2). These results indicate that ORL8c and RSc cells retained the characteristics of parent Li23 and HuH-7 cells, respectively. However, it was notable that the expression levels of apolipoprotein A1 (APOA1), α-2-HS-glycoprotein (AHSG), and albumin were significantly higher in ORL8c cells than in Li23 cells, suggesting that ORL8c is selected as a specific clone from Li23 cell populations.

Expression profiles of representative genes whose expression levels showed drastic differences between Li23 and HuH-7 cells among human hepatic cell lines

Regarding the 17 genes selected above, we performed comparative analyses by RT–PCR using Li23, HuH-7, HuH-6, HepG2, HLE, HLF, PLC/PRF/5 and PH5CH8 cells in order to clarify whether or not these genes exhibit Li23-specific expression profiles. The results of the RT–PCR performed after optimization of PCR conditions in each gene resulted in the classification of the 17 genes into three types (A, B and C in Fig. 2). NY-ESO-1 and DEFB1 (high expression in Li23 only), and LGALS3/Galectin-3 (no expression in Li23 only) belonged to type A, which showed a Li23-specific feature. Type B showed that the expression levels in Li23, HLE, HLF, PLC/PRF/5 and/or PH5CH8 cells were greatly higher or lower than those in HuH-7, HuH-6 and HepG2 cells. Type B consisted of cancer antigen 45, A5 (CT45A5), MAGEA6, four-and-a-half LIM domains 1 (FHL1), Thymosin B4, X-linked (TMSB4X), lectin, galactoside-binding, soluble 1 (LGALS1) and IFN-induced transmembrane protein 2 (IFITM2) – all of which were highly expressed in Li23 cells – and APOA1, AHSG and UGT2B4, which were highly expressed in HuH-7 cells. The remaining five genes were assigned to type C and showed more complex expression profiles (Fig. 2). For instance, Gap junction protein-α 43 kDa (GJA1) expression was observed in HuH-7, HLE, HLF, PLC/PRF/5 and PH5CH8 cell lines, but not in Li23, HuH-6 or HepG2 cell lines. In addition, IGFBP2 expression was observed in Li23, HuH-6 and PH5CH8 cell lines, but not in the other cell lines. Together, these results indicate that the Li23 cell line possesses a distinct expression profile among frequently used hepatic cell lines.

Table 2 Representative genes showing pronounced differences in gene expression between Li23 and HuH-7 cells

Gene	Accession no.	Li23	Li23-derived ORL8c	HuH-7	HuH-7-derived RSc
Cancer antigen 45, A5 (CT45A5)	NM_001007551	15 857†	10 508	8	23
Cancer testis antigen 1A (NY-ESO-1/CTAG1A)	U87459	9 005	5 503	5	8
β-Defensin-1 (DEFB1)	U73945	18 311	8 326	31	7
Melanoma-specific antigen family A6 (MAGEA6)	U10691	15 168	17 050	42	35
Four-and-a-half LIM domain 1 (FHL1)	NM_001449	21 851	13 428	77	79
Insulin-like growth factor binding protein 2 (IGFBP2)	NM_000597	17 429	8 931	117	13
Lectin, galactoside-binding, soluble 1 (LGALS1)	NM_002305	26 694	27 098	379	11
Thymosin β4, X-linked (TMSB4X)	NM_021109	34 273	26 199	648	307
IFN-induced transmembrane protein 2 (IFITM2)	NM_006435	20 762	9 645	595	637
Lectin, galactoside-binding, soluble 3 (LGALS3/Galectin 3)	BC001120	41	70	10 973	6 020
UDP glycosyltransferase 2 family polypeptide B4 (UGT2B4)	NM_021139	40	57	2 863	7 546
Arylacetamide deacetylase (AADAC)	NM_001086	57	73	2 282	4 746
Transmembrane 4 superfamily member 3 (TM4SF3)	NM_004616	95	51	3 220	1 265
Gap junction protein-α 43 KDa (GJA1)	NM_000165	951	2	19 090	19 485
Apolipoprotein A1 (APOA1)	X02162	673	7 230	16 920	15 202
α-2-HS-glycoprotein (AHSG)	NM_001622	308	6 373	18 436	26 000
Albumin	AF116645	4 304	30 111	30 234	33 140
	D16931	1 387	23 615	30 668	39 144

†Signal intensity in human genome U133 Plus 2.0 array.

DISCUSSION

IN THIS STUDY, we assigned 17 known genes that showed drastic differences between Li23 and HuH-7 cells, and classified the expression profiles of these genes into at least three types among frequently used hepatic cell lines. Three genes (NY-ESO-1, DEFB1 and LGALS3/Galectin-3) were identified as the representative showing Li23-specific expression.

NY-ESO-1 is a well-characterized cancer-testis antigen (CTAG) that appears to be the most immunogenic CTAG known to date.[14] NY-ESO-1 is expressed in malignant tumors such as melanoma, lung carcinoma and bladder cancer, which are called "CTAG-rich" tumor types, but are expressed solely in the testis among normal adult tissues.[15] Because a spontaneous immune response to NY-ESO-1 is frequently observed in patients with malignant tumors including hepatocellular carcinoma,[16] cancer vaccine trials based on NY-ESO-1 are currently underway.[15] However, the biological role of NY-ESO-1 in both tumors and testis remains poorly understood. Accordingly, the Li23 cell line may be useful for the study of the biological role of NY-ESO-1.

Human defensins, which are small cationic peptides produced by neutrophils and epithelial cells, form two genetically distinct subfamilies, α-defensin and β-defensin. DEFB1, identified in this study, is one of six members belonging to β-defensins and appears to be involved in the antimicrobial defense of the epithelia of surfaces.[16,17] Although α-defensins consisting of six members are known to be expressed in a variety of tumors, DEFB1 is downregulated in some tumor types in which it could behave as a tumor suppressor protein.[18] Our study revealed that except DEFB1 in Li23 cells, no α- or β-defensin members were expressed in the

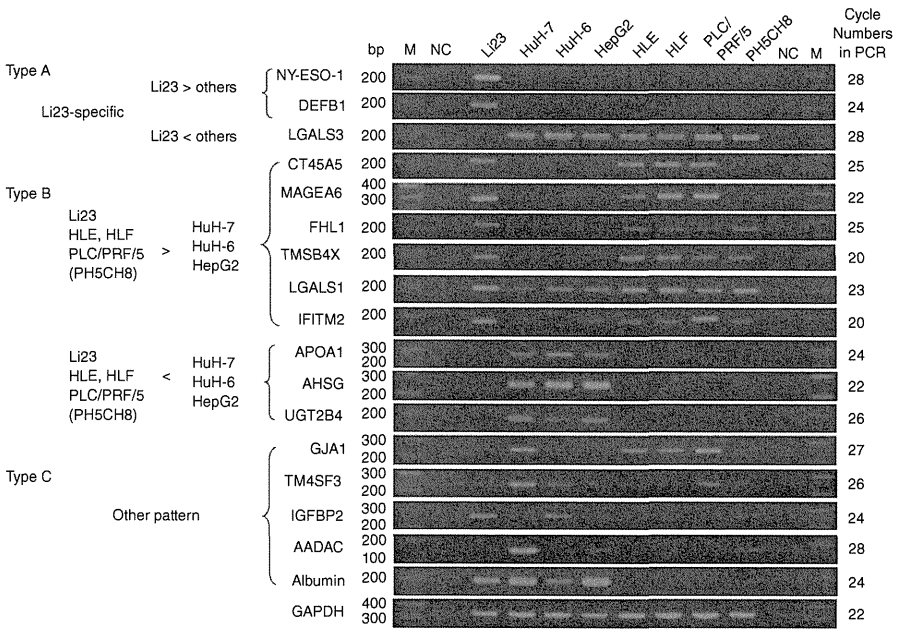

Figure 2 Expression profiles of representative genes, whose expression levels showed drastic differences between Li23 and HuH-7 cells, among human hepatic cell lines. Reverse transcription polymerase chain reaction (RT–PCR) analysis was performed as described in Methods. PCR products were detected by staining with ethidium bromide after separation by electrophoresis on 3% agarose gels.

hepatic cell lines tested in this study (data not shown). Because the molecular mechanism underlying DEFB1 expression or its role in oncogenesis remains to be clarified, Li23 cells may be useful for a study like that.

LGALS3/Galectin-3 is the most studied member of the galectin family, which is characterized by specific binding of β-galactosides through the carbohydrate-recognition domain.[19] LGALS3/Galectin-3 is ubiquitously expressed in numerous cell and tissue types; it is located in both nuclei and cytoplasm, and is secreted through a non-classical pathway. To date, LGALS3/Galectin-3 was found to be involved in many regulations including development, immune reaction, tumorigenesis, and tumor growth and metastasis.[19,20] Indeed, the overexpression of LGALS3/Galectin-3 in cirrhotic and hepatocellular carcinoma has also been reported.[21] In such situations, the absence of LGALS3/Galectin-3 expression in the Li23 cell line is a unique feature among hepatic cell lines, which show high expression levels. Accordingly, the Li23 cell line might be useful as a LGALS3/Galectin-3-null cell line for various studies including those on tumor growth and metastasis.

Although we identified Li23-specific genes showing distinct expression levels among hepatic cell lines examined, microarray analysis revealed that the expression profiles of Li23 and HuH-7 cells, both of which possess an environment for robust HCV replication, differed considerably. Accordingly, such differences may affect the properties or multiplications of HCV, such as susceptibility to anti-HCV reagents, the mutation rate of the HCV genome and the efficiency of HCV replication. Further comparative analysis using Li23 and HuH-7 cells will help to resolve these uncertain subjects.

ACKNOWLEDGMENTS

WE THANK NAOKO Kawahara for her technical assistance. This work was supported by a Grant-in-Aid for research on hepatitis from the Ministry of Health, Labor and Welfare of Japan. K. M. was supported by a Research Fellowship from the Japan Society for Promotion of Science for Young Scientists.

REFERENCES

1 Nakabayashi H, Taketa K, Miyano K, Yamane T, Sato J. Growth of human hepatoma cells lines with differentiated functions in chemically defined medium. *Cancer Res* 1982; **42:** 3858–63.
2 Lohmann V, Körner F, Koch J-O, Herian U, Theilman L, Bartenschlager R. Replication of subgenomic hepatitis C virus RNAs in a hepatoma cell line. *Science* 1999; **285:** 110–13.
3 Wakita T, Pietschmann T, Kato T *et al.* Production of infectious hepatitis C virus in tissue culture from a cloned viral genome. *Nat Med* 2005; **11:** 791–6.
4 Kato N, Sugiyama K, Namba K *et al.* Establishment of a hepatitis C virus subgenomic replicon derived from human hepatocytes infected in vitro. *Biochem Biophys Res Commun* 2003; **306:** 756–66.
5 Ikeda M, Abe K, Dansako H, Nakamura T, Naka K, Kato N. Efficient replication of a full-length hepatitis C virus genome, strain O, in cell culture, and development of a luciferase reporter system. *Biochem Biophys Res Commun* 2005; **329:** 1350–9.
6 Ariumi Y, Kuroki M, Abe K *et al.* DDX3 DEAD-box RNA helicase is required for hepatitis C virus RNA replication. *J Virol* 2007; **81:** 13922–6.
7 Kato N, Mori K, Abe K *et al.* Efficient replication systems for hepatitis C virus using a new human hepatoma cell line. *Virus Res* 2009; **146:** 41–50.
8 Tokiwa T, Doi I, Sato J. Preparation of single cell suspensions from hepatoma cells in culture. *Acta Med Okayama* 1975; **29:** 147–50.
9 Aden DP, Fogel A, Plotkin S, Damjanov I, Knowles BB. Controlled synthesis of HBsAg in a differentiated human liver carcinoma-derived cell line. *Nature* 1979; **282:** 615–16.
10 Doi I, Nambe M, Sato J. Establishment and some biological characteristics of human hepatoma cell lines. *Gann* 1975; **66:** 385–92.
11 Alexander JJ, Bey EM, Geddes EW, Lecatsaa G. Establishment of a continuously growing cell line from primary carcinoma of the liver. *S Afr Med J* 1976; **50:** 2124–8.
12 Ikeda M, Sugiyama K, Mizutani T *et al.* Human hepatocyte clonal cell lines that support persistent replication of hepatitis C virus. *Virus Res* 1998; **56:** 157–67.
13 Dansako H, Naganuma A, Nakamura T, Ikeda F, Nozaki A, Kato N. Differential activation of interferon-inducible genes by hepatitis C virus core protein mediated by the interferon stimulated response element. *Virus Res* 2003; **97:** 17–30.
14 Yoshida N, Abe H, Ohkuri T *et al.* Expression of the MAGE-A4 and NY-ESO-1 cancer-testis antigens and T cell infiltration in non-small cell lung carcinoma and their prognostic significance. *Int J Oncol* 2006; **28:** 1089–98.
15 Caballero OL, Chen YT. Cancer/testis (CT) antigens: potential targets for immunotherapy. *Cancer Sci* 2009; **100:** 2014–21.
16 Korangy F, Ormandy LA, Bleck JS *et al.* Spontaneous tumor-specific humoral and cellular immune responses to NY-ESO-1 in hepatocellular carcinoma. *Clin Cancer Res* 2004; **10:** 4332–41.
17 Bensch KW, Raida M, Magert HJ, Schulz-Knappe P, Forssmann WG. HBD-1: a novel bta-defensin from human plasma. *FEBS Lett* 1995; **368:** 331–5.
18 Droin N, Hendra JB, Ducoroy P, Solary E. Human defensins as cancer biomarkers and antitumour molecules. *J Proteomics* 2009; **72:** 918–27.
19 Dumic J, Dabelic S, Flögel M. Galectin-3: an open-ended story. *Biochim Biophys Acta* 2006; **1760:** 616–35.
20 Danguy A, Camby I, Kiss R. Galectins and cancer. *Biochim Biophys Acta* 2002; **1572:** 285–93.
21 Hsu DK, Dowling CA, Jeng KC, Chen JT, Yang RY, Liu FT. Galectin-3 expression is induced in cirrhotic liver and hepatocellular carcinoma. *Int J Cancer* 1999; **81:** 519–26.

The ESCRT System Is Required for Hepatitis C Virus Production

Yasuo Ariumi[1]*, Misao Kuroki[1], Masatoshi Maki[2], Masanori Ikeda[1], Hiromichi Dansako[1], Takaji Wakita[3], Nobuyuki Kato[1]

1 Department of Tumor Virology, Okayama University Graduate School of Medicine, Dentistry, and Pharmaceutical Sciences, Okayama, Japan, **2** Department of Applied Molecular Biosciences, Graduate School of Bioagricultural Sciences, Nagoya University, Nagoya, Japan, **3** Department of Virology II, National Institute of Infectious Diseases, Tokyo, Japan

Abstract

Background: Recently, lipid droplets have been found to be involved in an important cytoplasmic organelle for hepatitis C virus (HCV) production. However, the mechanisms of HCV assembly, budding, and release remain poorly understood. Retroviruses and some other enveloped viruses require an endosomal sorting complex required for transport (ESCRT) components and their associated proteins for their budding process.

Methodology/Principal Findings: To determine whether or not the ESCRT system is needed for HCV production, we examined the infectivity of HCV or the Core levels in culture supernatants as well as HCV RNA levels in HuH-7-derived RSc cells, in which HCV-JFH1 can infect and efficiently replicate, expressing short hairpin RNA or siRNA targeted to tumor susceptibility gene 101 (TSG101), apoptosis-linked gene 2 interacting protein X (Alix), Vps4B, charged multivesicular body protein 4b (CHMP4b), or Brox, all of which are components of the ESCRT system. We found that the infectivity of HCV in the supernatants was significantly suppressed in these knockdown cells. Consequently, the release of the HCV Core into the culture supernatants was significantly suppressed in these knockdown cells after HCV-JFH1 infection, while the intracellular infectivity and the RNA replication of HCV-JFH1 were not significantly affected. Furthermore, the HCV Core mostly colocalized with CHMP4b, a component of ESCRT-III. In this context, HCV Core could bind to CHMP4b. Nevertheless, we failed to find the conserved viral late domain motif, which is required for interaction with the ESCRT component, in the HCV-JFH1 Core, suggesting that HCV Core has a novel motif required for HCV production.

Conclusions/Significance: These results suggest that the ESCRT system is required for infectious HCV production.

Citation: Ariumi Y, Kuroki M, Maki M, Ikeda M, Dansako H, et al. (2011) The ESCRT System Is Required for Hepatitis C Virus Production. PLoS ONE 6(1): e14517. doi:10.1371/journal.pone.0014517

Editor: Gian Maria Fimia, INMI, Italy

Received May 6, 2010; **Accepted** December 15, 2010; **Published** January 11, 2011

Funding: This work was supported by a Grant-in-Aid for Scientific Research (C) from the Japan Society for the Promotion of Science (JSPS), by a Grant-in-Aid for Research on Hepatitis from the Ministry of Health, Labor, and Welfare of Japan, by the Viral Hepatitis Research Foundation of Japan, by the Kawasaki Foundation for Medical Science, Medical Welfare, by the Okayama Medical Foundation, and by Ryobi Teien Memory Foundation. MK was supported by a Research Fellowship from the JSPS for Young Scientists. The funders had no role in study design, data collection and analysis, decision to publish, or preparation of the manuscript.

Competing Interests: The authors have declared that no competing interests exist.

* E-mail: ariumi@md.okayama-u.ac.jp

Introduction

Hepatitis C virus (HCV) is a causative agent of chronic hepatitis, which progresses to liver cirrhosis and hepatocellular carcinoma. HCV is an enveloped virus with a positive single stranded 9.6 kb RNA genome, which encodes a large polyprotein precursor of approximately 3,000 amino acid residues. This polyprotein is cleaved by a combination of the host and viral proteases into at least 10 proteins in the following order: Core, envelope 1 (E1), E2, p7, nonstructural protein 2 (NS2), NS3, NS4A, NS4B, NS5A, and NS5B [1]. HCV Core, a highly basic RNA-binding protein, forms a viral capsid and is targeted to lipid droplets [2–6]. The Core is essential for infectious virion production [7]. NS5A, a membrane-associated RNA-binding phosphoprotein, is also involved in the assembly and maturation of infectious HCV particles [8,9]. Intriguingly, NS5A is a key regulator of virion production through the phosphorylation by casein kinase II [9]. Recently, lipid droplets have been found to be involved in an important cytoplasmic organelle for HCV production [4]. Indeed, NS5A is known to colocalize with the Core on lipid droplets [5], and the interaction between NS5A and the Core is critical for the production of infectious HCV particles [3]. However, the host factor involved in HCV assembly, budding, and release remains poorly understood.

Budding is an essential step in the life cycle of enveloped viruses. Endosomal sorting complex required for transport (ESCRT) components and associated factors, such as tumor susceptibility gene 101 (TSG101, a component of ESCRT-I), charged multivesicular body protein 4b (CHMP4b, a component of ESCRT-III), and apoptosis-linked gene 2 interacting protein X (ALIX, a TSG101- and CHMP4b-binding protein), have been found to be involved in membrane remodeling events that accompany endosomal protein sorting, cytokinesis, and the budding of several enveloped viruses, such as human immunodeficiency virus type 1 (HIV-1) [10–12]. The ESCRT complexes I, II, and III are sequentially, or perhaps concentrically recruited to the endosomal membrane to sequester cargo proteins and drive vesicularization into the endosome. Finally, ESCRT-III recruits Vps4 (two isoforms, Vps4A and Vps4B), a member of the AAA-family of ATPase that disassembles and thereby terminates and recycles the ESCRT machinery.

Since HCV is also an enveloped RNA virus, we hypothesized that the ESCRT system might be required for HCV production. To test this hypothesis, we examined the release of HCV Core into culture supernatants from cells rendered defective for ESCRT components by RNA interference. The results provide evidence that the ESCRT system is required for HCV production.

Materials and Methods

Cell Culture

293FT cells (Invitrogen, Carlsbad, CA) were cultured in Dulbecco's modified Eagle's medium (DMEM; Invitrogen) supplemented with 10% fetal bovine serum (FBS). The HuH-7-derived cell line, RSc cured cells that cell culture-generated HCV-JFH1 (JFH1 strain of genotype 2a) [13] could infect and effectively replicate [14–16] and OR6c and OR6 cells harboring the genome-length HCV-O RNA with luciferase as a reporter were cultured in DMEM with 10% FBS as described previously [17,18].

Plasmid Construction

To construct pcDNA3-FLAG-Alix, a DNA fragment encoding Alix was amplified from total RNAs derived from RSc cells by RT-PCR using the follwing pairs of primers: Forward 5′-CGGGATCCAAGATGGCGACATTCATCTCGGT-3′ and reverse 5′-CCGGCGGCCGCTTACTGCTGTGGATAGTAAG-3′. The obtained DNA fragment was subcloned into *Bam*HI-*Not*I of pcDNA3-FLAG vector [19], and the nucleotide sequences were determined by Big Dye termination cycle sequencing using an ABI Prism 310 genetic analyzer (Applied Biosystems, Foster City, CA, USA). The plasmid of pJRN/3-5B was based on pJFH1 [13] and was constructed as previously described [20].

RNA synthesis, RNA transfection, and Selection of G418-resistant cells

Plasmid pJRN/3-5B were linearized by *Xba*I and used for the RNA synthesis with the T7 MEGAScript kit (Ambion, Austin, TX). *In vitro* transcribed RNA was transfected into OR6c cells by electroporation [17,18]. The transfected cells were selected in culture medium containing G418 (0.3 mg/ml) for 3 weeks. We referred to them as OR6c/JRN 3-5B cells.

Immunofluorescence and Confocal Microscopic Analysis

Cells were fixed in 3.6% formaldehyde in phosphate-buffered saline (PBS) and permeabilized in 0.1% Nonidet P-40 (NP-40) in PBS at room temperature as previously described [21]. Cells were incubated with anti-HCV Core antibody (CP-9 and CP-11 mixture; Institute of Immunology, Tokyo, Japan), anti-Myc-Tag antibody (PL14; Medical & Biological Laboratories, MBL, Nagoya, Japan), anti-Alix antibody (Covalab, Villeurbanne, France), and/or anti-FLAG polyclonal antibody (Sigma, St. Louis, MO) at a 1:300 dilution in PBS containing 3% bovine serum albumin (BSA) at 37°C for 30 min. Cells were then stained with fluorescein isothiocyanate (FITC)-conjugated anti-rabbit antibody (Jackson ImmunoResearch, West Grove, PA) or anti-Cy3-conjugated anti-mouse antibody (Jackson ImmunoResearch) at a 1:300 dilution in PBS containing BSA at 37°C for 30 min. Lipid droplets and nuclei were stained with BODIPY 493/503 (Molecular Probes, Invitrogen) and DAPI (4′,6′-diamidino-2-phenylindole), respectively. Following extensive washing in PBS, cells were mounted on slides using a mounting media of 90% glycerin/10% PBS with 0.01% *p*-phenylenediamine added to reduce fading. Samples were viewed under a confocal laser-scanning microscope (LSM510; Zeiss, Jena, Germany).

RNA Interference

The following siRNAs were used: human TSG101 (siGENOME SMARTpool M-003549-01-0005 and 5′-CCUCCAGUCUUCUCUCGUCUU-3′ sense, 5′-GACGAGAGAAGACUGGAGGUU-3′ antisense), human Alix/PDCD6IP (siGENOME SMARTpool M-004233-02-0005), human Vps4B (siGENOME SMARTpool M-013119-02-0005), human CHMP4b (siGENOME SMARTpool M-018075-00-0005), and siGENOME Non-Targeting siRNA Pool#1 (D-001206-13-05) (Dharmacon, Thermo Fisher Scientific, Waltham, MA) as a control. siRNAs (50 nM final concentration) were transiently transfected into either RSc cells [14–16] or OR6 cells [17,18] using Oligofectamine (Invitrogen) according to the manufacturer's instructions. Oligonucleotides with the following sense and antisense sequences were used for the cloning of short hairpin (sh) RNA-encoding sequences against TSG101, Alix, Vps4B, or CHMP4b in lentiviral vector: TSG101i, 5′-GATCCCC GGAGGAAATGGATCGTGCCTTCAAGAGAGGCACGATCCATTTCCTCCTTTTTGGAAA-3′ (sense), 5′-AGCTTTTCCAAAAAGGAGGAAATGGATCGTGCCTCTCTTGAAGGCACGATCCATTTCCTCCGGG-3′ (antisense); Alixi, 5′-GATCCCC GGAGGTGTTCCCTGTCTTGTTCAAGAGACAAGACAGGGAACACCTCCTTTTTGGAAA-3′ (sense), 5′-AGCTTTTCCAAAAAGGAGGTGTTCCCTGTCTTGTCTCTTGAACAAGACAGGGAACACCTCCGGG-3′ (antisense); Vps4Bi, 5′-GATCCCC GGAGAATCTGATGATCCTGTTCAAGAGACAGGATCATCAGATTCTCCTTTTTGGAAA-3′ (sense), 5′-AGCTTTTCCAAAAAGGAGAATCTGATGATCCTGTCTCTTGAACAGGATCATCAGATTCTCCGGG-3′ (antisense); CHMP4bi, 5′-GATCCCC GAGGAGGACGACGACATGATTCAAGAGATCATGTCGTCGTCCTCCTCTTTTTGGAAA-3′ (sense), 5′-AGCTTTTCCAAAAAGAGGAGGACGACGACATGATCTCTTGAATCATGTCGTCGTCCTCCTCGGG-3′ (antisense); Broxi, 5′-GATCCCCGGATGACAGTACTAAACCCTTCAAGAGAGGGTTTAGTACTGTCATCCTTTTTGGAAA-3′ (sense), 5′-AGCTTTTCCAAAAAGGATGACAGTACTAAACCCTCTCTTGAAGGGTTTAGTACTGTCATCCGGG-3′ (antisense). The oligonucleotides above were annealed and subcloned into the *Bgl*II-*Hin*dIII site, downstream from an RNA polymerase III promoter of pSUPER [22], to generate pSUPER-TSG101i, pSUPER-Alixi, pSUPER-Vps4Bi, and pSUPER-CHMP4bi, respectively. To construct pLV-TSG101i, pLV-Alixi, pLV-Vps4Bi, and pLV-CHMP4bi, the *Bam*HI-*Sal*I fragments of the corresponding pSUPER plasmids were subcloned into the *Bam*HI-*Sal*I site of pRDI292 [23], an HIV-1-derived self-inactivating lentiviral vector containing a puromycin resistant marker allowing for the selection of transduced cells, respectively.

Lentiviral Vector Production

The vesicular stomatitis virus (VSV)-G-pseudotyped HIV-1-based vector system has been described previously [24–26]. The lentiviral vector particles were produced by transient transfection of the second-generation packaging construct pCMV-ΔR8.91 [24–26] and the VSV-G-envelope-expressing plasmid pMDG2 as well as pRDI292 into 293FT cells with FuGene6 (Roche Diagnostics, Basel, Switzerland).

HCV Infection Experiments

The supernatants was collected from cell culture-generated HCV-JFH1 [13]-infected RSc cells [14–16] at 5 days post-

infection and stored at −80°C after filtering through a 0.45 μm filter (Kurabo, Osaka, Japan) until use. For infection experiments with HCV-JFH1 virus, RSc cells (1×10^5 cells/well) were plated onto 6-well plates and cultured for 24 hours (hrs). Then, we infected the cells with 50 μl (equivalent to a multiplicity of infection [MOI] of 0.1) of inoculum. The culture supernatants were collected and the levels of HCV Core were determined by enzyme-linked immunosorbent assay (ELISA) (Mitsubishi Kagaku Bio-Clinical Laboratories, Tokyo, Japan). Total RNA was isolated from the infected cellular lysates using RNeasy mini kit (Qiagen, Hilden, Germany) for quantitative RT-PCR analysis of intracellular HCV RNA. The infectivity of HCV in the culture supernatants was determined by a focus-forming assay at 48 hrs post-infection. The HCV infected cells were detected using anti-HCV Core antibody (CP-9 and CP-11). Intracellular HCV infectivity was determined by a focus-forming assay at 48 hrs post-inoculation of lysates by repeated freeze and thaw cycles (three times).

Quantitative RT-PCR Analysis

The quantitative RT-PCR analysis for HCV RNA was performed by real-time LightCycler PCR (Roche) as described previously [17,18]. We used the following forward and reverse primer sets for the real-time LightCycler PCR: TSG101, 5′-ATGGCGGTGTCGGAGAGCCA-3′ (forward), 5′-AACAGGTTTGAGATCTTTGT-3′ (reverse); Alix, 5′-ATGGCGACATTCATCTCGGT-3′ (forward), 5′-TACTGGGCCTGCTCTTCCCC-3′ (reverse); Vps4B, 5′-ATGTCATCCACTTCGCCCAA-3′ (forward), 5′-ATACTGCACAGCATGCTGAT-3′ (reverse); CHMP4b, 5′-ATGTCGGTGTTCGGGAAGCT-3′ (forward), 5′-ATCTCTTCCGTGTCCCGCAG-3′ (reverse); Brox, 5′-ATGACCCATTGGTTTCATAG-3′ (forward), 5′-CCTGGATGACCTCAAGTCAT-3′ (reverse); β-actin, 5′-TGACGGGGTCACCCACACTG-3′ (forward), 5′-AAGCTGTAGCCGCGCTCGGT-3′ (reverse); and HCV-JFH1, 5′-AGAGCCATAGTGGTCTGCGG-3′ (forward), 5′-CTTTCGCAACCCAACGCTAC-3′ (reverse).

MTT Assay

Cells (5×10^3 cells/well) were plated onto 96-well plates and cultured for 24, 48 or 72 hrs, then, subjected to the colorimetric 3-(4,5-dimethylthiazol-2-yl)-2,5-diphenyltetrazolium bromid (MTT) assay according to the manufacturer's instructions (Cell proliferation kit I, Roche). The absorbance was read using a microplate reader (Multiskan FC, Thermo Fisher Scientific) at 550 nm with a reference wavelength of 690 nm.

Renilla Luciferase (RL) Assay

OR6 cells (1.5×10^4 cells/well) [17,18] were plated onto 24-well plates and cultured for 24 hrs. The cells were transfected with siRNAs (50 nM) using Oligofectamine and incubated for 72 hrs, then, subjected to the RL assay according to the manufacturer's instructions (Promega, Madison, WI). A lumat LB9507 luminometer (Berthold, Bad Wildbad, Germany) was used to detect RL activity.

Western Blot Analysis

Cells (2×10^5 cells/well) were plated onto 6-well plates and cultured for 24 or 48 hrs. Cells were lysed in buffer containing 50 mM Tris-HCl (pH 8.0), 150 mM NaCl, 4 mM EDTA, 1% NP-40, 0.1% sodium dodecyl sulfate (SDS), 1 mM dithiothreitol (DTT) and 1 mM phenylmethylsulfonyl fluoride (PMSF). Supernatants from these lysates were subjected to SDS-polyacrylamide gel electrophoresis, followed by immunoblot analysis using anti-TSG101 antibody (BD Transduction Laboratories, San Jose, CA), anti-Alix antibody, anti-Vps4B antibody (Abnova, Taipei, Taiwan) (A302-078A; Bethyl Laboratories, Montgomery, TX), anti-CHMP4B antibody (sc-82557; Santa Cruz Biotechnology, Santa Cruz, CA), anti-HCV Core antibody, anti-β-actin antibody (Sigma), anti-Myc-Tag antibody, anti-FLAG antibody (M2; Sigma), anti-Chk2 antibody (DCS-273; MBL), anti-heat shock protein (HSP) 70 antibody (BD), Living Colors A.v. monoclonal antibody (JL-8; Clontech, Mountain View, CA), anti-HCV NS5A monoclonal antibody (no. 8926; a generous gift from A Takamizawa, The Research Foundation for Microbial Diseases of Osaka University, Japan), or anti-HCV NS5A polyclonal antibody (a generous gift from K Shimotohno, Chiba Institute of Technology, Chiba, Japan).

Immunoprecipitation Analysis

Cells were lysed in buffer containing 10 mM Tris-HCl (pH 8.0), 150 mM NaCl, 1% NP-40, 1 mM PMSF, and protease inhibitor cocktail containing 104 μM 4-(2-aminoethyl)benzenesulfonyl fluoride hydrochloride, 80 nM aprotinin, 2.1 μM leupeptin, 3.6 μM bestatin, 1.5 μM pepstatin A, and 1.4 μM E-64 (Sigma). Lysates were pre-cleaned with 30 μl of protein-G-Sepharose (GE Healthcare Bio-Sciences). Pre-cleaned supernatants were incubated with 5 μl of Living Colors A.v. monoclonal antibody or anti-FLAG antibody at 4°C for 1 hr. Following absorption of the precipitates on 30 μl of protein-G-Sepharose resin for 1 hr, the resin was washed four times with 700 μl lysis buffer. Proteins were eluted by boiling the resin for 5 min in 1× Laemmli sample buffer. The proteins were then subjected to SDS-PAGE, followed by immunoblotting analysis using either anti-FLAG antibody, Living Colors A.v. monoclonal antibody or anti-HCV Core antibody.

Statistical Analysis

Statistical comparison of the infectivity of HCV in the culture supernatants between the knockdown cells and the control cells was performed using the Student's *t*-test. *P* values of less than 0.05 were considered statistically significant. All error bars indicate standard deviation.

Results

The ESCRT system is required for HCV production

To investigate the potential role(s) of the ESCRT system in the HCV life cycle, we first used lentiviral vector-mediated RNA interference to stably knockdown the ESCRT components, including TSG101, Alix, Vps4B, or CHMP4b in HuH-7-derived RSc cured cells that cell-culture-generated HCVcc (HCV-JFH1, genotype 2a) [13] could infect and effectively replicate [14–16]. We used puromycin-resistant pooled cells 10 days after the lentiviral transduction in all experiments. Western blot and real-time LightCycler RT-PCR analyses for TSG101, Alix, Vps4B, or CHMP4b demonstrated a very effective knockdown of each ESCRT component in RSc cells transduced with lentiviral vectors expressing the corresponding shRNAs (Fig. 1A–E). Importantly, we noticed that the depletion of ESCRT components did not affect the levels of several cellular proteins, including HSP70, Chk2, and b-actin (Fig. 1A). To test the cell toxicity of each shRNA, we examined colorimetric MTT assay. In this context, we demonstrated that the shRNAs did not affect the cell viabilities (Fig. 1F). We next examined the levels of HCV Core and the infectivity of HCV in the culture supernatants as well as the level of HCV RNA in the TSG101, Alix, Vps4B, or CHMP4b stable knockdown RSc cells 97 h after HCV-JFH1 infection at an MOI of 0.1. The results showed that the release of HCV Core into the culture supernatants

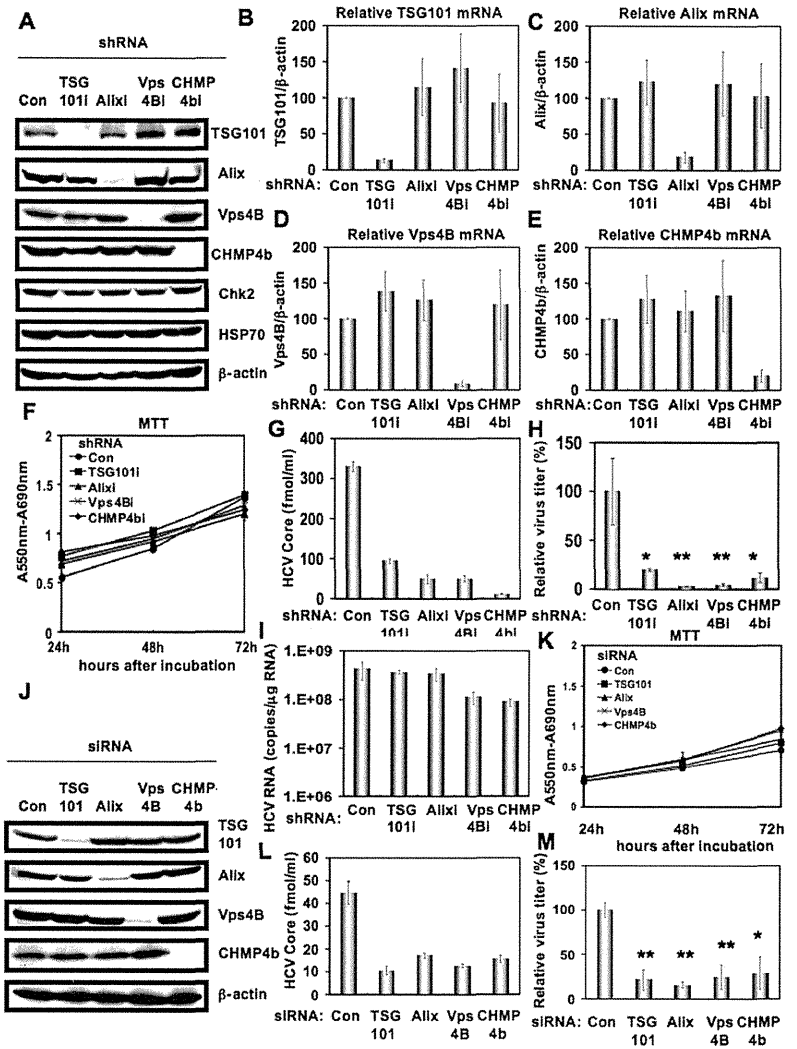

Figure 1. ESCRT components are required for the infectious HCV production. (A) Inhibition of TSG101, Alix, Vps4B, or CHMP4b protein expression by shRNA-producing lentiviral vectors. The results of the Western blot analysis of cellular lysates with anti-TSG101, anti-Alix, anti-Vps4B, anti-CHMP4b, anti-Chk2, anti-HSP70, or anti-β-actin antibody in RSc cells expressing shRNA targeted to TSG101 (TSG101i), Alix (Alixi), Vps4B (Vps4Bi), or CHMP4b (CHMP4bi) as well as in RSc cells transduced with a control lentiviral vector (Con) are shown. Real-time LightCycler RT-PCR for TSG101 (B), Alix (C), Vps4B (D), or CHMP4b mRNA (E) was performed as well as for β-actin mRNA in triplicate. Each mRNA level was calculated relative to the level in RSc cells transduced with a control lentiviral vector (Con) which was assigned as 100%. Error bars in this panel and other figures indicate standard deviations. (F) MTT assay of each knockdown RSc cells at the indicated time. (G) The levels of HCV Core in the culture supernatants from the stable knockdown RSc cells 97 h after inoculation of HCV-JFH1 at an MOI of 0.1 were determined by ELISA. Experiments were done in triplicate and columns represent the mean Core protein levels. (H) The infectivity of HCV in the culture supernatants from the stable knockdown RSc cells 97 hrs after inoculation of HCV-JFH1 at an MOI of 0.1 was determined by a focus-forming assay at 48 hrs post-infection. Experiments were done in triplicate and each virus titer was calculated relative to the level in RSc cells transduced with a control lentiviral vector (Con) which was assigned as 100%. Asterisks indicate significant differences compared to the control treatment. *$P<0.05$; **$P<0.01$. (I) The level of intracellular genome-length HCV-JFH1 RNA in the cells at 97 hrs post-infection was monitored by real-time LightCycler RT-PCR. Results